



Summary Report 278-S-01

For Project

Development of Optimized Welding Solutions for X100 Line Pipe Steel

Prepared for the

Design, Materials, and Construction Technical Committee of
Pipeline Research Council International, Inc.
Project MATH-1 Catalog No. L5XXXX

and

U.S. Department of Transportation
Pipeline and Hazardous Materials Safety Administration
Office of Pipeline Safety
Agreement Number DTPH56-07-T-000005

Prepared by
M.A. Quintana, The Lincoln Electric Company

With Major Contributions From
J. Hammond, Consultant
J.A. Gianetto and W.R. Tyson, CANMET-MTL
V.B. Rajan, R. Panday and J. Daniel, The Lincoln Electric Company
Y. Wang and Y. Chen, CRES

September 2011

This research was funded in part under the Department of Transportation, Pipeline and Hazardous Materials Safety Administration's Pipeline Safety Research and Development Program. The views and conclusions contained in this document are those of the authors and should not be interpreted as representing the official policies, either expressed or implied, of the Pipeline and Hazardous Materials Safety Administration, or the U.S. Government.



Catalog No. L5XXXX

Summary Report 278-S-01

For Project

Development of Optimized Welding Solutions for X100 Line Pipe Steel

Prepared for the

Design, Materials, and Construction Technical Committee of
Pipeline Research Council International, Inc.
Project MATH-1 Catalog No. L5XXXX

and

U.S. Department of Transportation
Pipeline and Hazardous Materials Safety Administration
Office of Pipeline Safety
DOT Project BAA DTHP56-07-0001

Prepared by

M.A. Quintana, The Lincoln Electric Company

With Major Contributions From

J. Hammond, Consultant
J.A. Gianetto and W.R. Tyson, CANMET-MTL
V.B. Rajan and R. Panday, The Lincoln Electric Company
Y. Wang and Y. Chen, CRES

September 2011

Version	Date of Last Revision	Date of Uploading	Comments
Draft	April 2011	April 2011	
Final	September 2011	September 2011	

This report is furnished to Pipeline Research Council International, Inc. (PRCI) under the terms of PRCI contract [278-PR- 348 - 074513], between PRCI and the MATH-1 contractors:

- Electricore (prime contractor),
- Center for Reliable Energy Systems, CANMET, NIST, and The Lincoln Electric Company (sub-contractors).

The contents of this report are published as received from the MATH-1 contractor and subcontractors. The opinions, findings, and conclusions expressed in the report are those of the authors and not necessarily those of PRCI, its member companies, or their representatives. Publication and dissemination of this report by PRCI should not be considered an endorsement by PRCI of the MATH-1 contractor and subcontractors, or the accuracy or validity of any opinions, findings, or conclusions expressed herein.

In publishing this report, PRCI and the MATH-1 contractors make no warranty or representation, expressed or implied, with respect to the accuracy, completeness, usefulness, or fitness for purpose of the information contained herein, or that the use of any information, method, process, or apparatus disclosed in this report may not infringe on privately owned rights. PRCI and the MATH-1 contractors assume no liability with respect to the use of, or for damages resulting from the use of, any information, method, process, or apparatus disclosed in this report. By accepting the report and utilizing it, you agree to waive any and all claims you may have, resulting from your voluntary use of the report, against PRCI and the MATH-1 contractors.

Pipeline Research Council International Catalog No. L5XXXX

PRCI Reports are Published by Technical Toolboxes, Inc.

3801 Kirby Drive, Suite 520
Houston, Texas 77098
Tel: 713-630-0505
Fax: 713-630-0560
Email: info@ttoolboxes.com

PROJECT PARTICIPANTS

PROJECT TEAM MEMBER	COMPANY AFFILIATION	PROJECT TEAM MEMBER	COMPANY AFFILIATION
Arti Bhatia	Alliance	Jim Costain	GE
Jennifer Klementis	Alliance	Gilmar Batista	Petrobras
Roger Haycraft	Boardwalk	Marcy Saturno de Menezes	Petrobras
David Horsley	BP	Dave Aguiar	PG&E
Mark Hudson	BP	Ken Lorang	PRCI
Ron Shockley	Chevron	Maslat Al-Waranbi	Saudi Aramco
Sam Mishael	Chevron	Paul Lee	SoCalGas
David Wilson	ConocoPhillips	Alan Lambeth	Spectra
Satish Kulkarni	El Paso	Robert Turner	Stupp
Art Meyer	Enbridge	Gilles Richard	TAMSA
Bill Forbes	Enbridge	Noe Mota Solis	TAMSA
Scott Ironside	Enbridge	Philippe Darcis	TAMSA
Sean Keane	Enbridge	Dave Taylor	TransCanada
Laurie Collins	Evraz	Joe Zhou	TransCanada
David de Miranda	Gassco	Jason Skow	TransGas
Adriaan den Herder	Gasunie	Ernesto Cisneros	Tuberia Laguna
Jeff Stetson	GE	Vivek Kashyap	Welsun
		Chris Brown	Williams

CORE RESEARCH TEAM	
RESEARCHER	COMPANY AFFILIATION
Yaoshan Chen	Center for Reliable Energy Systems
Yong-Yi Wang	Center for Reliable Energy Systems
Ming Liu	Center for Reliable Energy Systems
Dave Fink	Lincoln Electric Company
Marie Quintana	Lincoln Electric Company
Vaidyanath Rajan	Lincoln Electric Company
Joe Daniel	Lincoln Electric Company
Radhika Panday	Lincoln Electric Company
James Gianetto	CANMET Materials Technology Laboratory
John Bowker	CANMET Materials Technology Laboratory
Bill Tyson	CANMET Materials Technology Laboratory
Guowu Shen	CANMET Materials Technology Laboratory
Dong Park	CANMET Materials Technology Laboratory
Timothy Weeks	National Institute of Standards and Technology
Mark Richards	National Institute of Standards and Technology
Dave McColskey	National Institute of Standards and Technology
Enrico Lucon	National Institute of Standards and Technology
John Hammond	Consultant Metallurgist & Welding Engineer

This Page Intentionally Left Blank

FINAL REPORT STRUCTURE

Focus Area 1 - Update of Weld Design, Testing, and Assessment Procedures for High Strength Pipelines		
Report #	Description	Lead Authors
277-T-01	Background of Linepipe Specifications	CRES/CANMET
277-T-02	Background of All-Weld Metal Tensile Test Protocol	CANMET/Lincoln
277-T-03	Development of Procedure for Low-Constraint Toughness Testing Using a Single-Specimen Technique	CANMET/CRES
277-T-04	Summary of Publications: Single-Edge Notched Tension SE(T) Tests	CANMET
277-T-05	Small Scale Tensile, Charpy V-Notch, and Fracture Toughness Tests	CANMET/NIST
277-T-06	Small Scale Low Constraint Fracture Toughness Test Results	CANMET/NIST
277-T-07	Small Scale Low Constraint Fracture Toughness Test Discussion and Analysis	CANMET/NIST
277-T-08	Summary of Mechanical Properties	CANMET
277-T-09	Curved Wide Plate Tests	NIST/CRES
277-T-10	Weld Strength Mismatch Requirements	CRES/CANMET
277-T-11	Curved Wide Plate Test Results and Transferability of Test Specimens	CRES/CANMET
277-S-01	Summary Report 277 Weld Design, Testing, and Assessment Procedures for High Strength Pipelines	CRES

Focus Area 2 - Development of Optimized Welding Solutions for X100 Linepipe Steel		
Report #	Description	Lead Authors
278-T-01	State of The Art Review	Lincoln
278-T-02	Material Selection, Welding and Weld Monitoring	Lincoln/CANMET
278-T-03	Microstructure and Hardness Characterization of Girth Welds	CANMET/Lincoln
278-T-04	Microstructure and Properties of Simulated Weld Metals	CANMET/Lincoln
278-T-05	Microstructure and Properties of Simulated Heat Affected Zones	CANMET/Lincoln
278-T-06	Essential Welding Variables	Lincoln/CANMET
278-T-07	Thermal Model for Welding Simulations	CRES/CANMET
278-T-08	Microstructure Model for Welding Simulations	CRES/CANMET
278-T-09	Application to Other Processes	Lincoln/CANMET
278-S-01	Summary Report 278 Development of Optimized Welding Solutions for X100 Line Pipe Steel	Lincoln

EXECUTIVE SUMMARY

This investigation is part of a major consolidated program of research sponsored by the US Department of Transportation (DOT) Pipeline Hazardous Materials Safety Administration (PHMSA) and the Pipeline Research Council International (PRCI) to advance weld design, establish weld testing procedures, improve assessment methodologies, and develop optimized welding solutions for joining high strength steel pipe. This project focused specifically on development of optimized welding solutions for X100 line pipe steel. It was undertaken in direct response to growing industry demand for greater predictability in overall weld performance and mechanical properties. In general, the more exacting requirements imposed by strain based design are driving industry demand for improved performance as indicated by two PHMSA sponsored government industry forums - the first on pipeline research and development in March 2005 and the second on welding research in January 2006.

Accordingly, a research team was assembled in consideration of the key capabilities required to develop welding solutions for X100 in a comprehensive manner. John Hammond, Consultant Metallurgist and Welding Engineer, provided historical perspective on X100 development to date. The Lincoln Electric Company provided welding process and materials expertise as well as technical program management. CANMET-MTL provided materials expertise and significant experience in testing and characterization of X100 pipe welds. The organizations expertise in conducting thermal simulation studies was also essential to the project. CRES played an essential role with expertise in analytical methods and numerical modeling.

The first task of this project was a state of the art review of X100 in order to identify the major challenges facing the industry. This would also help the team focus the work scope for the program. The priority needs identified for field installation of X100 include welding processes and materials for seam welding, double jointing, tie-in and repair, as well as, for mainline welds. Mechanized gas metal arc welding (GMAW) was considered a proven and effective method for field welding of X100. Even so, ensuring consistent performance using GMAW still presented certain challenges, such as:

- Improvements were needed in the ability to define and control the welding parameter envelope to ensure performance targets are satisfied consistently.
- There is an ongoing effort by the industry to achieve higher levels of productivity with GMAW using advanced welding waveforms, tandem, and dual tandem variants of the process. This creates an ongoing need for development of welding processes and materials to achieve the required balance of weld strength, ductility and toughness.

The themes that underlay nearly all of the challenges presented fell into two focus areas.

- Reconsider the design standards, materials properties targets and assessment methods in the context of strain based design for high strength pipelines.
- Understand the fundamental interactions between the welding process and the materials being welded well enough to effect improvements in productivity, quality and weld properties simultaneously.

A team was dedicated to each focus area, and technical results were shared across projects.

This report presents the methodology, major results and conclusions from the research focused on X100 welding processes and welding materials, specifically the optimization of GMAW methods for X100 pipe line girth welds. The objective was to achieve a high level of reliability and consistency in X100 girth weld mechanical performance in order to support larger scale implementation of the material in pipe line projects.

The technical approach involved a reassessment of essential welding variables for pulse gas metal arc welding (GMAW-P) that aimed directly at the welding thermal cycle and the response of welding consumables and pipe steels to the welding process. The researchers used analytical numerical methods to determine the most probable primary welding process drivers. These key variables became the object of extensive experimental trials involving multiple base pipe and weld metal chemical compositions. From the standpoint of welding process control, the team placed an emphasis on welding variables known to influence the weld thermal cycle. In parallel, the team studied the response of base pipe and weld metal to simulated thermal cycles in detail from the standpoint of microstructure development and resulting properties (i.e., hardness and toughness).

Results clearly demonstrate the strong influence of the welding process on weld properties and indicate that the welding procedure is key in achieving the required weld properties. There is sufficient interaction between welding practice and material chemical composition (base pipe or weld) that the control of both key inputs is critical for the level of consistency and predictability desired for strain based design. This is a paradigm shift from traditional practice which has considered the welding procedure almost exclusively as a tool in achieving productivity and weld soundness.

By considering the fundamental aspects of the welding process, the materials, and their interactions in a holistic way, this report presents an alternative to the standardized treatment of essential variables. The authors have developed a methodology for welding process control based on True Energy™ and True Heat Input that can be used to significantly reduce the variation in weld thermal cycles and, therefore, improve weld performance. Also, a methodology was developed for welding material assessment based on Gleeble® thermal simulations that will improve the reliability of selecting the best welding materials for an application, thereby further enhancing weld performance. The major research outcomes are summarized as follows:

- The results demonstrate an approach to GMAW-P process control based on the concept and measurement of True Energy™ that allows for informed choices about welding process changes that can minimize variation in weld performance. Operators can establish and monitor procedure limits real time with the appropriate instrumentation. The resulting data from this program is also useful for post weld assessment of test results.
- Researchers show that the prediction of welding thermal cycles are accurate using the True Heat Input derived from True Energy™ measurements. They can assess the robustness of various welding materials under different scenarios by using $\Delta t_{800\ 500}$ estimates from the thermal cycles in conjunction with the CCT diagrams generated from the thermal simulation experiments.
- Connecting the welding process knowledge with the fundamental understanding of how the materials will respond to the process is key to making the best welding material selection. Conversely, the same kind of analysis will identify the boundaries of a welding process required to ensure a given material performs as expected.
- The same methodology applies to an assessment of the HAZ. The evaluation of simulated HAZ regions provides an excellent method for comparing and ranking the pipe steels. This eliminates the complexity and cost associated with the evaluation of real welds where complex distributions and narrow width of HAZ regions are often encountered.

Clearly, the results of this program demonstrate a higher level of predictability and consistency for X100 with this approach than has been possible previously. Even though this project was focused on X100, the technical approaches and general problem solving methods can be applied to any GMAW application to improve reliability and consistency.

TABLE OF CONTENTS

EXECUTIVE SUMMARY	vii
TABLE OF CONTENTS	x
LIST OF FIGURES	xi
LIST OF TABLES	xii
ABSTRACT	1
1 BACKGROUND	2
1.1 Historical Review - X100 Development	4
1.2 Industry Successes	15
1.3 Challenges Remaining	16
1.4 Opportunities	18
2 OBJECTIVES & OVERALL APPROACH	19
3 EXPERIMENTAL METHODS	23
3.1 Materials, Welding Processes and Weld Process Monitoring	23
3.2 Material Characterization	31
3.3 Mechanical Testing	36
4 ANALYTICAL METHODS	39
4.1 Thermal Cycle Predictions	40
4.2 Microstructure Models and Hardness Predictions	46
5 MATERIALS AND PIPE WELD PERFORMANCE	50
5.1 Heat Affected Zones	50
5.2 Weld Metal	53
6 WELDING CONSIDERATIONS	57
6.1 Essential Welding Variables	57
6.2 Considerations for Other Welding Processes	61
7 CONCLUDING REMARKS	62
8 FUTURE RESEARCH OPPORTUNITIES	64
9 ACKNOWLEDGEMENTS	65
10 REFERENCES	66

LIST OF FIGURES

Figure 1. World Marketed Energy Use by Fuel Type	2
Figure 2. History of X100 Experience	4
Figure 3. Carbon Content and Processing for High Strength Pipe Steel	7
Figure 4. Transverse pipe yield strength with weld overmatch	9
Figure 5. Longitudinal pipe yield strength	10
Figure 6. WERC dual tandem GMAW-P	14
Figure 7. Consolidated Program Schematic	19
Figure 8. Schematic narrow groove pipe joints	26
Figure 9. Comparison of "constant" and pulsed current welding outputs	30
Figure 10. Cross-sectional view of thermocouple placement	30
Figure 11. Material characterization, single torch example (807)	31
Figure 12. Material characterization, dual torch example (883)	32
Figure 13. Typical micro-hardness map for staggered weld, 300G Hv (883)	32
Figure 14. CCT behavior, (a) NiMo80 and (b) PT1	34
Figure 15. CCT behavior, (a) X100-5 and (b) X100-4	36
Figure 16. Narrow gap weld cross-section and hardness distribution (807J)	38
Figure 17. Schematic, mechanical properties specimen locations	38
Figure 18. An integrated thermal-microstructure model for welding simulation	40
Figure 19. GMAW-P girth weld and its partitioned finite element mesh	41
Figure 20. Work flow of thermal model development, verification, and applications	41
Figure 21. Predicted vs. measured cooling time, WERC research data	43
Figure 22. Comparison of predicted with measured thermal cycles (807J)	44
Figure 23. Microstructure and hardness predictions for thermal simulation	49
Figure 24. Comparison of micro-hardness distribution, (a) measured vs. (b) predicted	49
Figure 25. Comparison of simulated HAZ softening for three pipe steels	51
Figure 26. Comparison of CVN transition behavior for pipe steel X100-5	52
Figure 27. Tensile test summary NiMo80 and X100-5	54
Figure 28. Charpy V-notch impact toughness, NiMo80	55
Figure 29. Continuous cooling transformation behavior	56
Figure 30. Schematic comparison of GMAW-P waveforms	58
Figure 31. Effect of welding variables on HAZ cooling time	59

LIST OF TABLES

Table 1. Historical Development of Modern X100 (Year of Manufacture)	6
Table 2. Estimate of X100 Pipe Production to 2007	8
Table 3. Generic Alloying System for X100 Line Pipe (Parent Metal)	8
Table 4. X100 Tensile Test Requirements (PSL2)	9
Table 5. Summary of Chemical Compositionsof X100 Test Seam Welds	12
Table 6. GMAW performance from early trials	13
Table 7. Welding consumable types, WERC Research	13
Table 8. GMAW-P weld metal properties performance, WERC Research	14
Table 9. Comparison of Essential Welding Variables	21
Table 10. Experimental Test Plan, Test Welds	24
Table 11. Chemical composition X100 base pipe	25
Table 12. Chemical composition X100 weld metal	27
Table 13. Comparison of Average and True Power, "constant" and pulsed DC current	29
Table 14. Influence of cooling time and alloy level on hardness and impact toughness	34
Table 15. CVN summary for X100-5 and X100-4	36
Table 16. Small scale test summary	37
Table 17. Summary simulated HAZ Charpy V-notch properties	51



TECHNICAL REPORT

No. TH-0233

FROM

**The Lincoln Electric
Company**

30 September 2011

M.A. Quintana

PREPARED FOR

**Pipeline Research
Council International
(PRCI)
&
Pipeline Hazardous
Materials Safety
Administration
(PHMSA)**

PRCI MATH-1, Project 2 watermark PHMSA DTPH56-07-T-000005, Project 278

Summary Report 278-S-01

Development of Optimized Welding Solutions for X100 Line Pipe Steel

ABSTRACT

This investigation is part of a major consolidated program of research sponsored by the US Department of Transportation (DOT) Pipeline Hazardous Materials Safety Administration (PHMSA) and the Pipeline Research Council International (PRCI) to advance weld design, establish weld testing procedures, improve assessment methodologies, and develop optimized welding solutions for joining high strength steel pipe. The work presented in this summary report addresses the optimization of gas metal arc welding (GMAW) methods for X100 pipe line girth welds.

Specifically, the project focused on achieving a higher level of reliability and consistency in X100 girth weld mechanical performance to support larger scale implementation of the material in pipe line projects. To that end, the team began with a state of the art review to identify the major challenges facing the industry with regard to X100 and to help focus the work scope for the program. The technical approach involved a re-assessment of essential welding variables for pulse gas metal arc welding that aimed directly at the welding thermal cycle and the response of welding consumables and pipe steels to the welding process.

By considering the fundamental aspects of the welding process, the materials, and their interactions in a holistic way, the researchers developed a methodology for welding process control based on True Energy™ and True Heat Input which can significantly reduce the variation in weld thermal cycles and, therefore, weld performance. Also, the team developed a method for welding material assessment based on Gleeble®¹ thermal simulations. This research will improve the reliability of selecting the best welding materials for an application, thereby further enhancing weld performance.

This report presents results for several GMAW welding consumables that achieve a range of strength mismatch conditions in order to illustrate the application for improving the reliability and consistency in weld performance.

KEYWORDS

GMAW, GMAW-P, X100 pipe welding, weld metal, HAZ, thermal cycle, strength, microhardness, toughness, True Power, True Heat Input, Average Heat Input, True Energy™

¹ Gleeble® is a registered trademark of Dynamic Systems Inc. Corporation New York P.O. Box 123, Route 355 Poestenkill New York 12140

1 BACKGROUND

The primary field of application for high strength steel line pipe is envisaged as high pressure, large diameter pipelines for the transmission of dry natural gas, particularly for long distance systems. In such pipelines, the economic advantages of high strength steel can be exploited effectively in mechanical design and construction of the pipeline and in optimizing compression systems and operating costs. Although the primary driving force is for gas transmission, there may be instances where it can be utilized elsewhere. For example, its use in oil pipelines is a possibility but there is less of an economic advantage.

Most recently, the focus has been on increasing strength because of the potential for significant cost reduction. [1, 2] The major potential is in capital expenditure (CAPEX) associated with the construction and commissioning of long distance gas pipelines through:

- Reduced steel tonnage,
- Reduced transportation cost, and
- Increased construction efficiency.

The drive for cost effectiveness is a very powerful incentive for ongoing investment in materials development. While the major commercial benefit comes from reducing CAPEX, there is benefit also in the potential for design optimizations and lower operating expenditure (OPEX). The potential to increase capacity with higher operating pressures provides some additional incentive at a time when oil and gas demand is growing, Figure 1. Effective industry response to this increasing demand requires implementation of advances in line pipe steel technology more rapidly than experienced historically for X80, which took nearly twenty years from its initial application in 1985.

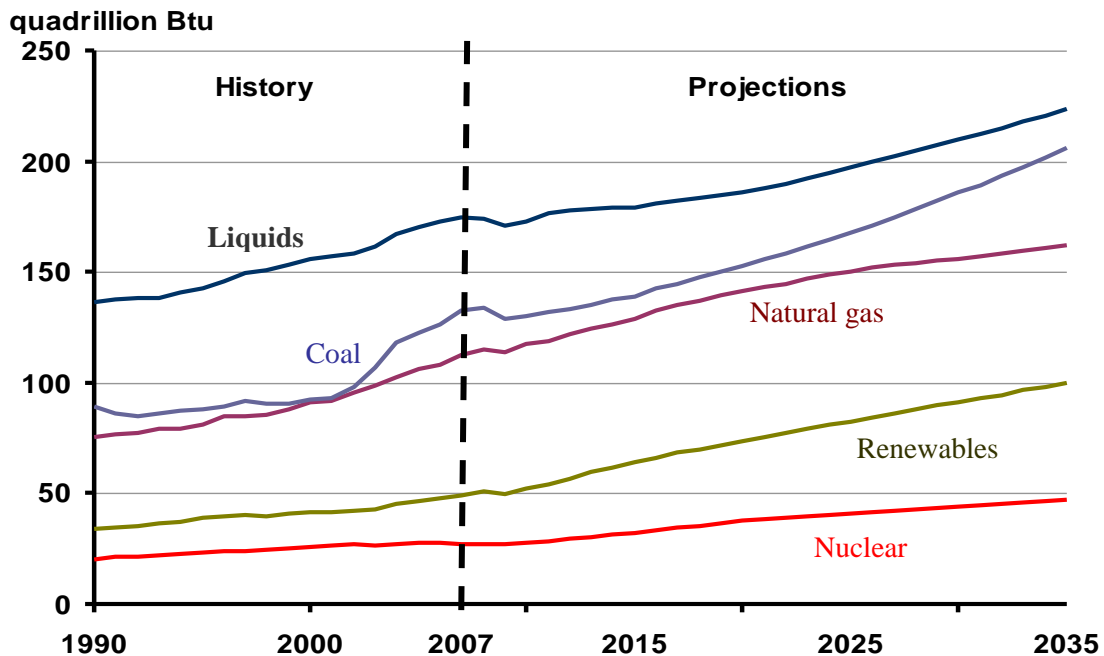


Figure 1. World Marketed Energy Use by Fuel Type [3]

Historically, developments in line pipe technology needed to satisfy increasing demand have been evolutionary in nature and have, to some extent, paralleled improvements in steel making practice. Over the past 40 years, pipelines have been constructed in a range of steels from API Grade B (ISO Grade L 245) up to Grade X80 (ISO L 555). For large diameter oil and gas lines constructed between 1980 and 1990, modified grade X65 (L 450) and later X70 (L 485) were used extensively. These have been the “workhorse” steels in the pipeline industry for twenty to thirty years. Over time, refinements in thermo-mechanical control process (TMCP) of steel plate for pipe increased the availability of leaner composition steels with improved weldability. This resulted in X65 and X70 with very little metallurgical difference. Accordingly, the use of X70 and later X80 was encouraged as welding process and consumable development caught up with the improvements in base material. Over this same period of time, welding practice in pipe welding shifted from manual and semi-automatic welding processes to more mechanized or automated methods.

X80 can be considered a small evolutionary step from X70 with only minor changes to chemical composition. In terms of both steel and welding development, the transition from X65 to X70 to X80 can be viewed as incremental development. Improvements in manufacturing technology made possible the optimizations of basic materials and welding technology needed for implementation of the new steels without major changes in governing codes and standards.

Even before X80 became more widely used, investigation of the possibilities offered by even higher strength steels were a priority, driven by the prospect of very long, high pressure gas trunk pipelines in increasingly remote areas. By the 1990s, the target was X100 steel that would achieve a minimum pipe yield strength (YS) of 100 ksi (690 MPa) in the application with high levels of toughness and weldability.

While considerable advances in steelmaking and pipeline construction have occurred, innovations in welding process technology generally lag pipeline industry needs. Clearly, the number of historically viable welding options declines as pipe strength increases. Weld strength becomes more sensitive to cooling rate variation, cold cracking sensitivity increases, and overall weldability declines. Also, achieving the necessary balance among weld strength, toughness, and ductility necessary for pipeline performance requires more highly controlled welding practice, procedures and pass sequence. As a result, greater control of essential variables is needed to satisfy increasingly stringent weld property requirements. This must be achieved with the range of manual, semi-automatic and automatic welding processes needed for double jointing and mainline girth welding, as well as tie-in and repair welding.

If the pipeline industry is to realize the full potential of X100, large-scale implementation must occur on an aggressive time scale consistent with estimates for increasing energy demand. However, it must be accomplished in a manner that manages the potential risks and provides high levels of protection for the environment, security of supply and public safety. A major technological challenge is achieving the necessary weld properties with sufficient reliability and consistency to ensure pipeline weld performance using a broad enough range of welding processes for the existing production conditions and contractor capabilities.

1.1 Historical Review - X100 Development

A comprehensive review of the state of knowledge was necessary to ensure that this project would build effectively on past experience and the most recent developments in line pipe and proposed pipeline designs. Thus, a state of the art review was commissioned to assess pipeline industry experience with X100 and to identify major technology gaps as a foundation for this research. While the initial focus of this review was a consolidation of knowledge based on publicly available information, it was recognized that much of the detail would still be held closely by the companies that had invested heavily in the development efforts. Through a series of surveys and private communications with industry leaders and organizations most recently engaged in the development and implementation of high strength line pipe, additional proprietary information that could be released also was included in the review. The review [4,5] traced the history of X100 use in the field; presented the evolution of steel technology and pipe manufacture; reviewed the state of welding technology as it applies to pipe fabrication and field construction; and critically assessed practical drivers and resource constraints to reach conclusions regarding key technology gaps and research needs.

In order to provide context for the current program of research, major elements of the review are summarized to provide a foundation for ongoing development aimed at improving pipe line weld performance.

1.1.1 Field Trials and Large Scale Tests

At the time of reporting, no purpose designed X100 pipeline has been built. Therefore, practical experience is best illustrated by the chronology of test sections and large scale tests. As part of the ongoing development of materials, pipe and fabrication techniques, test sections of X100 were built into expansions or loops of existing pipeline systems with for the purpose of demonstrating that welding, bending and pipelay was feasible under practical site conditions. Other large scale trials involved test loops for fracture control (burst) tests, for evaluation of long term environmental effects, or for operational experience. The history of this large scale experience is illustrated in Figure 2.

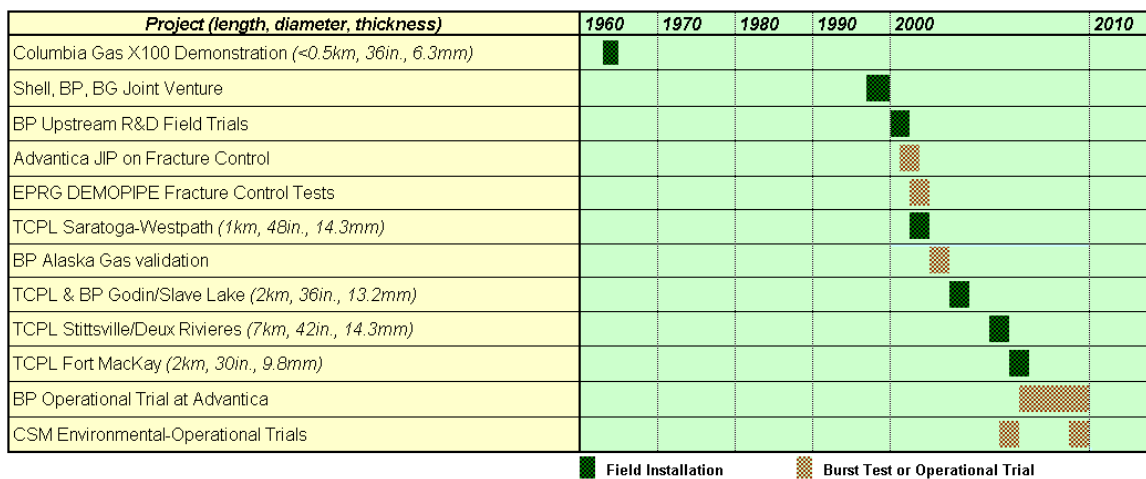


Figure 2. History of X100 Experience

The earliest reported application of an X100 pipeline [6] goes back to the 1960s when Atlantic Seaboard Corporation (subsidiary of Columbia Gas) laid an 1185 foot long test section that was ultimately used for storage. The material from which the pipe was formed was quenched and tempered steel. Mechanized gas metal arc welding (GMAW) was used for field fabrication. Although the developer's concluded that X100 was a feasible product for long distance gas pipelines no further interest was shown in the topic until the 1990's with a Shell, BP Exploration (BP), and British Gas (BG) joint venture.

The first pipeline construction with a modern X100 occurred in September 2002 when TransCanada Pipelines (TCPL) tied a 1 km section into an X80 main line [7-9]. Single wire (ER90S-G over ER70S-G root) mechanized pulsed gas metal arc welding (GMAW-P) was employed by a contractor that had been trained specifically in the welding practice needed for X100. The few weld defects were repaired with shielded metal arc welding (SMAW). This trial proved that X100 could be welded and laid by a commercial contractor under site conditions but the early autumn weather could not be considered as a simulation for arctic pipelay in winter.

TCPL and BP responded with another test section in February 2004 [7-9]. Both conventional single wire and tandem GMAW-P were used for this 2 km X100 loop installed in an existing TCPL line. The tandem process nearly doubled the welding speed of the conventional single wire process. Contractors achieved target production rates with an extremely low repair rate. The remote location during the severity of a Canadian winter provided confirmation of field feasibility of X100.

A more extensive field trial was conducted by TCPL in July 2006 [10]. The 7 km loop included 5 km of longitudinal seam submerged arc welded (SAWL) pipe and 2 km of helical seam submerged arc welded (SAWH) pipe. For the girth welds, another commercial pipelay contractor employed mechanized GMAW-P with both single wire and hybrid-tandem techniques (ER90S-G over ER70S-G root). For tie-in and repair welds, a broader range of welding options was employed than in previous trials. Mechanized gas-shielded flux cored arc welding (FCAW-G) was used for the first time (E111T1-K3MJ-H4 over ER70S-G root) in addition to low hydrogen vertical down SMAW (E12018-G over E8010-G root/hot).

A less extensive field trial conducted by TCPL in 2007 [10] installed 2 km of SAWH X100 pipe using single wire GMAW-P. An ER100S-G wire electrodes was used with root passes deposited over an internal backing bar. Due to the short length of the loop, only two tie in welds were needed, one at each end of the section. GMAW-P was used for both welds.

In addition to the field trials, several fracture control (burst) tests [10, 11] and one operational trial [12-14] were conducted over the past decade. While the details and results of the fracture control (burst) tests generally remain proprietary to the sponsors and their contractors, their position in the chronology illustrates an increasing level of interest in X100 and an increasing need to understand the behavior of the material under varying conditions of running fracture. Since these are highly engineered tests designed to reveal specific aspects of the material under dynamic loading, the girth welds are expected to be prototypical of pipelay welding under field conditions.

By contrast, the operational trial of X100 [12] commissioned by BP in 2006 required the construction of a test loop using conventional techniques. The 0.8 km loop incorporated X100 cold bends and SAWL pipe from two suppliers. The test section was fabricated using mechanized tandem GMAW-P over single wire GMAW-P root passes and ER100S-G wire electrodes. Tie-ins and repairs were made using semi-automatic FCAW-G (E111T1-K3MJ-H4) over GMAW-STT (ER80S-G) root passes. The operational trial was run for a two year period under conditions simulating a forty year operational life of a high pressure pipeline. Results have not been made public.

Thus far, all the X100 projects have been demonstrations that suitable linepipe can be produced and that pipelines can be constructed using conventional pipelay methods. Since most trial sections were installed in systems designed for lower strength grades of pipe material, these installations do not fully exploit the X100 pipe properties and hence do not prove the operational capability of X100. In service, these sections of high strength pipeline are not operating at stress levels that would apply in a full economic exploitation of the material. Only the longer term full scale operational trials begin to prove operational suitability [14].

Even so, the steel and welding developments completed to ensure success of these projects were significant. Many welding consumables were evaluated to assess their operational characteristics and potential to produce weld metal with requisite mechanical properties. Significant strides were made in welding process and procedure development in terms of both the productivity objectives and the weld performance targets.

1.1.2 Evolution of Steel and Line Pipe Capability

While some producers report laboratory trials as early as 1985, Table 1, development of the modern X100 steels began in the mid 1990's with separate collaborations between steel makers and individual companies of the oil and gas user industry [4]. The X100 steel pipes made to date have been the subject of extensive and incremental technical development. For large diameter onshore applications, manufacture has been by the basic oxygen steel making process followed by ladle treatments and vacuum degassing resulting in low carbon steel with micro-alloy additions and exceptionally low sulfur and phosphorus content [15]. The recent development of seamless X100 pipe for offshore uses electric furnace steel.

Table 1. Historical Development of Modern X100 (Year of Manufacture)

Manufacturer	A	B	C	D	E	F
Lab Trial Heats of X100	1985	1985	1996	1994	2005	2003
Prototype Commercial Manufacture of X100	2003	1999	2000	1995	2006	2005
Normal Commercial Manufacture of X100	-	-	2002	2003	-	-

Specific chemical compositions were developed to suit individual mill practice (e.g. plate rolling capacity, accelerated cooling control, and pipe forming capacity). While much of the detailed information on X100 remains proprietary to each steel mill, Figure 3 illustrates three different

approaches for achieving target mechanical and physical properties considering the trade-offs between chemical composition and mill processing parameters [16]. Approach “A” describes a relatively high carbon content and carbon equivalent. While this is an easier composition for the steel maker to process because it allows X100 properties to develop in the plate at a low cooling rate and high accelerated cooling stop temperature, it has the disadvantage of lower weldability. Approach “B” describes a relatively low carbon and carbon equivalent. This would improve weldability but also requires greater process controls in the plate rolling mill to achieve desired properties. Also, the leaner chemical composition may result in excessive heat affected zone (HAZ) softening adjacent the pipe seam weld. Approach “C” at an intermediate carbon level and carbon equivalent tends to optimize production flexibility produces high levels of toughness and weldability.

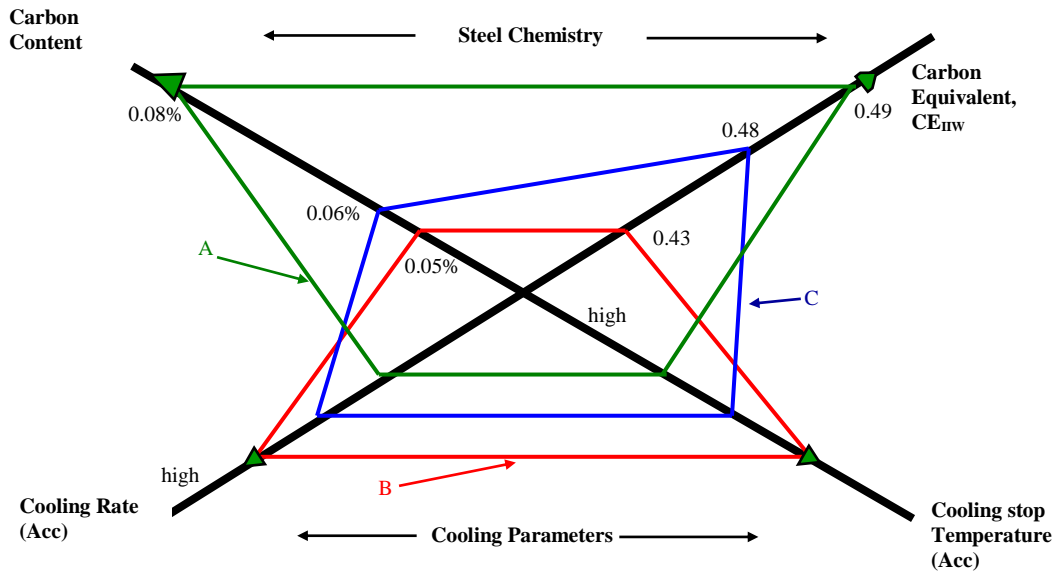


Figure 3. Carbon content and processing for high strength pipe steel [16]

Much of the X100 pipe produced to date is in the 762 - 914 mm (30 - 36 in.) diameter range and with wall thicknesses for SAWL type from 12.0 - 19.1 mm. Smaller quantities of larger diameter and higher wall thickness X100 have been manufactured with the upper end of the diameter reaching 1219 - 1320 mm (48 - 52 in.) and wall thickness ranging typically from 16 - 20 mm. One manufacturer reported 1420 mm (56 in.) diameter X100 pipe at 19 mm wall thickness. In the case of X100 SAWH pipe the wall thickness range is at the lower end, typically 9.8 mm and 12.7 mm for 762 mm and 1067 mm (30 in. and 42 in.) diameter pipe, respectively. This reflects the products supplied by the major manufacturers and indicates significant manufacturing experience. All have been manufactured from TMCP strip or plate.

Table 2 summarizes manufacturer capability by diameter and wall thickness at the time research started for the state of the art review [4]. At present, the situation concerning X100 seamless pipe development is less diverse as pipes of only one diameter 323 mm (12.75 in.) and two wall thicknesses (15 and 25 mm) have been manufactured and tested.

Table 2. Estimate of X100 Pipe Production to 2007

Manufacturer	A	B	C	D	E	F
Total X100 Pipes Produced	100*	114	300	283	>300**	90
Type	SAWL	SAWL	SAWL	SAWL	SAWH	SMLS
Minimum Diameter (mm)	762	762	914	762	762	324
Maximum Diameter (mm)	1321	1220	1220	1420	1067	324
Min. Wall Thickness (mm)	14.0	12.7	13.2	12.5	9.8	15
Max. Wall Thickness (mm)	25.0	20.6	18.4	25.4	12.7	25
Condition	TMCP	TMCP	TMCP	TMCP	TMCP	Q & T

* approximate number quoted by manufacturer

** Quoted as a km figure - 12 meter long pipes assumed for calculated number

Mill practice and wall thickness are primary drivers for determination of chemical composition. Given the range of variation possible, particularly for onshore applications, alloying strategies are expected to change from one manufacturer to another. Table 3 summarizes the generic alloying systems used for X100 pipe [4]. In general, most X100 has been produced to a 0.05 - 0.07% C, high Mn composition with varying amounts of other major alloy elements, typically Cu, Mo, Ni and in some instances Cr, with micro-alloy additions of Ti and Nb and in one instance V. This results in a parent metal CE_{IIW} value of typically 0.46 - 0.49, indicating that some preheat will be needed to weld these alloys and that hydrogen controlled welding procedures should be used. The P_{cm} values fall within the range 0.19 - 0.23. Such values imply that the X100 steels will have good weldability with preheat application. The exception may be the second alloying system from Manufacturer A with a CE_{IIW} of 0.60, but a P_{cm} within range of the others. At this time, it is not known if P_{cm} or CE_{IIW} is a better predictor of X100 weldability.

Table 3. Generic Alloying System for X100 Line Pipe (Parent Metal)

Manufacturer	Generic Alloying System (Alloy Element Weight % where quoted)	CE_{IIW}	P_{cm}
A	0.06 C, 1.9 Mn, 0.04 Nb, 0.01Ti + other alloy	0.46	0.19
	0.03 C, 1.9 Mn, 0.04 Nb, 0.01Ti + other alloy	0.60	0.22
B	0.06 C, 1.85 Mn + Cu, Mo, Ni alloy + Nb, Ti microalloy	0.49	0.20
C	0.05-.0.07 C, 1.8-2.0 Mn + Cu, Mo, Ni alloy + Nb, Ti	0.46	0.20
D	0.06-0.07 C, 1.8 - 2.0 Mo + Cu, Mo, Ni, Cr alloy + Nb, V, Ti*	0.47- 0.49	0.20- 0.21
E	Declared only as Nb+V micro alloyed steel		
F	0.10 C, 1.25 Mn = Cu, Mo, Ni, Cr alloy + Nb, Ti **	0.54	0.24
G	Not declared		

* May contain controlled addition of boron

** Q & T seamless pipe

The impact of such variation on strength can be significant. Table 4 summarizes the API 5L and ISO 3183:2007 tensile test requirements for X100 pipe. The values specified are for transverse

direction tensile tests (i.e. test specimen orientation perpendicular to the longitudinal axis of the pipe and tangential to the diameter). The specified range for X100 YS at 690-840 MPa is wider than the 690-810 MPa that some users would prefer. At the time the 44th edition of API 5L and ISO 3183:2007 standards were drafted, the pipe mills considered that the ranges specified would allow economic manufacture without unacceptable failure rates for YS above the maximum.

Table 4. X100 Tensile Test Requirements (PSL2)

Requirement	Pipe Body				Weld Seam
	Yield Strength, $R_{p0.2}$ (MPa)	Ultimate Tensile Strength, R_m (MPa)	Ratio $R_{p0.2}/R_m$	Elongation %	Ultimate Tensile Strength, R_m (MPa)
Min	690	760	--	12	760
Max	840	990	0.97	--	--

The consequence for operator-users and their contractors is greater difficulty in achieving overmatching weld strength, particularly as much of the early welding procedure development was based on overmatching pipe YS of 810 MPa maximum. This point is illustrated in Figure 4 [4]. The pipe transverse YS results are approximated by a normal bell curve. A typical distribution for a tightly controlled welding process is superimposed with a minimum weld YS set at the desired 810 MPa maximum for the pipe. If this weld metal range were to be shifted upward to coincide with the 840 MPa specification maximum, weld metal alloy levels would increase and the availability of welding consumables and welding process options would be further limited. The result would be smaller operational envelopes for welding with essential parameters being specified more tightly, a greater sensitivity to cooling rate, a greater risk of cold cracking, increased hardness and decreased toughness.

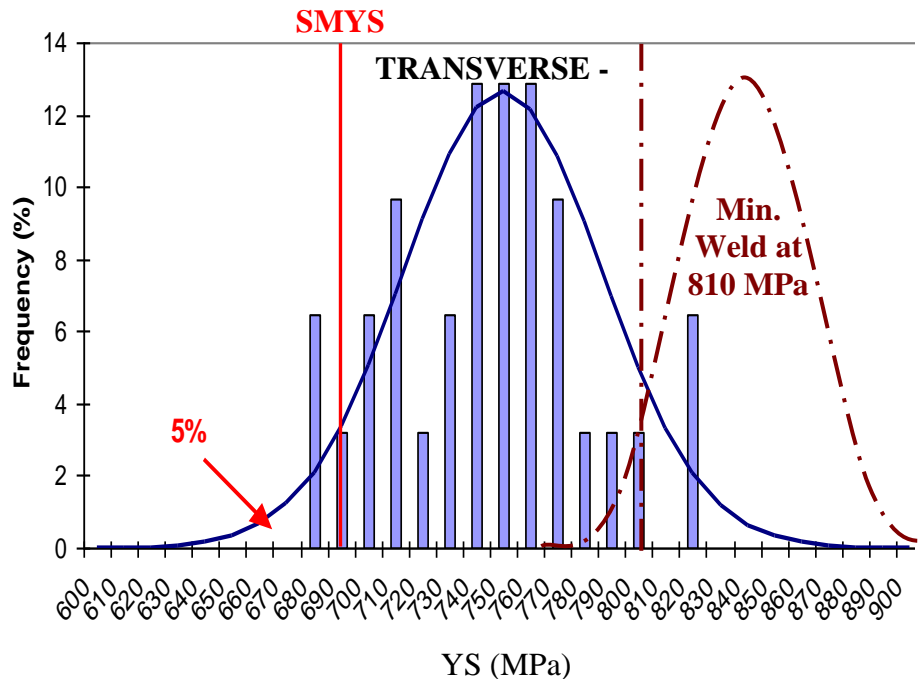


Figure 4. Transverse pipe yield strength with weld overmatch

The tensile properties of X100 line pipe in the longitudinal direction are not specified in either the API or ISO standards but are often included in a purchaser's supplementary specifications. In such instances high strength in the parent pipe metal may be of secondary importance to achieving a high strain capacity in the longitudinal direction. It should be noted that the yield and tensile strengths in the longitudinal direction will be lower than for the transverse direction for SAWL pipe. The situation for SAWH or seamless pipe may be completely different and cannot be covered here from available data. The frequency distribution for strength in the longitudinal direction was taken from the same data and presented in Figure 5. Here again, there is a wide spread of actual YS values but the mode value is some 50 MPa less than the transverse direction. On the basis that the purchasers specified a minimum YS of 630 MPa in the longitudinal direction, the under-strength reject rate would have been less than 5%. A positive aspect is that any girth welding consumable selected to overmatch the transverse direction YS should comfortably overmatch the longitudinal YS.

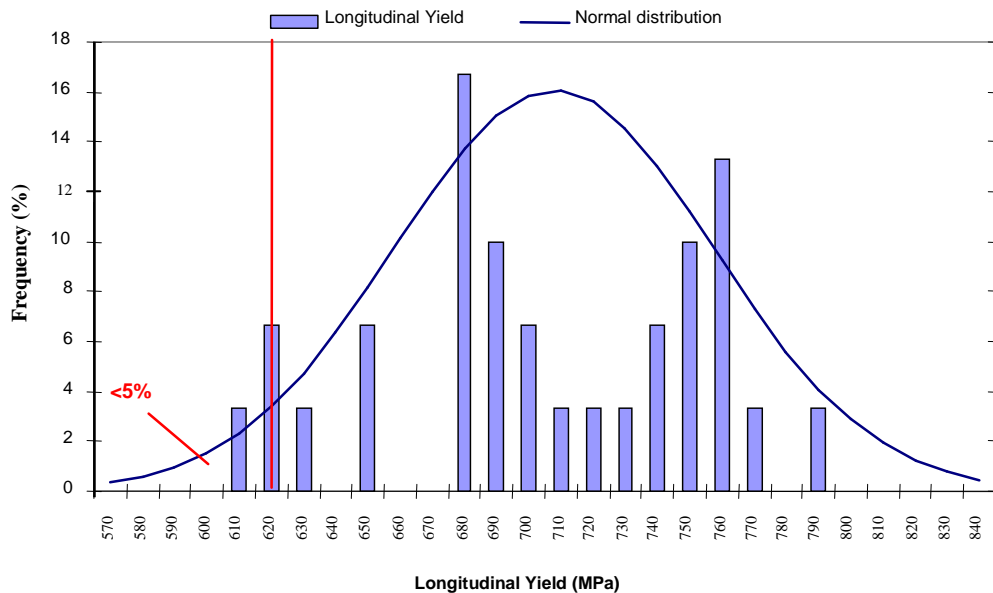


Figure 5. Longitudinal pipe yield strength

The concept and level of weld metal YS overmatching the actual YS of the parent pipe deserves further consideration as, given that significant anisotropy exists in most X100 line pipe, a minimum all-weld metal YS of 810 MPa will generally overmatch the actual YS of the pipe in the longitudinal direction, in which the highest levels of operational strain are likely to be experienced. The transverse direction YS of the X100 pipe will generally be higher, so an automatic overmatch by an 810 MPa YS weld metal cannot be guaranteed. However, the supporting effect of the adjacent higher strength parent metal on a girth weld of marginally lower strength may make it fit for purpose, although this should be proved in each case by further testing.

Far more detail regarding X100 steel and line pipe development is available in Hammond's review [4]. Those aspects that seem most relevant to the optimization of welding solutions have been summarized here.

1.1.3 Welding Processes and Consumables

Most of the welding development focused on main line welding options that had offered the highest potential for success. The main objective was to extend the use of conventional welding techniques to X100, if possible. Any development done to improve SAWL or SAWH for seam welds was conducted by the pipe mills themselves and most of the details remain confidential.

1.1.3.1 Seam Welds

Throughout the development of X100 steel and line pipe, the pipe mills refined the welding techniques for the SAWL seam welds with each new project. While most of the work is still considered proprietary there are a few reports published that provide some insight as to the technical challenges faced with X100 SAWL [18-20]. Seam welds in line pipe are made in two passes, one each from outside and inside diameter (OD and ID), using multiple wire SAW. Little problem was associated with achieving the required strength. The weld metal could be alloyed to ensure the entire weld overmatched the base material with requisite toughness, particularly if the weld reinforcement was taken into consideration. However, the roughly 40 kJ/cm heat input caused the HAZ softening and variation in toughness expected.

Around 2000-2001, major technical development on X100 line pipe escalated. By about 2002, the mills were delivering second generation X100 steels as full-sized limited production prototypes. Pipe from three suppliers was used during girth welding trials. Thicknesses ranged from 14.9 to 19.0 mm in 30 to 36 in. pipe with CE_{IIW} and Pcm consistent with the ranges in Table 3. Based on the chemical test results for the seam welds, each supplier approached SAWL in a slightly different way.

Table 5 compares the seam weld and pipe compositions for the three suppliers - A, B and C. By either measure, Pcm or CE_{IIW} , it is apparent that two of the pipe suppliers are using welding consumables more highly alloyed than the base pipe being welded.

Table 5. Summary of Chemical Compositions of X100 Test Seam Welds

Supplier	C	Mn	P	S	Si	Cr	Ni	Mo	Cu	Nb	V	Ti	Pcm	CE
A (Pipe)	0.027	2.00	0.006	<0.005	0.2	0.43	0.48	0.43	0.46	0.05	0.07	0.015	0.22	0.61
A (ID)	0.037	1.64	0.006	<0.005	0.22	0.56	1.10	0.58	0.33	0.03	0.05	0.010	0.33	0.64
A (OD)	0.046	1.62	0.007	<0.005	0.20	0.50	1.09	0.51	0.31	0.03	0.04	0.010	0.33	0.62
B15 (Pipe)	0.066	1.91	0.008	<0.005	0.10	0.02	0.54	0.27	0.27	0.03	0.006	0.013	0.21	0.50
B15 (ID)	0.068	1.88	0.009	<0.005	0.13	0.46	0.39	1.04	0.24	0.02	0.007	0.013	0.28	0.73
B15 (OD)	0.063	1.87	0.008	<0.005	0.16	0.34	1.75	0.60	0.26	0.019	0.007	0.016	0.27	0.70
B19 (Pipe)	0.06	1.89	0.008	<0.005	0.18	0.02	0.50	0.26	0.30	0.06	0.005	0.018	0.20	0.49
B19 (ID)	0.06	1.99	0.008	<0.005	0.21	0.36	1.00	0.78	0.26	0.04	0.007	0.02	0.27	0.70
B19 (OD)	0.053	1.91	0.007	<0.005	0.20	0.33	2.03	0.63	0.26	0.03	0.007	0.018	0.26	0.72
C (Pipe)	0.55	1.91	0.010	<0.005	0.37	0.03	0.24	0.28	0.01	0.05	0.005	0.02	0.19	0.45
C (ID)	0.049	1.69	0.012	<0.005	0.38	0.04	0.17	0.34	0.01	0.03	0.06	0.03	0.19	0.42
C (OD)	0.05	1.64	0.012	<0.005	0.38	0.04	0.16	0.35	0.01	0.03	0.06	0.03	0.19	0.41

Note: Some weld deposits contained Boron; others did not.

Note: $P_{cm} = C + Mn/20 + Mo/15 + Ni/60 + Cr/20 + V/10 + Cu/20 + Si/30 + 5B$

$CE_{IIV} = C + Mn/6 + (Cr + Mo + V) / 5 + (Cu + Ni) / 15$

1.1.3.2 Girth Welds

The first comprehensive welding development was conducted in 1990's for a joint industry project funded by Shell, BP, and BG. Very little detail is published about this work, although it is understood that general weldability was assessed for both SMAW and GMAW.

The feasibility study drew upon field experience with mechanized welding of X80 and concluded that X100 was weldable. A major concern with any new application of high strength steel is the potential for hydrogen assisted cracking, particularly given the traditional use of SMAW with cellulosic electrodes. The study concluded that cellulosic electrodes were generally unacceptable for X100 because crack free welds could not be produced even at preheat temperatures as high as 140°C. This shifted the focus to lower hydrogen potential alternatives (i.e. SMAW, FCAW-G and GMAW) [16]. Many commercially available and some experimental welding consumables were evaluated during this process. Since the low hydrogen SMAW consumables at the time lacked the operational characteristics necessary for pipe line applications and the one candidate FCAW-G consumables failed to achieve 690 MPa SMYS for the pipe, this left the GMAW process and a few solid wire electrodes as the most viable option for X100 girth welding.

Table 6 summarizes the mechanized narrow gap GMAW properties from this early work [4].

Table 6. GMAW performance from early trials

Consumable AWS A5.28 root / fill	All-Weld Tensile Test		Root CVN @ -10°C (Joules)			Weld CTOD @ 0°C 2BxB (mm)	Max. Cap Hardness, Hv10 3:00 & 9:00 o'clock		
	0.2% YS (MPa)	UTS (MPa)	Weld	Fusion Line	Fusion Line + 2mm		Weld	HAZ	Parent Metal
ER90S-G ER 100S-G	772, 728	842, 826	62-77	226-252	242-262	$\delta_m = 0.14$	309	317	297
ER90S-G ER110S-G	821, 850	921, 931	49-95	225-247	234-259	$\delta_m = 0.10$	360	333	294

The escalation in X100 development that began in 2000 also marked the beginning of major technical advancements in girth welding techniques. BP and TCPL sponsored development work at The Welding Engineering Research Centre (WERC) of Cranfield University [21] from 2000 to 2004. Cranfield worked closely with key contractors and manufacturers of welding equipment and consumables to extend the reach of the technical development effort. The initial challenge was to achieve the minimum weld metal target YS of 810 MPa in order to overmatch the parent pipe. It was found that the strength level could be readily achieved. However, the task of simultaneously attaining high elongation, Charpy toughness and CTOD together with acceptable hardness proved much more difficult to achieve.

In all, five welding consumable manufacturers supplied twenty-one different welding consumables for various purposes in support of this research, Table 7. Some of the consumables were used in multiple trials, not all of which produced satisfactory results. One consumable might produce acceptable results with one welding process variant but not with another. Note also that variation of process parameters within a single process or procedure also seemed to cause weld properties to vary.

Table 7. Welding consumable types, WERC Research

Root Passes	Fill & Cap	Additional Electrodes & Wires for Tie-ins & Repair
ER70S-6 ER90S-G E70C-6C, E70C-6M	ER100S-G ER100S-1 ER110S-G ER120S-1 ER120S-G	E11018-M E11018-G E111T1-GH4 E101T1-GH4
4 consumables from 3 suppliers	10 consumables from 6 suppliers	8 consumables from 3 suppliers

The initial objective was the development of welding process and practices that achieved the targeted 810 MPa minimum weld metal YS (i.e. achieve an adequate overmatch of parent pipe YS). The requisite ductility (tensile elongation %) and toughness (Charpy V-notch (CVN) and

crack tip opening diameter (CTOD)) proved more difficult to achieve. Procedures were developed for 5G position, narrow-gap welding with three variants of GMAW-P (i.e. single wire, dual wire, and tandem torch). Some conventional short-circuit GMAW, SMAW and FCAW-G was also investigated. However, the early trials with GMAW-P demonstrated it to have the highest potential for achieving the desired results.

The primary focus of the research was to better understand the factors influencing X100 girth weld mechanical properties under field conditions. Results were dependent upon a strong interaction between the welding consumable and the details of the welding process. In the end, procedures were qualified successfully with careful control of welding practice. Mechanical properties achieved, Table 8, and show that 810 MPa YS weld metal is achievable through careful process control. These tensile properties were achieved with generally acceptable levels of hardness and weld toughness.

Table 8. GMAW-P weld metal properties performance, WERC Research

Wires, Torches	All-Weld Tensile Test			Average Root CVN @ (Joules)				CTOD (mm) @ -10°C	Hv10
	0.2% YS (MPa)	UTS (MPa)	EL (%)	-20°C	-40°C	-60°C	-80°C		
Single	791-971	833-1017	10-20	93-226	55-191	58-203	39-165	0.08-0.27	267-375
Tandem	876-967	926-1004	12-18	93-189	55-191	58-173	39-194	0.13-0.24	319-376
Dual	793-884	840-949	12-19	146-190	81-197	60-197	38-161	0.14-0.37	255-360

Perhaps the most significant results of the WERC research were the development and refinement of the dual wire and tandem torch concepts, Figure 6. Weld metal properties targets were achieved through advances in welding process control. This was accomplished simultaneously with innovations in the tandem and dual torch processes that made possible significant increases in productivity and quality.

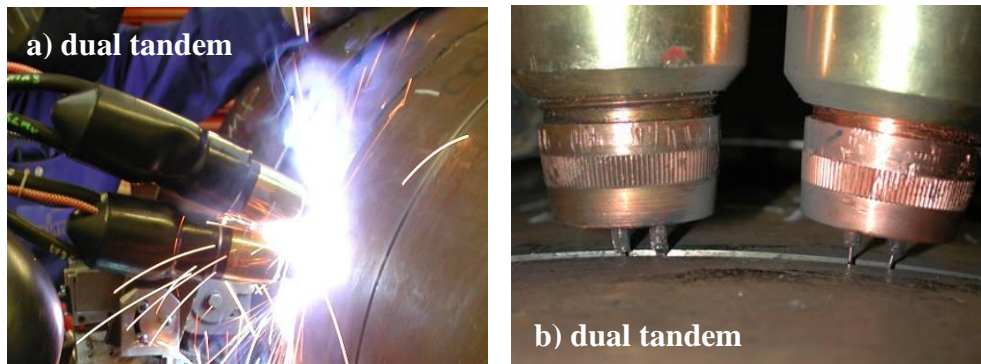


Figure 6. WERC dual tandem GMAW-P

The basic conclusions from this research were that X100 weld metal properties could be achieved with the desired levels of YS overmatch and toughness using all three GMAW-P process variants. However, welding consumables had to be selected carefully and a high level of welding process control was required. This resulted in relatively narrow ranges of operation for any individual procedure, which put considerable constraints on welding operations that have to produce defect free welds with the necessary properties. The welding procedures were highly

individual and could not be arbitrarily transferred from one contractor to another with any guarantee of success. Even a change of equipment or welding process variables by the same contractor was likely to result in deviation from desired properties in the weld metal and HAZ. As a result, the concept of essential welding variables extended well beyond the minimum requirements in several ways:

- **Welding Consumable Design** - Selection of welding consumable or alloy variant was welding process type related to a far greater extent than for lower grades of line pipe. The strong interaction between welding consumable and welding process variables suggested that a separate qualification should be run for each welding wire design.
- **Weld Joint Dimensions** - Minor changes in weld bevel profile had so much of an influence on the mechanical properties that machine prepared bevels having tight dimensional tolerances had to be stipulated for main-line welding.
- **Welding Power Source and Setup** - Because of the strong influence of the welding process on the weld metallurgy, welding power-source type/model, pulse mode and wave form must all be considered as essential variables.
- **Welding Torch Design** - In the case of dual wire, since complete electrical isolation is required between the contact tips in the single nozzle, specific torch designation, wave form and the synergic curves must also be considered unique to the procedure. Phasing between dual power sources, where they are used, also needs to be specified with some precision.

In short, pipeline girth welding became more of a precision business with X100 than for lower strength pipe grades. The Cranfield work established the feasibility of X100 mainline welding, subject to using the requisite process and materials controls. A great deal was learned regarding the interplay between welding consumable composition and welding process variables. However, a better understanding is still required of welding processes with respect to relevant welding process variables.

1.2 Industry Successes

After a period of development and full scale trial applications lasting over fifteen years, the modern X100 line pipe has gained acceptance with several major oil and gas operating companies and can be considered as on the threshold of commercial application. It remains some way off being a widely used grade of material but offers economic potential as the construction material for some long distance gas pipelines.

The level of industry wide collaboration required to bring the new technology to practical application in the field as it was being developed is a tremendous accomplishment. The WERC model where key commercial stakeholders, from fabricators to owners, are actively engaged as the research is unfolding was highly effective in this case. The evidence is in the success of the field trials in which the technology has been deployed to date.

The ground rules have been established for mainline welding and have been validated by several commercial fabricators. Furthermore, a foundation has been established for understanding the complexity of interactions between steel/weld composition and welding processes parameters.

1.3 Challenges Remaining

The near and long term challenges for large scale implementation of X100 are identified as unanswered technology gaps and priority needs in Hammond's State Of The Art Review [4]. The technology needs are somewhat different for onshore and offshore applications for X100. Onshore applications focus on the large diameter welded pipe used for transmission where most of the technology gaps relate to optimization of welding processes and materials. Since it is assumed that large diameter X100 will not find application in the offshore environment, priorities for offshore relate to seamless pipe of smaller diameter for risers and flow lines. While there is the potential for cross-over of welding technology, the performance assessment for offshore includes a greater emphasis on fatigue, corrosion fatigue, collapse testing, and electrochemical studies for a wide variety of environments. The basis for the assessment of onshore technology gaps is the expectation that the mechanical performance demands will be higher for X100 than for lower grade applications. Further, simple transfer of technologies from lower grade materials is not likely to achieve the desired performance for X100.

1.3.1 Pipe - Mill and Shop

There is still opportunity for further optimization of X100 pipe. While the steel development is considered to be mature, the technology gaps are associated with the welding operations.

The current practice of pipe manufacture using multiple wire SAW for the weld seam requires weld metal more highly alloyed than the pipe to achieve required strength. Lower alloy seam weld deposits need to be considered to minimize hardening where the pipe seams intersect the girth welds. It is acknowledged that lower welding heat inputs would be required to achieve necessary weld properties, which would compromise welding speed and the economics of pipe manufacture. The challenge is one of balancing the need for mechanical properties at a cost that enables the industry to take advantage of the higher pipe strength. There has been little activity on these issues to date because of the limited demand for X100 in practice.

Seam welding consumables tailored to particular steels and applications may become necessary with broader use of X100 in long distance pipe lines. While the initial application of this steel grade was for arctic applications, the possibility exists for its use in temperate or equatorial climate zones with widely diverse zones of habitation. A greater diversity in the ambient conditions will drive greater variability in requirements from project to project. As demand increases, the availability of tailored welding consumables is expected to become a larger challenge than it is at present.

The wide HAZ and associated line of local softening adjacent SAW seam welds is a topic of concern. While there is no evidence that softened HAZ have contributed to failures, the issue remains open because none of the installations to date have used the full potential of X100 in terms of design factor. Given the potential for strain localization and failure initiation in a softened HAZ, Hammond identifies mitigation of the effect of HAZ softening as a priority need. He views changes in welding process to be more viable than changes in base pipe chemical composition.

1.3.2 Pipe - In Line Fittings and Double Jointing

Technology developments that would benefit both mill and field operations for onshore applications involve fittings and double jointing. Development of welding methods and consumables for pipe fittings is viewed as a technology gap requiring attention. The lack of compatible in-line fittings is expected to inhibit the use of X100 as the alternative is simply the use of heavier wall, lower strength items resulting in potentially excessive thickness mismatches and awkward transition joints. In some cases, strength transition will need to be dealt with in regard to girth welds, in which case the weld joint designs will become very important.

Double jointing of X100 that achieves the consistent performance required of main line girth welds is a technology gap that will become a priority need with larger projects. To date, X100 has been supplied as single joints, which adequately served the small scale projects of the past ten to fifteen years. For larger projects, every pre-existing double joint obviates the need for a field weld and significantly accelerates pipe lay. The greatest benefit will be in the case of long distance pipe lines in remote locations.

1.3.3 Field Installation

The priority needs identified for field installation of X100 include welding processes and materials for tie-in and repair as well as for mainline welds. Mechanized GMAW is a proven and effective method for field welding of X100. To date, no other welding process has been able to achieve the same level or consistency of performance as GMAW in X100 pipe line applications. Even so, the ensuring the consistency of performance using GMAW still presents certain challenges.

First, improvements are needed in the ability to define and/or control the welding parameter envelope to ensure performance targets are satisfied consistently. Second, the ongoing effort to achieve higher levels of productivity with GMAW using advanced welding waveforms, tandem, and/or dual tandem variants of the process create an ongoing need for development of welding processes and materials to achieve the required balance of weld strength, ductility and toughness. Finally, development of tie-in and repair techniques/materials for X100 has received little attention to date. While the current technologies in the form SMAW and FCAW-G are able to deliver results from the standpoint of weld soundness, achieving the desired strength with adequate toughness remains a technology gap.

1.3.4 Performance Targets and Assessment Methods

Hammond indicates also that materials properties targets and assessment methods present certain challenges in the case of X100. Revision of the main pipeline design standards is needed to include X100 and similar higher strength pipe. Although the industry is moving increasingly towards strain based design, it must be recognized that each application is unique and that specifications may have to be customized to enhance specific mechanical characteristics necessary for the strain based design to succeed in the particular application. For X100, this will require detailed definition of the stress-strain curve and the use of tensile testing methods that are not normally used. For strain based designs in particular, more information is needed regarding uniform elongation and longitudinal pipe properties. While Hammond's comments seem to be focused on line pipe properties, the same challenge exists for target weld properties.

1.4 Opportunities

The historical review of X100 development provides a valuable basis for continuous improvement and innovation. However, the decisions taken and approaches used for demonstration projects of limited scope are not necessarily optimum in all fabrication environments, although they do form an essential basis from which to evolve. The practical application of the developing technologies in field trials of limited size and scope brought clarity to the assessment of the remaining challenges. The identification of priority research needs benefit also from Hammond's own experience as an active participant in the development and deployment of X100 technology during his career at BP. With the many challenges now so clearly presented, the current program of research had to focus on just a few key opportunities that would establish a new foundation for larger scale implementation of X100.

The themes that underlay nearly all of the challenges presented fall into two focus areas:

- Reconsider the design standards, materials properties targets and assessment methods in the context of strain based design for high strength pipelines.
- Understand the fundamental interactions between the welding process and the materials being welded well enough to effect improvements in productivity, quality and weld properties simultaneously. "Improvements in weld properties" can be translated to better results, more consistent results, and more predictable results.

In considering how best to approach either of these, it becomes apparent that they are interdependent. The standards by which improvements in quality and weld performance are measured depend upon the materials properties targets and assessment methods that are driven by the design standards. Any reevaluation of design standards requires at least a high level understanding of the performance levels possible from the materials that are available.

Accordingly, a consolidated program of research was viewed as having the best opportunity for resolving the fundamental technical issues in both focus areas, Figure 7.

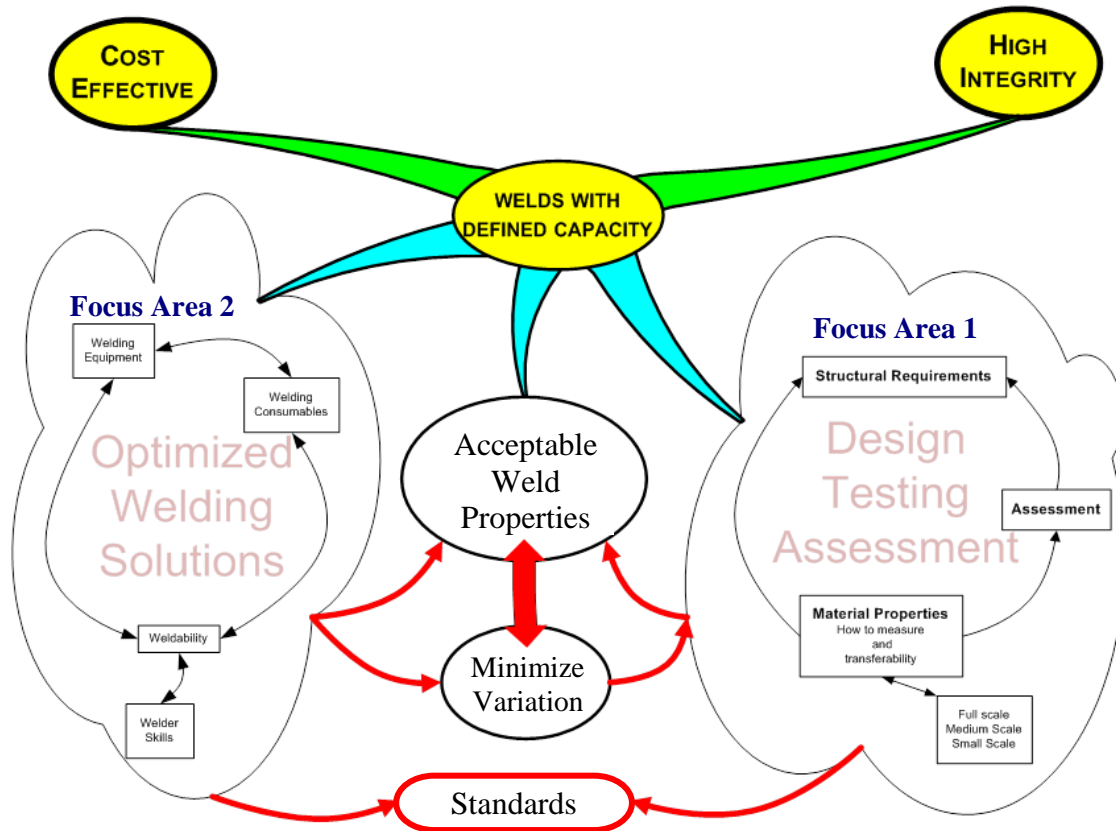


Figure 7. Consolidated Program Schematic

2 OBJECTIVES & OVERALL APPROACH

The research program was organized to address these two focus areas in a collaborative way with two technical teams - one for each focus area. Under the consolidated program, technical synergy was built into the work plans and technical results were shared across projects. At the highest level, the overriding objective was to develop solutions that would enable the pipe line industry to achieve a higher level of reliability and integrity in high strength pipeline girth welds with a specific emphasis on X100.

This report presents the methodology, major results and conclusions from the research focused on optimizing welding solutions for X100 line pipe steel, Focus Area 2. The project had four major objectives:

- Overview of available resources for welding high strength line pipe and the major challenges facing the industry;
- Fundamental understanding of the factors controlling attainment of high weld strength and toughness for the welding processes of greatest relevance to the industry;
- Functional understanding of how the controlling factors translate to essential welding variables and recommendations for appropriate ranges of these variables; and
- Method for achieving the necessary level of control over essential welding variables in practice.

The State of the Art Review [4], which formed the basis for the historical review in the previous section, is the overview indicated in the first objective. Also, it provided the necessary foundation for the remaining work. The early surveys and literature reviews provided baseline information on the current status of X100 materials and welding technology development.

This baseline information helped also to inform decisions about welding processes and materials that later became focal points for the project. For mainline welding of X100, the only viable welding process was GMAW-P starting with the conventional single wire process and extending the research to the dual torch variant of GMAW-P later in the project. Similarly, the baseline starting point for the welding consumable was the ER90S-G solid wire electrode that had been used for many of the field trials. This starting point allowed for comparison with published work as the methods for welding process monitoring and control were being developed. As work progressed, the range of weld metal chemical compositions expanded based on what the team learned regarding the relative importance of weld chemistry, welding process variables, and the interactions among them. In total, four different weld metal chemical composition ranges were included in the experiments. With regard to X100 pipe composition, the choices were based on availability of supply rather than on a deliberate decision to target a range of compositions. The team was fortunate that TCPL and CANMET were generous with the excess pipe remaining from completed projects. In total, three different pipe compositions were included in the experiments.

Developing a fundamental understanding of the factors controlling weld and HAZ properties required an assessment of materials variables, welding process variables, and their interactions. At a base level, the weld metal performance attributes of primary interest (i.e., strength, hardness and toughness) are controlled by chemical composition and the microstructures that form during the welding thermal cycles. For a given chemical composition, the final weld microstructure is determined by the thermal cycles. In the case of a HAZ, the starting microstructure before thermal cycling must also be considered. In turn, the welding thermal cycles are controlled by the welding process variables for a given size and thickness of pipe.

This situation is analogous to the interaction between the pipe mill processing parameters and the pipe steel composition that is illustrated in Figure 3. However, there is a major difference between the pipe mill example and the situation with welding variables. In the case of the pipe mill, the cause and effect relationship between the essential steel and pipe process parameters and the pipe performance is fairly well established. In the case of welding variables, the cause and effect relationship with performance is not as clear. Thus, determining which welding variables are really essential to performance is a challenge. This is evident in the limited comparison of requirements for essential welding variables presented in Table 9 for multiple pass GMAW with minimum toughness requirements. The standards selected for comparison are not necessarily the most current, but all have been used in the pipe line industry for standardization and control of GMAW.

Table 9. Comparison of Essential Welding Variables (multiple pass GMAW butt weld without supplementary filler and with toughness requirements)

Welding Variable	API 1104 [23]	ASME, Section IX [22]	CSA Z662-03 [24]	BS4515-1 [25] EN 288-9 [26]
Joint geometry	X		X	X
Base material alloy type	X (strength range)	X (alloy group)	X (CE range)	X (ladle chemistry & CE range)
Base material supply				X
Base material thickness	X (group)	X (range)	X (range)	X (range)
Pipe diameter			X (range)	X (range)
Filler metal alloy type	X (strength / class group)	X (alloy group)	X (CE range)	X (trade name)
Filler metal diameter		X	X	X (range)
Filler metal classification	X	X	X	X
Welding process	X	X	X	X
Welding position	X	X	X	X
Welding direction	X	X	X	X (range)
Current type & polarity	X	X	X	X
Manual vs. automatic			X	X
Transfer mode		X		X
Number of wires/electrodes		X		
Shielding gas type	X	X	X (range)	X
Shielding gas flow rate	X	X	X (range)	X
Pass sequence		X	X (range)	
Heat input		X (range)	X (range)	X
Wire feed speed / current			X (range)	X (range)
Travel speed	X (range)		X (range)	X (range)
Electrical stick out				X (range)
Voltage			X (range)	X (range)
Preheat temperature	X (range)	X (range)	X (range)	X (range)
Interpass temperature			X (range)	X (range)
Interpass time delay	X (Δt root-hot)			X (cellulosic)
Post weld heat treatment	X	X	X (range)	X
Removal of line up clamp				X
Number of welders			X	X

Notes:

1. An “X” indicates a welding variable identified by the code/standard to be essential to achieve a minimum acceptable standard for weld soundness and mechanical properties including toughness
2. Parentheses indicate how the variable is defined by the code/standard or if some variability within a range is permitted without having to requalify the welding procedure.
3. No entry in a cell indicates that the code does not indicate the variable to be essential.

Of the twenty-nine welding variables listed, less than half are considered in all four standards to be essential, as indicated by the shaded cells in Table 9. Even for those variables that are common to all four standards, there are differences in acceptable variation and methods of control. Considering many of the variables that directly influence the welding operation (e.g., voltage, current, electrical stick out, heat input), there is not as much alignment as one might expect. Basically, the treatment of essential welding variables is not consistent among four standards of relevance to the pipe line industry. Hammond’s conclusions [4] from the WERC research [21] further suggest that the traditional treatment of essential welding variables is actually insufficient for welding high strength steels, particularly with modern power sources

that enable a much wider range of welding process variables than recognized in the Table 9 examples. This comparison is not intended to raise doubt about existing installations of lower grade line pipe, but rather to highlight the need to reconsider the treatment of essential welding variables if higher levels of consistency and predictability in weld performance are necessary. The WERC research demonstrates this need for higher strength materials where a higher level of performance and predictability is required with materials (pipe and weld) that are more significantly influenced by welding thermal cycles.

The task then before the research team was to reassess essential welding variables for X100 by considering the relationships and interactions among:

- Mechanical performance, chemical composition and the microstructure,
- Microstructure, chemical composition and welding thermal cycles, and
- Thermal cycles and the welding process variables.

The team used a combination of experimental and analytical methods and drew upon their collective expertise in welding metallurgy, welding engineering, pipeline applications, and weld process monitoring and control in developing the detailed overall approach.

The team re-assessed as much available raw data as possible from the WERC research. [21] Their re-assessment was in the context of current knowledge about control of welding process parameters in GMAW-P and about how they are likely to influence welding thermal cycles. In addition, carefully monitored welds were produced and tested under specific welding conditions to provide more detailed information about the relationship among welding variables and the resulting thermal cycles in both weld metal and HAZ. These data were used to refine existing analytical thermal and microstructure models to improve their reliability for predicting self-consistent trends in weld and HAZ performance. Using these analytical models, it was possible to vary welding parameters numerically in a virtual environment to predict trends in behavior and focus subsequent experiments on the welding parameters expected to have the largest influence on weld performance. This methodology made it possible to quickly differentiate primary drivers of weld performance from secondary drivers and kept the time consuming experimental work focused where it would have the greatest impact. Subsequent experiments then varied these high value welding parameters systematically, first in test plates and then in pipe welds. Results from microstructure characterization, hardness, strength and toughness were then correlated with the welding variables under investigation.

In parallel with the welding process investigation, the metallographic characterizations performed for these welds provided a starting point for understanding the evolution of microstructures in X100 welds over a range of chemical compositions and a limited range of welding thermal cycles. The correlations between weld performance and microstructure for the different alloying strategies were more clearly established using thermal simulations techniques where performance over a wider range of cooling rates could be assessed under more controlled conditions.

The mechanical properties test results from all pipe welds were used by both technical teams. A large number of tensile, hardness, CVN, CTOD, low constraint fracture toughness, and curved

wide plate tests were conducted to support the work on Focus Area 1 (FA1)—Development of Test Protocols, Materials Properties Targets and Assessment Methods, as well as Focus Area 2 (FA2)—Essential Welding Variables. Conversely, the development of test protocols, most notably the tensile test protocol, and materials properties targets helped to refine and focus the experimental work throughout this project.

3 EXPERIMENTAL METHODS

Experiments were conducted in a sequence of increasing complexity, starting with the basic relationships for single torch welding and progressing to the more complex interactions. Initial experiments involved a single weld metal composition and a single base pipe composition. Additional chemical composition and welding process variants were introduced toward the end of the test program. There were three rounds of narrow gap pipe welds and an extensive series of narrow gap plate welds. Weld metal and HAZ microstructures were characterized and compared with microhardness measurements that mapped the entire weld cross-section. Weld properties and weld thermal cycles were measured in both weld metal and HAZ regions until the predictive capabilities of the thermal models were well established. The microstructure models evolved to the point where self-consistent trends in hardness as a function of welding parameter changes could be predicted with confidence, which helped economize on the total number of experiments needed. All of the pipe welds were produced by experienced welding contractors, CRC-Evans and Serimax-North America. All of the plate welds were produced by The Lincoln Electric Company.

Table 10 summarizes the overall test weld plan. Details can be found in the various topical reports for this project [27-31].

The microstructure characterization of the test welds was supplemented by two studies that used thermal simulation techniques to evaluate the evolution of microstructures for a range of chemical compositions and a broader range of weld cooling rates than could be efficiently evaluated with test welding. Microstructures were characterized and correlated with microhardness and CVN results [32, 33].

3.1 Materials, Welding Processes and Weld Process Monitoring

This section describes the welding operations and methods used to monitor the key process variables associated with the test plan outlined in Table 10. All welding operations were closely monitored and controlled to ensure a high level of integrity in the results. High speed data acquisition enabled weld process monitoring at the frequency necessary to assess the linkages with weld thermal cycles. Experimental methods were developed for monitoring HAZ and weld metal temperatures as welding progressed.

3.1.1 Materials & Weld Preparation

In general, X100 base material was in very short supply because there were no active projects involving X100. Procuring a heat of steel and pipe manufacture simply was not feasible from a budget or schedule perspective. Further, this approach would not have supported the need to

include multiple chemical composition variants in the study. Consequently, TransCanada PipeLines made available pipe material remaining from previous projects.

Table 10. Experimental Test Plan, Test Welds

Test Series	Test Conditions	Test ID	Purpose
First Round Pipe Welds	GMAW-P 1G rolled Single torch	807F	Baseline correlation between single torch welding variables and weld thermal cycles, HAZ and weld metal FA2 Microstructure characterization, HAZ and weld metal FA2 Microhardness traverses and full section maps FA2 Tensile, CVN and CTOD properties for single weld and pipe chemical composition FA1 and FA2 Low constraint fracture toughness, SE(B) and SE(T) FA1 Curved wide plate tests FA1
		807G	
		807H	
		807I	
		807J	
Second Round Pipe Welds	GMAW-P 5G Single torch	883G	Relate weld thermal cycles and True Heat Input to single torch welding variables and changes in clock position FA2 Microstructure characterization, HAZ and weld metal FA2 Microhardness traverses and full section maps FA2 Tensile, CVN and CTOD properties for single torch weld and pipe chemical composition FA1 and FA2
		883D	
	GMAW-P 1G rolled Dual torch	883E	Baseline correlation between dual torch welding variables and weld thermal cycles, HAZ and weld metal FA2 Microstructure characterization, HAZ and weld metal FA2 Microhardness traverses and full section maps FA2 Tensile, CVN and CTOD properties for single weld and pipe chemical composition FA1 and FA2 (results used by both projects in the program) Low constraint fracture toughness, SE(B) and SE(T) FA1 Curved wide plate tests FA1
		883F	
	GMAW-P 5G Dual torch	883H	Relate weld thermal cycles and True Heat Input to single torch welding variables and changes in clock position FA2 Microstructure characterization, HAZ and weld metal FA2 Microhardness traverses and full section maps FA2 Tensile, CVN and CTOD properties for single weld and pipe chemical composition FA1 and FA2
GMAW-P 1G rolled Single torch Dual torch Staggered passes	883J 883I	Assess the effect of reheating by subsequent passes on microstructure formation and its correlation to micro-hardness and thermal cycles FA2	
Flat Plate Welds	GMAW-P Single torch Dual torch 1G	29 total test welds	Introduce multiple weld metal chemical composition variants FA2 Verify the essential welding variables identified by virtual experiment FA2 Quantify relationship between essential welding variables and weld performance FA2 Establish control methodology to minimize weld performance variation for subsequent 5G pipe welds FA2
Third Round Pipe Welds	GMAW-P 5G Single torch Dual torch	952D	Contractor evaluation of proposed control methodology FA2 Two weld metal chemical composition variants plus two base metal chemical composition variants FA2
		952F	
GMAW 5G Single torch Dual torch	PRCI3 PRCI4 PRCI1 PRCI2	PRCI3	Mechanical properties correlated with chemical composition and proposed essential welding variables FA1 and FA2
		PRCI4	

The girth welding for the first two rounds was carried out on 914 mm (36 in.) diameter X100 pipes with a wall thickness of 19 mm (0.75 in.). The pipe ends were prepared using the standard

CRC-Evans joint preparation, Figure 8a. The contractor’s standard GMAW-P narrow gap procedures with 85% Ar - 15% CO₂ shielding gas were used. Pipe strings were fabricated using two 30 in. long pipe sections welded to a central 60 in. long section.

In order to get the most from the material available, pipe remaining after removal of the test specimens was cut and flattened for the twenty-nine flat plate welds used for the welding process variable experiments. These were prepared using the CRC Evans joint without the ID root pass bevel and offsets that varied according to the experimental test plan [27, 34, 35]. Because testing of the flat plate welds was limited to the passes above the root, eliminating this step helped keep the experimental work moving at the necessary pace.

The girth welding in the Round 3 was carried by two welding contractors with pipes from two different mills. These pipes were 1067 mm (42 in.) in diameter with a wall thickness of 14.1-14.3 mm (0.555-0.563 in.). Because the primary purpose for the Round 3 welds was contractor evaluation of the proposed welding control methodology, the contractors following Table 10 maintained their standard joint geometries and procedures as much as possible. Accordingly, CRC-Evans used their GMAW-P procedures for both single and dual torch welds with the joint geometry illustrated in Figure 8a, while Serimax used their GMAW procedures for both single and dual torch welds with the joint geometry illustrated in Figure 8b. The base pipe compositions are summarized in Table 11. All details are reported by Panday, Daniel, and Rajan [27, 34, 35].

Table 11. Chemical composition X100 base pipe

Test Series		%C	%Mn	%Si	%S	%P	%Ni	%Cr	%Mo	%Cu
Round 1&2 Plate Welds	X100-5	0.07	1.83	0.11	0.005	0.005	0.52	0.03	0.27	0.30
	Round 3	X100-A	0.06	1.88	0.30	0.001	0.012	0.23	0.03	0.23
	X100-B	0.05	1.87	0.16	<0.001	0.007	0.45	0.54	0.10	0.44
Gleeble HAZ Simulations	X100-2	0.06	1.80	0.09	0.001	0.002	0.63			
	X100-5	0.06	1.76	0.10	0.002	0.006	1.07			
	X100-4	0.05	1.87	0.19	0.001	0.007	1.54			
Test Series		%Al	%Nb	%Ti	%N	Ti/N	CE _{ITW}	P _{cm}	CEN	
Round 1&2 Plate Welds	X100-5	0.042	0.027	0.009	0.004	2.25	0.49	0.21	0.31	
	Round 3	X100-A	0.032	0.043	0.017	-	-	0.46	0.20	0.28
	X100-B	0.006	0.002	0.010	-	-	0.55	0.21	0.31	
Gleeble HAZ Simulations	X100-2	0.073			0.006	1.67	0.43	0.18	0.27	
	X100-5	0.079			0.002	4.80	0.47	0.20	0.28	
	X100-4	0.044			0.003	3.33	0.55	0.21	0.30	

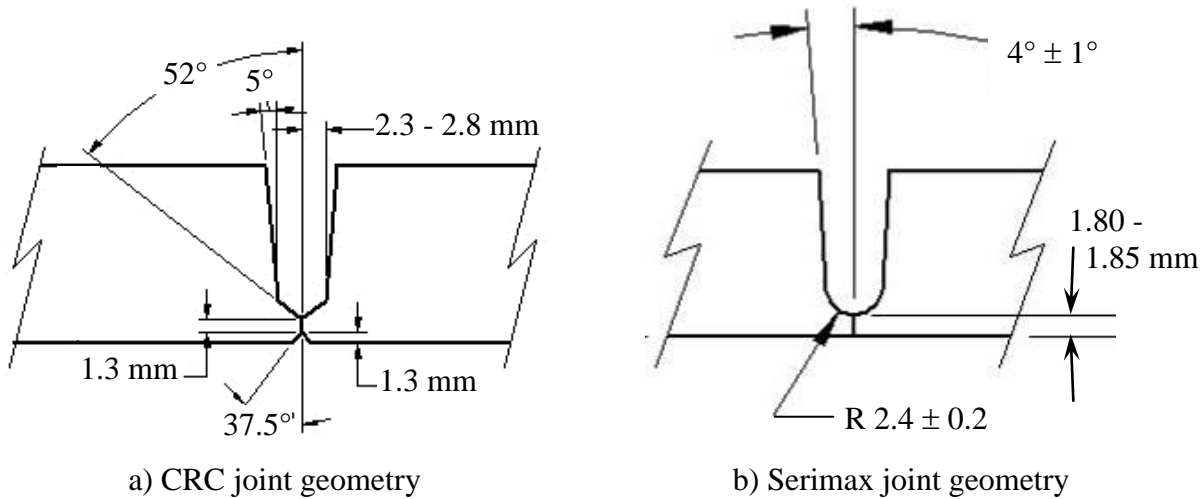


Figure 8. Schematic narrow groove pipe joints

All welds for Round 1 and 2 were produced using the same AWS A5.28 ER90S-G type welding wire electrode used for much of the GMAW on the X100 demonstration projects [4]. This allowed the initial experiments to focus on the influence of welding process variables on weld thermal cycles and weld performance. Therefore, baseline was established using Union NiMo80. Two prototype wire electrodes, PT1 and PT2, were introduced with the flat plate weld and Round 3 pipe welds for the specific purpose of assessing the influence of chemical composition on weld performance. The weld metal composition summary is presented in Table 12. The chemical composition ranges represent the full range of welding process variations employed. It is important to recognize that the Round 3 pipe welds represent both GMAW-P using 85% Ar - 15% CO₂ shielding gas and GMAW using 50% Ar - 50% CO₂ shielding gas.

3.1.2 Weld Process Monitoring

The WERC research suggested that the traditional approach to weld process monitoring and essential welding variables is insufficient for higher strength materials with the potential for greater performance variation with seemingly small shifts in process variables [4, 21]. Clearly, when it is suggested that the list of essential welding variables expand to include welding power-source type/model, pulse mode and wave form details, it becomes apparent that industry has not yet adequately addressed the root causes of mechanical performance variation in pipe welds. The implication is that greater precision if not accuracy is needed for monitoring those aspects of the welding process that influence performance. Consequently, all the welds were closely controlled and monitored to record all potentially relevant weld process data. Correlation with weld performance and the ultimate determination of the essential welding variables would not be possible without this.

The welding contractors employed their respective best practices for documenting in process welding data. These practices are based on code requirements, typical customer requests for additional information, and their respective quality assurance procedures. Contractor systems recorded the voltage, current, wire feed speed, and travel speed. In addition preheat temperatures, interpass temperatures, shielding gas types, and shielding gas flow rates were

controlled and documented. The sampling frequency for the electrical parameters was such that only Average Heat Input could be determined from this data.

Table 12. Chemical composition X100 weld metal

Test Series	Filler Metal ID	%C	%Mn	%Si	%S	%P	%Cr	%Ni	%Mo
Rounds 1 & 2	NiMo80	0.11	1.42-1.48	0.55-0.59	0.010-0.011	0.014	0.05-0.07	0.95-0.99	0.35-0.37
Flat Plate Welds	LA100	0.05-0.06	1.52-1.63	0.31-0.40	0.004-0.006	0.003-0.008	0.03-0.07	1.64-1.91	0.40-0.43
Round 3 & Flat Plate Welds	PT1	0.089-0.094	1.50-1.65	0.46-0.49	0.006-0.010	0.014-0.015	0.16-0.29	1.23-1.39	0.37-0.44
	PT2	0.093-0.097	1.60-1.69	0.57-0.66	0.008-0.010	0.009-0.013	0.22-0.40	1.54-1.95	0.45-0.51
Gleeble Weld Metal Simulations	LA90	0.084	1.6	0.41	0.005	0.006	0.02	0.15	0.40
	LA100	0.064	1.5	0.31	0.003	0.005	0.04	1.60	0.39
	NiMo80	0.100	1.4	0.49	0.009	0.012	0.05	0.89	0.34
	PT1	0.087	1.5	0.40	0.005	0.013	0.18	1.30	0.42
	PT2	0.097	1.6	0.59	0.008	0.012	0.30	1.80	0.49
Test Series	Filler Metal ID	%Cu	%Al	%Ti	%N	%O	CE _{IIW}	Pcm	CEN
Rounds 1 & 2	NiMo80	0.13-0.14	0.004-0.008	0.035-0.039	0.004	0.025-0.033	0.50-0.52	0.25-0.26	0.39-0.40
Flat Plate Welds	LA100	0.11-0.19	0.001-0.015	0.016-0.022	0.003-0.008	0.028-0.038	0.53-0.55	0.21-0.22	0.30-0.32
Round 3 & Flat Plate Welds	PT1	0.17-0.39	0.001-0.011	0.028-0.036	0.004-0.005	0.030-0.051	0.54-0.64	0.24-0.28	0.36-0.43
	PT2	0.15-0.25	0.002-0.004	0.024-0.037	0.004-0.005	0.029-0.042	0.59-0.71	0.26-0.30	0.40-0.49
Gleeble Weld Metal Simulations	LA90	0.25	0.008	0.008	0.004	0.044	0.46	0.22	0.32
	LA100	0.14	0.005	0.015	0.005	0.042	0.52	0.21	0.31
	NiMo80	0.16	0.007	0.029	0.007	0.045	0.48	0.24	0.36
	PT1	0.20	0.005	0.028	0.005	0.040	0.56	0.25	0.37
	PT2	0.18	0.005	0.022	0.007	0.032	0.65	0.28	0.44

High speed data acquisition supplemented the contractors' measurements. Electrical parameters were measured at a minimum frequency of 10 kHz to enable True Power and True Heat Input determination for all welds. Comparisons were made with Average Heat Input determined by contractor normal practices. Details are reported by Panday, Daniel and Rajan [27, 34].

3.1.2.1 Average Heat Input vs. True Heat Input

In this work, the primary focus was on the factors directly influencing the weld thermal cycles, which lead directly to a reassessment of the traditional approach to welding heat input. Because of the effect it has on the welding thermal cycle and ultimately the mechanical properties of the weld and the HAZ, an accurate representation is of utmost importance in achieving consistent and reliable weld performance. Traditional methods of calculating heat input involve the measuring of either average or RMS voltage and average or RMS current.

$$Heat\ Input_{AVG} = (Voltage_{AVGorRMS} * Amperage_{AVGorRMS}) * \left(\frac{60}{Travel\ Speed_{AVG}} \right)$$

Equation 1. Average Heat Input

While not necessarily accurate, this method produces relatively self-consistent results when the welding process used is traditional spray GMAW (GMAW-S). Even in the early days of GMAW-P, this method served well as a self-consistent indicator of heat input because the basic form of the pulsed wave form was consistent over a wide range of power sources. With modern welding power sources now able to create wide variation in pulsed wave forms and with fabricators taking advantage of that flexibility to achieve higher levels of productivity and weld quality, the use of average heat input has become less consistent and less accurate for short circuiting and pulsed GMAW due to the rapidly changing output of the power sources [27, 36].

Consequently, accurate assessment of heat input for GMAW-P became a priority for this project. Since it is not practical to define and control all possible aspects of the welding wave form that could possibly influence weld thermal cycle, a more practical solution was devised that focused on the true power output of the waveform. Considering that the first parenthetical term in Equation 1 is the average power, this approach is consistent with long standing industry practice with the advantage of improving both precision and accuracy.

The correct method for calculating the True Power, particularly with time-varying signals employed in many welding processes, is shown in Equation 2 [27, 37]. The True Energy™ is then represented two ways in Equation 3. In this way, a True Heat Input can be calculated, Equation 4, which represents an average over the period of travel or bead length of particular interest. In a 5G pipe weld, for example, one can average the True Heat Input over an entire weld pass or any part of the weld pass that is of interest.

$$True\ Power = \frac{1}{n} \sum_{i=1}^n (v_i * i_i)$$

Equation 2. True Power; accurate for any signal type

v = instantaneous voltage, i = instantaneous current

$$True\ Energy = \frac{1}{n} \sum_{i=1}^n (v_i * i_i * t_i) \quad \text{or} \quad True\ Energy = \left(\frac{1}{n} \sum_{i=1}^n (v_i * i_i) \right) * Arc\ Time$$

Equation 3. True Energy; accurate for any signal type

$$True\ Heat\ Input_{AVG} = \frac{True\ Power}{Travel\ Speed} \quad \text{or} \quad True\ Heat\ Input_{AVG} = \frac{True\ Energy}{Weld\ Bead\ Length}$$

Equation 4. True Heat Input calculated from True Power or True Energy

The American Society of Mechanical Engineers (ASME) very recently incorporated this approach as a more accurate alternative for GMAW-P and GMAW-S where relatively complex

welding wave forms often are employed. There are two methods presented for calculating True Heat Input, Equation 5 [22], as follows:

$$True\ Heat\ Input_{AVG} = True\ Power * \frac{Arc\ Time}{Weld\ Bead\ Length}$$

Equation 5(a). True Heat Input calculated from instantaneous power
True Heat Input=J/in (or J/mm), True Power=W, Arc Time=s, Weld Bead Length=in. (or mm)

$$True\ Heat\ Input_{AVG} = \frac{True\ Energy}{Weld\ Bead\ Length}$$

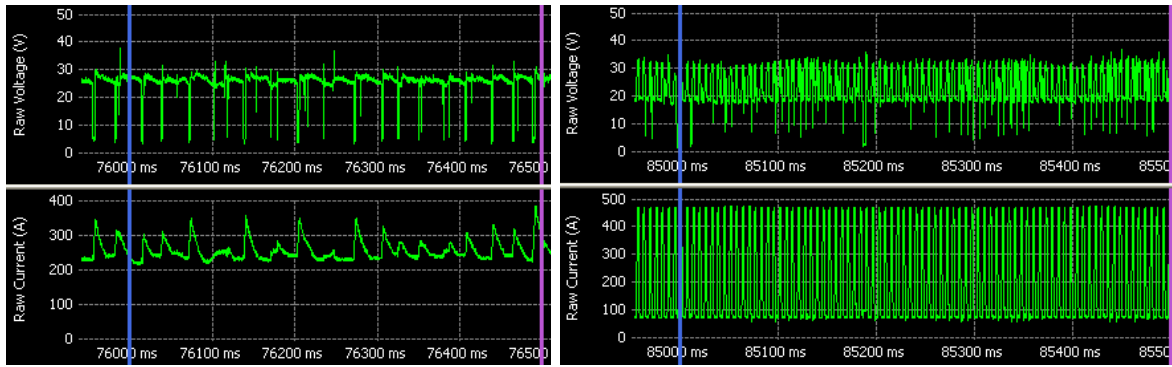
Equation 5(b). True Heat Input calculated from instantaneous energy
True Heat Input = J/in (or J/mm), True EnergyTM = J, Weld Bead Length = in. (or mm)

These methods can be used for any signal type including constant DC signals, but must be used on time-varying signals to get an accurate result. Voltage and current are still multiplied together, but on an instantaneous basis at high enough frequency to capture the time varying nature of the waveform in use.

To illustrate the differences between the traditional average power approach and the True Power approach, consider the results summarized in Table 13 for the examples illustrated in Figure 9. For “constant” DC, the error for average power is 0.1%. However, for pulsed current, the error is over 15%. These errors translate directly into calculated heat inputs. Different welding power sources or different types of GMAW-P waveforms can produce accuracy error from 10% to 20%. The degree of inaccuracy is not a fixed amount; different welding power sources and/or different welding waveforms will produce different amounts of error. The welding processes used in this study were generally in the range of 8% to 22% error [34]. By using the True Power method, an accurate determination of heat input is possible without having to control individual wave form attributes or the power source type/model.

Table 13. Comparison of Average and True Power, "constant" and pulsed DC current

Welding Output	Average			True Power (W)	% Difference Average from True Power
	Voltage	Current (A)	Power (W)		
Figure 9(a) “constant” DC	25.25	252.65	6384.02	6384.02	-0.1%
Figure 9(b) pulsed current	24.01	201.15	4672.71	5505.75	-15.1%



(a) GMAW “constant” DC output
(PRCI 1, Side 2, Fill Pass 1)

(b) GMAW-P pulsed current output
(952-D, Side 1, Fill Pass 1)

Figure 9. Comparison of "constant" and pulsed current welding outputs

3.1.3 Thermal Cycle Measurements

After having determined an appropriate means for monitoring the welding process, it was necessary to establish baseline data for the welding thermal cycles associated with the welding process choices. The first step was to develop a reliable means to measure the thermal histories in the weld metal and HAZ.

Thermal histories for single torch GMAW-P were established during Round 1 with thermocouples located within 1 to 2 mm of the fusion boundary in the HAZ associated with each weld pass. Placement from the pipe ID is illustrated in Figure 10. The detailed development of test equipment, methods and procedures to accomplish this work has been reported by Panday, Daniel and Chen [27, 38]. The resulting “grid” of thermocouples in the HAZ allowed for continuous monitoring of temperature adjacent each weld pass as welding progressed from start to finish. Weld metal cooling curves for each weld pass were recorded with thermocouples plunged into the trailing edge of the weld pool behind the welding arc. Accordingly, thermal histories were recorded for nearly all of the locations targeted, which made initial validation of the thermal models possible.

As the complexity of the welding process increased with each round of weld tests, additional thermal measurements were made to provide for experimental validation of predictive models for dual torch GMAW-P and 5G test conditions. In relatively short order, the reliability of the thermal models was established and no further verification or validation was considered necessary.

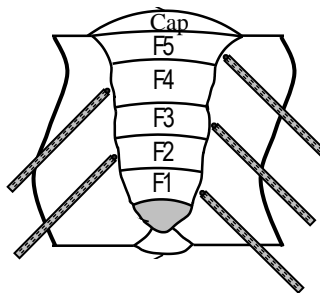


Figure 10 Cross-sectional view of thermocouple placement
Thermocouples are spaced apart 1-1¼ in. along the weld length.

3.2 Material Characterization

Baseline material characterization was conducted for both weld metal and HAZ from the various experimental pipe welds. Thermal simulation techniques were used to supplement the evaluation of baseline pipe welds with a more systematic assessment of the influence of weld cooling rates and chemical compositions. Microstructure comparisons were made between simulated weld metal and HAZ and the corresponding regions in experimental welds. Metallographic examination procedures were consistent for both types of experiments. All specimens were mounted in epoxy resin and further ground and subsequently polished using series of diamond suspensions and a final polish with a 0.05 μm colloidal silica suspension. All specimens were etched in 3% Nital solution for examination and evaluation using light optical microscopy.

3.2.1 Welds

Optical microscopy, hardness surveys and detailed microhardness mapping were used to characterize both pipe and plate welds fabricated with a single pipe chemical composition and a single weld metal. Weld metal and HAZ regions were examined with the purpose of identifying trends associated with the change from single to dual torch GMAW-P and identifying microstructure features that would help to explain both the level and consistency of weld properties. Standardizing on a single pipe composition and welding consumable made it possible to relate differences in microstructure to the welding conditions and weld pass sequence. Significant variation in the microstructure constituents was observed in both the weld metal and the HAZ, particularly at the faster cooling rates typical of narrow gap GMAW-P pipeline girth welds. The magnitude of that variation was most apparent by considering both the metallographic features and the microhardness patterns together. Examples are illustrated in Figure 11 and Figure 12 for single and dual torch welds, respectively. In many cases, the microhardness maps provided indication of the regions to be investigated further at higher magnification. Detailed procedures and microstructure observation have been reported by Gianetto [28].

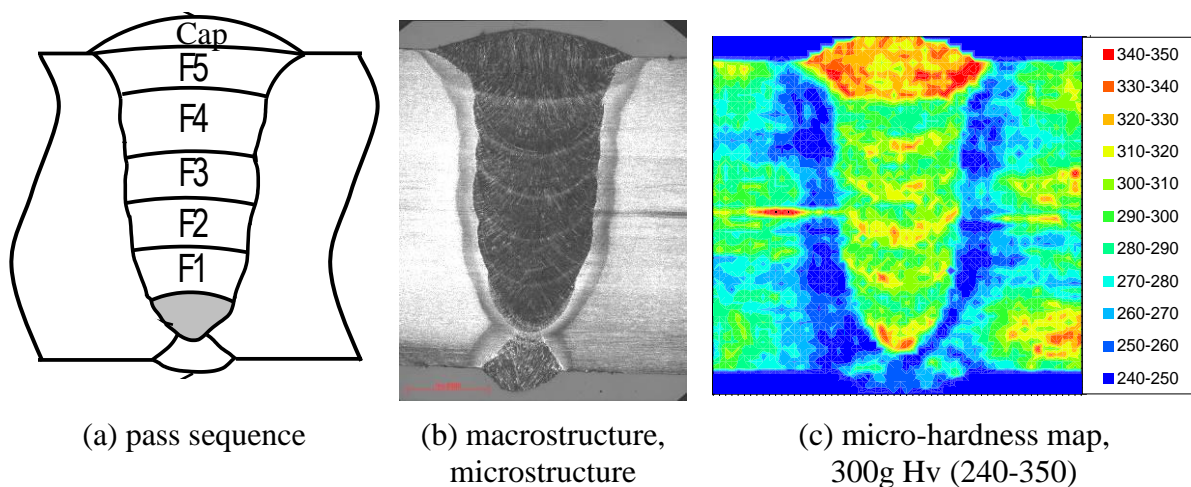


Figure 11. Material characterization, single torch example (807)

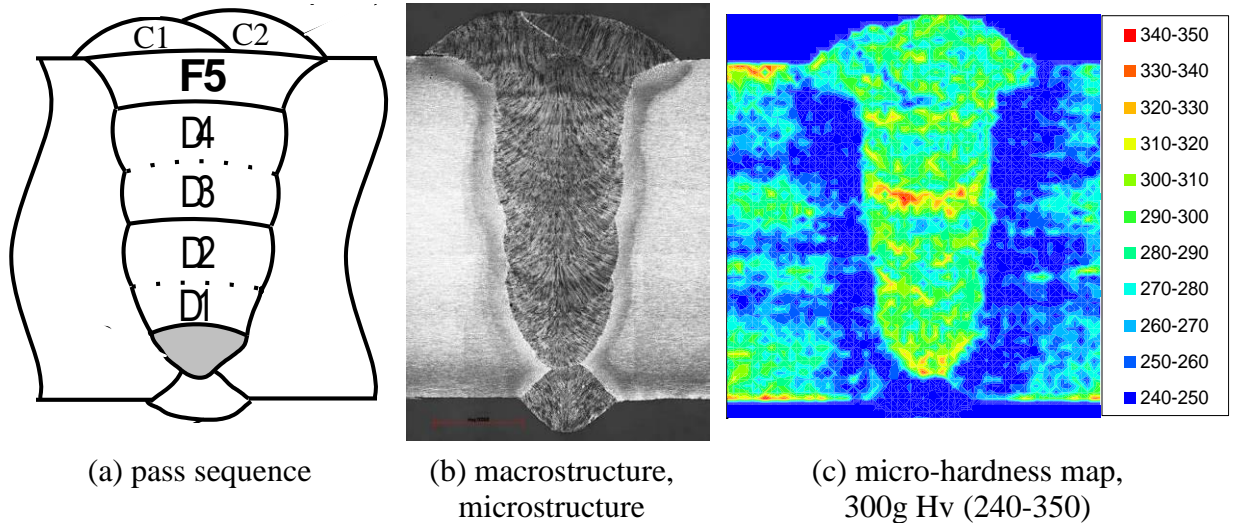


Figure 12. Material characterization, dual torch example (883)

The work on full pipe welds was supplemented by a series of staggered bead pipe welds using the same pipe steel. The staggered bead pipe welds provided a systematic assessment of microstructure development with the deposition of successive weld beads. While the microstructure and hardness characterization of full pipe welds revealed significant short range variation in both weld metal and HAZ regions that helps to establish baseline and trends with cooling rates, the staggered bead welds were more useful in revealing the evolution of microstructures from the as-deposited condition through to the reheated condition created by deposition of additional weld metal either by a subsequent weld pass or by the second torch in the dual torch process. Figure 13 is an example of micro-hardness results for a staggered dual torch weld.

The staggered welds proved useful for developing a better understanding of the evolution of microstructure with successive weld passes and clearly show the range of weld bead thicknesses, the relative distributions of AD and RH weld metal as well as the change weld metal and HAZ microhardness that occur with deposition of successive weld passes due to the influence of reheating and tempering.

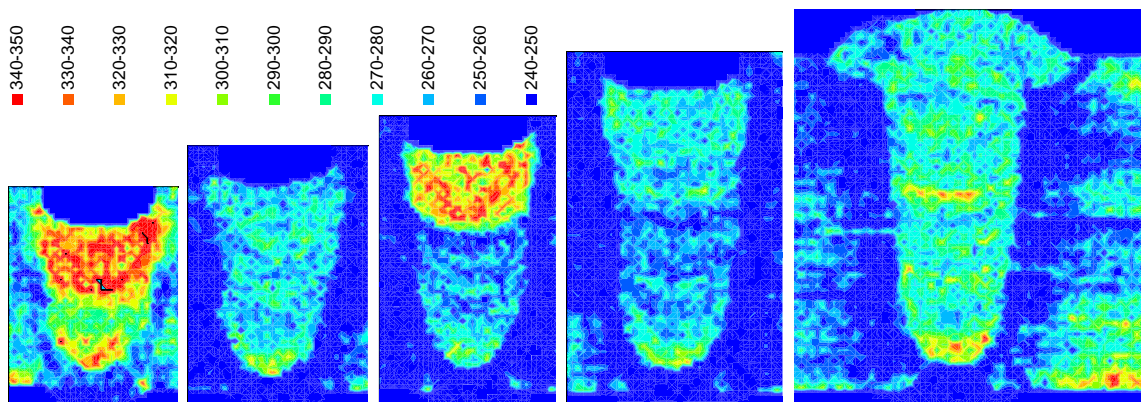


Figure 13. Typical micro-hardness map for staggered weld, 300g Hv (883)

Microstructure constituents are very much the same in both the AD and RH regions of the weld metal. They differed only in that the overall grain structure is equiaxed in the RH regions and columnar in the AW regions. The complex microstructures formed in the single torch pipe welds consisted of mixed martensite/bainite/ferrite with higher hardness in AD compared to RH regions. The cyclic nature of the hardness profile through thickness results from reheating and tempering of the underlying weld metal by each successive pass (e.g. Figure 11). In the dual torch pipe welds, higher hardness of the lead wire deposit is significantly altered by deposition of the trail wire (e.g. Figure 13).

Three HAZ structures/regions formed in the multiple pass pipe welds, which included the grain coarsened (GC) HAZ, super-critically reheated (SCR) GHAZ and intercritically reheated (ICR) GHAZ. The microstructures formed within these regions are consistent with the cyclic variation in through-thickness hardness and resultant constituent phases formed within the respective regions [28]. The finer details in the weld microstructures were often difficult to discern using optical methods. This was even more apparent for the HAZ microstructures than the weld metal microstructures.

Significant variation in the complex mixed bainite/martensite occurred in both the weld metal and HAZ regions, particularly at the faster cooling rates typical of narrow gap GMAW-P pipeline girth welds. As is evident in the limited data presented here, Figure 11-Figure 13, microstructure variation occurred over very short distances, making possible only general assessment of potential influence on overall weld performance. Therefore, thermal simulation methods were used to develop a more direct connection between microstructure and weld performance.

3.2.2 Thermal Simulations

Thermal simulation techniques were used to supplement the evaluation of baseline pipe welds with a more systematic assessment of weld cooling rates and chemical compositions on microstructure, hardness, and impact toughness. Gleeble® 2000 and Gleeble® 3800 were used for the thermal simulations. Full details are reported by Gianetto et al for weld metal [32] and HAZ [33] experiments and analyses.

For the weld metal investigation, the continuous cooling transformation (CCT) behavior was determined and correlated with microhardness at various cooling times, $\Delta t_{800-500}$, from 1.9 to 50 s. They provide a clearer indication than the pipe weld characterizations of the range of the fine-scale predominantly displacive martensite, bainite and acicular ferrite transformations that are likely to form in single and selected dual torch welds. In addition, weld metal thermal simulation was used to create specimens of relatively uniform microstructure for subsequent CVN impact testing at -20°C.

The weld metal CCT diagrams were developed for a total of five chemical compositions. Overall alloy levels ranged from 0.46 to 0.65 CE_{IW} and 0.22 to 0.28 P_{cm}, Table 12. Four of these chemical compositions are considered relevant for X100. The LA90 was not expected to achieve X100 level strength, but did serve as an experimental control being a relatively simple C-Mn-Si-Mo alloy system. Marked changes in microstructure and hardness were observed for relatively small increases in cooling time for all five compositions. The CVN results indicate the general

trend to lower toughness with increasing alloy content and fast cooling rates (i.e. short cooling time), where higher hardness microstructures are more likely to be formed [32]. The improvement in impact energies with slower cooling rates (i.e. longer cooling time) is consistent with the formation of AF dominated microstructures.

These results are consistent with what is expected for low alloy steel weld metal in general. What is different about the information from these thermal simulation experiments is the ability to correlate the microstructure with the hardness and -20°C CVN toughness over a range of cooling times relevant in GMAW-P pipe welds. Figure 14 and Table 14 illustrate this for NiMo80 at 0.48 CE_{IW} and PT1 at 0.56 CE_{IW}, for example. Consider the region from 3.5 to 20 s Δt₈₀₀₋₅₀₀. At 3.5 s, both alloys achieve nominally the same hardness with nominally the same microstructure. As the cooling time increases, average hardness is maintained at higher levels with PT1 at 0.56 CE_{IW} through 20 s with little difference in average -20°C CVN. Understanding the balance among alloy level, cooling time and relative performance will lead to more informed decisions regarding the optimum welding procedures for a given material, or the optimum material choice given the welding procedures.

Table 14. Influence of cooling time and alloy level on hardness and impact toughness

Δt ₈₀₀₋₅₀₀ (s)	NiMo80, CE _{IW} = 0.48			PT1, CE _{IW} = 0.56		
	Average Hv-300g	Average -20°C CVN		Average Hv-300g	Average -20°C CVN	
		J	% shear		J	% shear
5	334	67	80	364	63	72
10	281	116	88	309	112	85
20	260	164	96	275	156	90

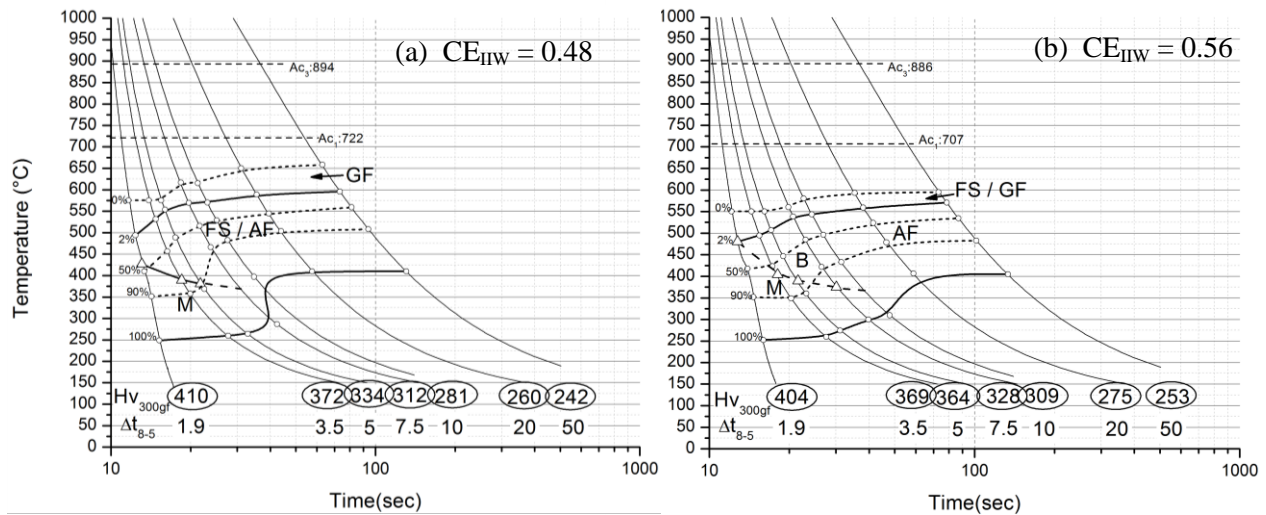


Figure 14. CCT behavior, (a) NiMo80 and (b) PT1

The HAZ investigation involved a number of thermal simulations scenarios. Single cycle thermal cycles over range of cooling times (Δt₈₀₀₋₅₀₀ ~1 to 50s) simulating the GCHAZ regions were correlated with microhardness used to develop CCT diagrams for the GCHAZ. In addition, thermal simulation was used to create specimens of relatively uniform microstructure for

subsequent development of full CVN transition curves. These thermal simulations represented GCHAZ at two cooling times, 6 and 10 s, ICR-GCHAZ (10% Ac₃) at 12 s, and a not totally reheated (NTR) ICR-GCHAZ at 12 s with interrupted cooling cycle typical of dual torch welds.

The HAZ CCT diagrams were developed for a total of three X100 chemical compositions. Overall alloy levels ranged from 0.43 to 0.55 CE_{IW} and 0.18 to 0.21 P_{cm}, Table 11. There are significant differences in microstructure and performance for the limited range of pipe steels investigated. GCHAZ microstructures with varying proportions of lath martensite and different morphologies of bainite were found with increasing cooling time. These changes and the overall coarsening of the transformed microstructures are consistent with the corresponding reduction in hardness observed for a given the pipe steel composition.

A performance comparison of X100-4 with X100-5 is presented in Table 15 and Figure 15. The pipe steel (X100-4) with the highest hardenability resulting from additions of Ni, Cr (instead of Mo), Cu and lower Nb with optimum Ti and N exhibited the best pipe steel and HAZ toughness. Steel X100-4 (CE = 0.55 and P_{cm} = 0.21) also exhibited the highest potential to maintain hardness as cooling times increases and achieved the highest HAZ toughness. This can be accounted for based on the formation of more favorable lath martensite with fine bainite microstructures as a result of the suppression of the $\gamma \rightarrow \alpha$ to lower temperatures and more gradual decrease in hardness that occurred. The lower toughness exhibited by the X100-5 GCHAZ regions is attributable to the formation of higher proportions of coarse bainite, which provide lower resistance to crack propagation as evidence by the large cleavage facets found on the fracture surfaces.

The further reduction in toughness for the ICRGCHAZ region was believed to be caused by formation of secondary phases at the prior austenite grain boundaries. The slightly better toughness of the NTR-ICR-GCHAZ relative to the ICRGCHAZ is related to the formation of greater proportions of austenite and subsequent transformation as a result of the longer cooling time $\Delta t_{800-500} = 12$ s. While it was possible to show clear trends in terms of transformation and notch toughness behaviors for the pipe steels investigated, detailed characterization of the secondary phases believed to be playing a role in the ICR-GCHAZ requires more advanced metallographic methods than employed for this work.

Even though the HAZ characterization is not as conclusive as the weld metal example presented previously, it is possible to use the information in a similar manner. The tendency for HAZ softening and toughness reduction is a function of thermal cycle controlled by welding practice. The steel composition can be assessed in relative terms using CCT for practical problem solving.

Table 15. CVN summary for X100-5 and X100-4

Material Condition	X100-5				X100-4			
	CVN @ -60°C		CVN @ -20°C		CVN @ -60°C		CVN @ -20°C	
	J	% shear						
Pipe Steel	223-246	88-100	278-300	100	262-309	100	312-319	100
GHAZ-6s	12-20	4	45-233	17-74	35-114	31-62	237-278	81-100
GHAZ-10s	13-34	0-6	34-114	-	32-98	17-33	229-273	77-88
ICR-GHAZ	16	6	41-52	21	27-58	17-27	222-248	78-82
NTR-ICR-GHAZ	25-46	11-17	84-93	43	-	-	-	-

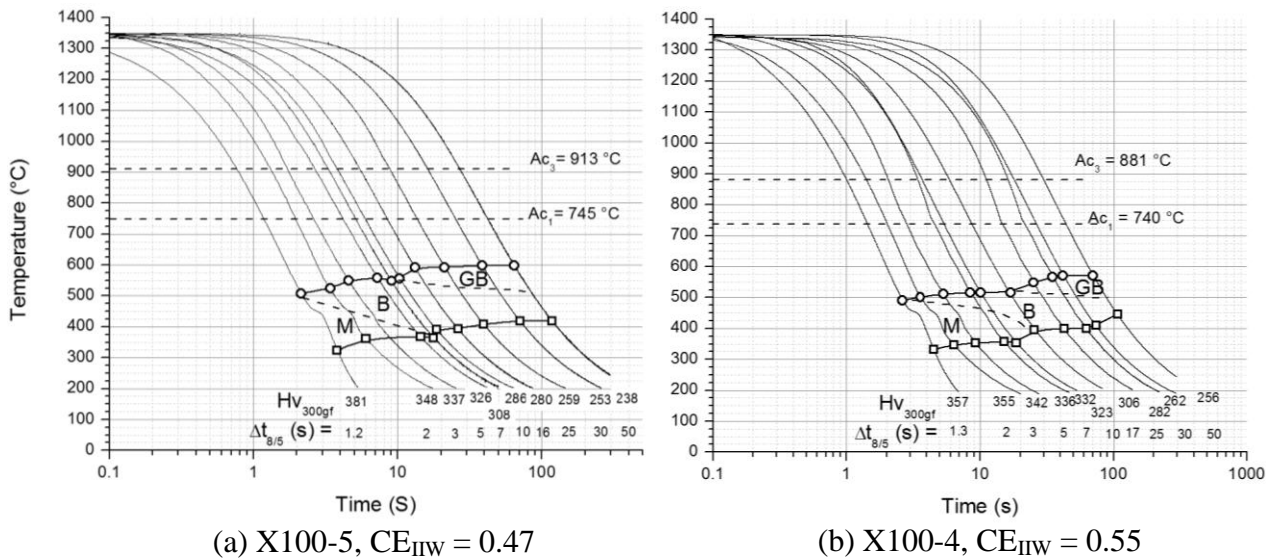


Figure 15. CCT behavior, (a) X100-5 and (b) X100-4

3.3 Mechanical Testing

A number of mechanical tests were conducted for the welded assemblies produced in this program. A baseline was established with some of the standardized tests normally required by codes and standards for qualification. For the base pipe, these included both round and full thickness strap tensile tests as well as CVN tests. For the welds from Round 1, these included round all-weld tensile, CVN and conventional CTOD single edged notched bending (SE(B)) tests. The CVN and CTOD SE(B) were conducted with notches placed through thickness in both weld metal and HAZ. This baseline was supplemented by the development and application of non-standardized testing techniques, which was an integral part of the program and led to more in depth understanding of the baseline welds. For both base pipe and welds, additional CVN tests were conducted to develop full transition curves. For welds, additional tensile tests were conducted using a strip specimen configuration. Also, for welds, additional fracture toughness evaluations were conducted, including the development of J resistance curves for conventional CTOD and some low-constraint (SE(T)) and single edge-notched bend (SE(B)) tests. All of these small scale tests were supplemented by a series of curved wide plate tests. These tests

served different purposes for the two focus areas in the program. Many of the tests conducted were for the purpose of developing assessment methods (FA1) and were not directly applicable to the development of welding solutions (FA2). While the details are reported by Gianetto [29], Table 16 presents a summary of the small scale tests and their applicability to each focus area.

Table 16. Small scale test summary

Material	Test Description	Purpose and Applicability
Pipe	Longitudinal tensile round & full thickness strap	Establish baseline pipe properties <i>FA1</i> Development of assessment methods <i>FA1</i>
	Charpy V-notch	
Weld Metal	All weld tensile - round	Establish baseline weld properties <i>FA1 & FA2</i> Development of testing protocols and assessment methods <i>FA1</i>
	All weld tensile - strip	
	Charpy V-notch	
	CTOD	Assess influence of welding variables on performance <i>FA2</i>
	J-SE(B)	
	J-R SE(T)	Development of assessment methods <i>FA1</i> Correlations with larger scale test results <i>FA1</i>
	Microhardness - traverses & maps	Assess variation in properties, correlations with microstructure, and facilitate the assessment of welding variables on performance <i>FA2</i>
HAZ	Charpy V-notch	Establish baseline weld properties <i>FA1 & FA2</i> Development of assessment methods <i>FA1</i> Assess influence of welding variables on performance <i>FA2</i>
	CTOD	
	J- SE(B)	Development of assessment methods <i>FA1</i>
	J-R SE(T)	Establish correlations with larger scale (CWP) test results <i>FA1</i>
	Microhardness - traverses & maps	Assess variation in properties, correlations with microstructure, and facilitate the assessment of welding variables on performance <i>FA2</i>

Two types of tensile specimens were used for characterization of weld metal properties: the conventional round bar and a strip specimen. Measurements using both types of specimens were made for the Round 1 welds only. By Rounds 2 and 3, the strip tensile had become the standard. The reason is simply that the welds are not homogenous and a small round specimen in a narrow gap weld does not represent the tensile properties of the weld metal as a whole. Figure 16 illustrates the variability in weld macrostructure and hardness, particularly in the through thickness direction. Hardness being a general indicator of tensile strength, it is clear that measured strength will vary significantly specimen location. Various specimen locations in a narrow gap weld cross-section are illustrated in Figure 17. At the typical location used for welding material and procedure qualifications, Figure 17(a), the small reduced section is sampling a very small fraction of the weld metal. Using two round tensile specimens, as in Figure 17(b), improves the coverage of the weld cross-section. The strip configuration in Figure 17(c) samples the largest amount of weld metal. Consequently, the strip provides the best measure of the overall narrow gap weld metal strength.

CVN specimens also were located differently from a standard qualification test situation, which requires a mid thickness location similar to the round tensile in Figure 18(a). Since the focus of this work was to assess the influence of welding variables on performance, most of the specimens were shifted toward the OD to minimize any possible influence from the root and hot

passes, Figure 17(e). Some weld metal specimens were shifted to the inside diameter (ID), incorporating root, hot, and fill passes, Figure 17(f). All fracture toughness test specimens were full thickness and prepared according to their respective standards.

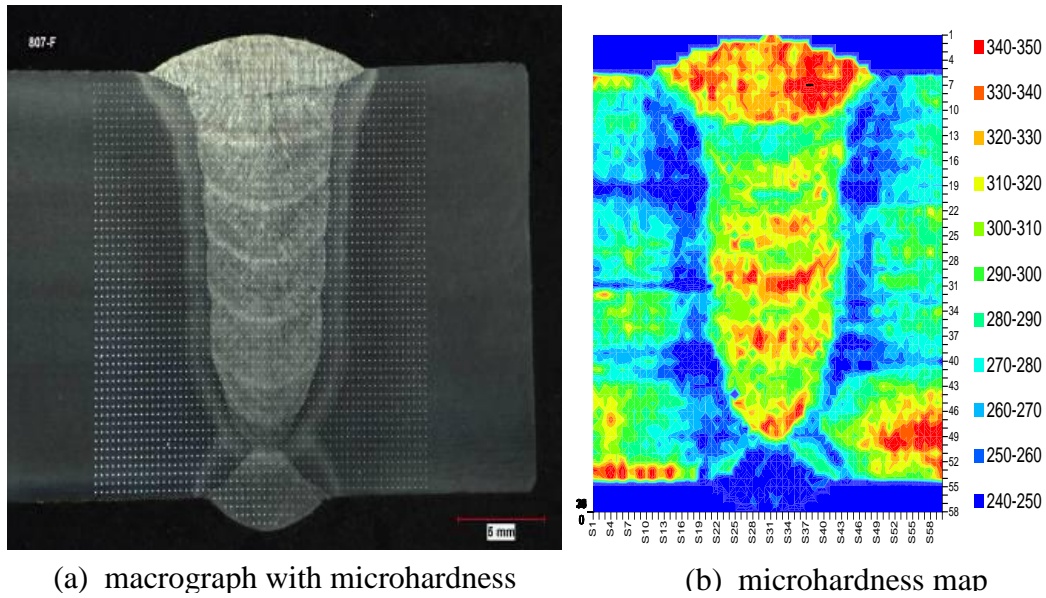


Figure 16. Narrow gap weld cross-section and hardness distribution (807J)

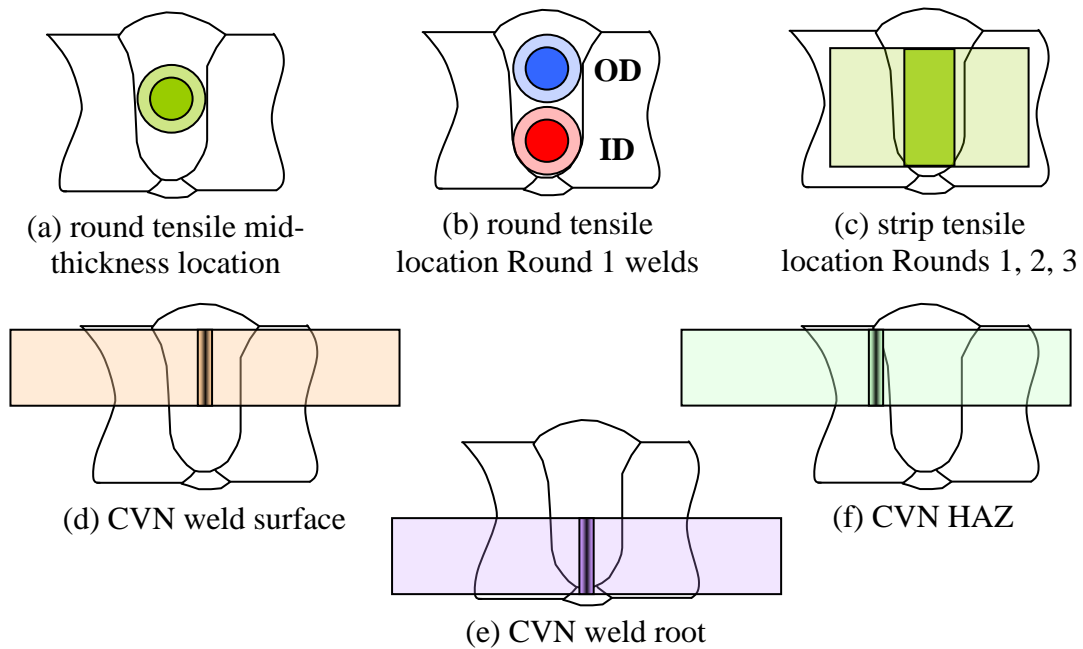


Figure 17. Schematic, mechanical properties specimen locations
(Darker centers indicate tensile specimen reduced section and CVN notches.)

4 ANALYTICAL METHODS

Analytical methods were extremely important to this project on several levels. A self-consistent means of predicting trends in weld and HAZ performance was an essential element of the experimental approach. This was accomplished through the development of numerical methods [38, 39]. In addition, the process of continually refining the analytical methods at each step in the project encouraged greater rigor in the analysis of empirical results. Specifically, the analytical methods were applied to:

- 1) Virtual experiments to assist identifying the welding essential variables;
- 2) Thermal simulations for dual torch GMAW to assist weld procedure designs; and
- 3) Cooling rate calculations for dual torch GMAW to provide information for design of the thermal simulation experiments.

Welding is a relatively complex process and is particularly challenging when considered on a fundamental level. The welding of micro-alloyed, thermo-mechanically processed, high strength steels such as X100 poses even greater challenges as a result of the demands imposed by modern pipeline design. Expectations for performance and consistency are higher than for lower strength grades. Yet, the mechanical properties of both weld metal and HAZ are more sensitive to variations in welding conditions than for those lower grade steels. The high-productivity multi-wire GMAW process variants, such as tandem-wire and dual-torch, introduce new welding variables and further complicate the relationship between weld properties and welding parameters.

For any given chemical composition, weld and HAZ microstructures that control performance are dependent on the thermal cycles experienced during the welding process. In order to understand the interactions of welding parameters, including those new variables associated with the multi-wire GMAW variants, and their influence on the final weld mechanical properties, an accurate knowledge of the thermal cycles in the weld metal and its HAZ is necessary. While there have been many analytical, empirical, and numerical solutions for single-torch welding processes, a very limited number of thermal models for multi-wire GMAW processes were developed.

The modeling effort undertaken in this project focused on GMAW-P process and its multi-wire variants in mainline welding, although the methodology easily can be expanded and implemented to cover other arc welding processes. The overall objective of the modeling effort was to identify and evaluate essential welding variables by analyzing, correlating and predicting the mechanical properties of the weld and HAZ. In the integrated thermal-microstructure model, Figure 18, given the welding process and its welding parameters, the thermal model calculates the thermal cycles first. Subsequently, the thermal cycle results are used by the microstructure model in the simulation of microstructure evolution.

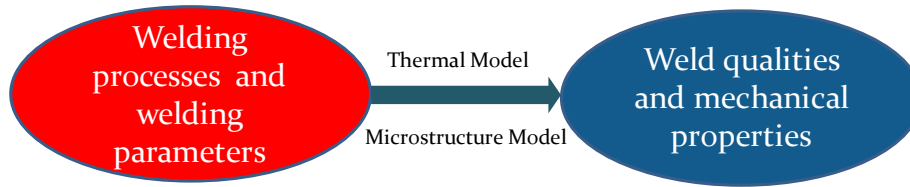


Figure 18. An integrated thermal-microstructure model for welding simulation

4.1 Thermal Cycle Predictions

4.1.1 Methodology

In any thermal model for welding processes, two components are critical: 1) the numerical treatment of the weld metal in its volume, geometry, and welding sequence; and 2) the heat flux imposed by the electrode onto the weld metal region. These two core issues are briefly described below.

4.1.1.1 Multi-Pass Girth Weld Partition

When modeling a multi-pass girth weld, an important part of the procedure is the partitioning of the girth weld according to the heat inputs associated with each welding pass. Since it is impossible to precisely locate the boundaries between successive passes, an accurate correlation between the welding parameters, in particular, the heat input, and the volume of weld metal, was developed and implemented. Given the welding parameters associated with each welding pass, the model calculates the volume of the weld metal for the pass. For the whole girth weld, its partition is made based on the calculated volumes of each pass.

4.1.1.2 Heat Flux Formulation

The thermal model procedure was based on the two-dimensional version of the Goldak model [40]. At its core is a new formulation for the application of the heat flux to the weld region. The current practice of the axis-symmetrical thermal model by the welding research community at large often includes empirical parameters for the heat flux evaluation that are based on a trial and error approach. The new heat flux formulation developed under this project combined the Goldak model with a characterization of the electrode power through the moving-source solution. This new approach introduced consistency and accuracy into the evaluation of the transient properties of the heat flux. Combined with the weld partitioning process, this new heat flux formulation proved to be critical in the automation of the thermal modeling procedure.

By using an axis-symmetrical model, an efficient thermal analysis procedure for the multi-pass, multi-wire GMAW-P girth weld was developed. Figure 19 shows a typical multi-pass girth weld and its partitioned finite element mesh generated by the model. Overall, the development of this procedure went through a series of steps that included its implementations, its verification against existing measurement thermal cycle data and thermal cycle data obtained from the current project works. It also included a number of applications of this thermal model to research activities performed for this project.

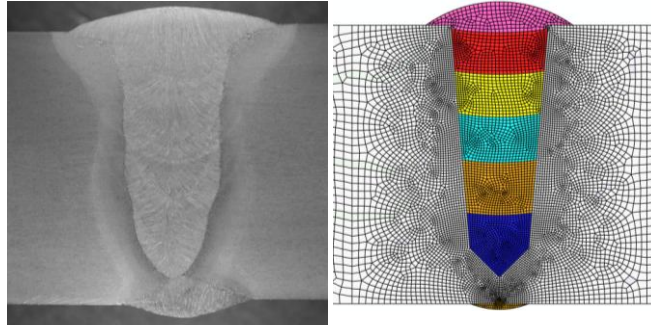


Figure 19. GMAW-P girth weld and its partitioned finite element mesh

The work flow diagram of these implementations, verifications, and applications is shown in Figure 20. The thermal analysis procedure was implemented first with ABAQUS®² finite element software. The predictions from this implementation were compared to the measured thermal cycle data from the WERC research by Hudson [21]. The procedure was then implemented through a generic finite element method in the format of stand alone software tool. This software tool was verified against thermal cycle data from the Round 1 girth welds and those from the Round 2 girth welds. After the thermal analysis software tool was verified and proved to be effective, it was used as the primary tool in a virtual experiment to evaluate and identify the essential variables. In addition, during the course of project work, this tool was used on numerous occasions to perform simulations and provide information for welding procedure design and Gleeble® test design.

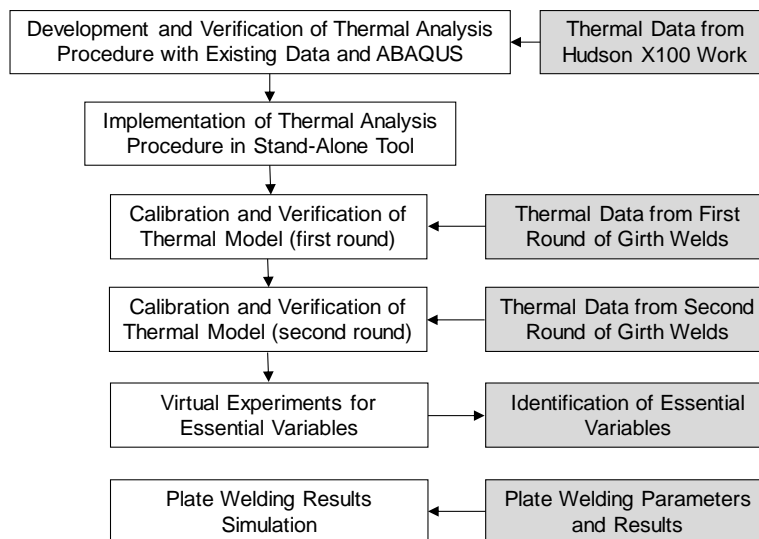


Figure 20. Work flow of thermal model development, verification, and applications

4.1.2 ABAQUS® Model Implementation

The purpose of this implementation was primarily to test the feasibility of the modeling approach, investigate the impacts of other process features, and verify its accuracy against

² ABAQUS® is a registered trademark of Abaqus, Inc. Corporation Rhode Island 1080 Main Street Pawtucket Rhode Island 02860

existing thermal cycle data. In the thermal model, the cavity radiation effect was included. The prediction results indicated that the impact of the cavity radiation was insignificant. Consequently, this feature was ignored in all the remaining modeling activities. The results of this implementation, the predicted cooling times T_{85} , T_{84} , and T_{83} were compared to those measured by Hudson [21] and satisfactory agreement was achieved.

4.1.3 Implementation with Finite Element Method and Stand-Alone Software Tool

After its successful development and verification against existing measurement data, the thermal model (together with the microstructure model) was implemented with a generic finite element procedure and a stand-alone software tool was produced. The primary purpose of implementing the thermal model in a finite element procedure is to automate the entire analysis procedure. Compared with the ABAQUS® thermal model, the stand-alone analysis software tool offered the following benefits:

1. Efficient analysis of a complicated thermal and microstructure process;
2. Consistently accurate results compared to a manual modeling process with third-party package;
3. Very robust in dealing with element activations and successive torch applications because the codes were designed and implemented for these special scenarios; and
4. Easy to incorporate new features.

The key components of this software tool include:

1. Input module;
2. Weld partitioning module;
3. Heat flux formulation module;
4. Transient finite element solver for temperature simulation;
5. Output of results.

The software was written in C++ in an object-oriented way. The software tool as a whole consists of several dynamic-linked libraries for different functionalities. An interface was developed for the execution of the program. Before the execution of the analysis, an input file that contains the complete information for the welding procedure needs to be compiled. The details for this input file are reported by Chen [38].

Before its use for welding simulation, the finite element code went through rigorous numerical convergence tests and stability tests. Computation results were compared to those from the ABAQUS® model under the same welding conditions, and the agreement was reasonably good.

The outputs of the program include the snapshots of peak temperature distributions over the entire model domain, which are recorded after each pass is completed. In addition, temperature histories at selected locations in weld and HAZ regions can be extracted for post-processing.

4.1.4 Verifications

In the process of thermal analysis procedures development and implementation, several experimental data were used to calibrate and verify the procedure. The major data sets include:

- 1) The thermal cycle measurement data by Hudson [21];
- 2) The thermal cycle measurement data from the Round 1 girth welds;
- 3) The thermal cycle measurement data from the Round 2 girth welds;

4.1.5 WERC Research Thermal Data by Hudson

In this effort, ABAQUS® software was used for the thermal analysis procedure. The thermal model, including the weld partition, mesh generation, heat flux formulation, boundary condition applications, was constructed using the technical procedure described previously. The measured thermal cycles for two series data were selected to verify the thermal model: one from the “pre-heat variation trials” and the other from the “process variation trials”. The former includes measured thermal cycles from girth welds made with three pre-heat temperatures: no pre-heat application, 100°C, 180°C. The “process variation trials data” were from girth welds made with four GMAW-P variants: single torch, tandem wire, dual torch, and dual tandem.

Measured cooling times, $\Delta t_{800-500}$, $\Delta t_{800-400}$, and $\Delta t_{800-300}$ were compared to those predicted by the model. Overall, generally good agreement was achieved, Figure 21. The correlation is better for $\Delta t_{800-500}$ and $\Delta t_{800-400}$ than for $\Delta t_{800-300}$. For $\Delta t_{800-300}$, because the low temperature tail of the predicted thermal cycle is sensitive to the heat convection at the pipe/bevel surfaces, improper selection of heat transfer coefficient at the surfaces could lead to significant discrepancy between the predicted $\Delta t_{800-300}$ and measured $\Delta t_{800-300}$.

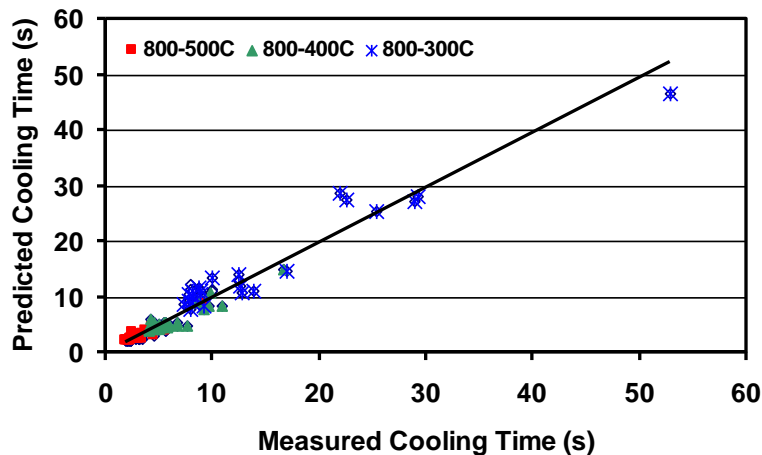


Figure 21. Predicted vs. measured cooling time, WERC research data
Predicted = 0.9879 x Measured, $R^2 = 0.9417$

The characteristics of the experimentally recorded thermal cycles from dual torch GMAW-P process were examined. In general, the leading weld pass experiences a twin-peak temperature thermal cycle and the trailing pass experience a single-peak temperature thermal cycle. In both

cases, model prediction indicated that the final cooling rates were dictated by that of the trailing torch. It was demonstrated from the model simulation results that the residual temperature left behind the wake of the leading torch is much higher than the nominal pre-heat or interpass temperatures. This residual temperature from the leading torch acts as an elevated “pre-heat” for the trailing torch. Consequently the resulting cooling times are much longer than for a single torch process with the same heat input.

4.1.6 First Round Girth Welds Thermal Data

All Round 1 girth welds were single torch GMAW-P. Two of the welds were instrumented for HAZ temperature measurements. One observation from the measured True Power data is that the True Heat Inputs for the welding waveform used were often about 15-20% higher than the Average Heat Inputs. The measured thermal cycles from hot pass to cap pass by one thermocouple were compared to the thermal model predictions using True Heat Input. The results illustrated in Figure 22 demonstrate that the agreement between prediction and measurement is excellent when an accurate heat input is used in the computations.

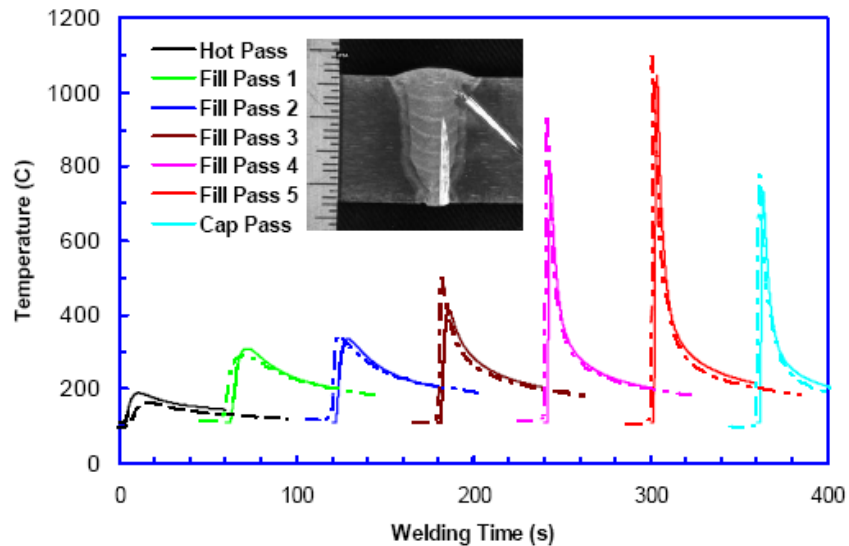


Figure 22. Comparison of predicted with measured thermal cycles (807J)
broken lines = measured thermal cycles, solid lines = predicted thermal cycles

Similar thermal cycles measured by another thermocouple were used to show the impact of True Heat Input. Predicted thermal cycles using averaged heat input and true heat input were compared to the measured data, and it showed that the model would under-predict the peak temperature of a thermal cycle if the Average Heat Input was used for the simulation.

A major conclusion drawn from this result is that for GMAW-P, the conventional Average Heat Input can be misleading when it is used for the evaluation of thermal cycles for GMAW-P. In practice, when information on True Heat Input is not available, estimated compensation must be made to thermal cycle evaluation.

4.1.7 Second Round Girth Welds Thermal Data

The Round 2 girth welds were made with single torch and dual torch GMAW-P processes, and in 1G and 5G positions. In addition to thermal cycles measured in HAZ regions, thermocouples were plunged manually into the weld pool immediately behind the arc to measure the thermal cycles in the weld metal.

Among the girth welds made during the Round 2 welding, the measured thermal cycles of two girth welds were used for the comparisons with results predicted by the thermal model. The first comparison was made between the cooling times $\Delta t_{800-500}$ and $\Delta t_{800-400}$ measured by the plunged thermocouples and the model prediction for a single torch girth weld. The agreement was very good. The second comparison was made for a dual torch girth weld. The predicted dual torch thermal cycles at a HAZ location agreed very well with the measurement data, not only in the repeated heating and cooling profiles, but also in the peak temperatures of the cycles. This result indicates that the combination of the new heat flux model and the superimposition principle works very well for the simulation of dual torch welding, particularly when using the True Heat Input for the computations.

4.1.8 Applications

The primary purpose for the development of predictive tools was a complete assessment of essential welding variables and improved understanding of the factors influencing properties of high strength steel pipeline girth welds and their performance. After the models went through three rounds of calibrations and verifications, they proved to be accurate in predicting thermal cycles for multi-pass, multi-wire GMAW-P and accurate in predicting changes in hardness. Consequently, the thermal model was used as the primary tool to conduct a virtual experiment to identify the welding essential variables.

The outputs of the virtual experiment were taken to perform a sensitivity study. This sensitivity study on the dependency of cooling times and weld metal hardness on the welding variables led to the identifications of welding essential variables. The details of this sensitivity study and its results are reported by Rajan [34]. The test matrix was developed by changing five welding parameters: bevel offset, pre-heat/interpass temperature, torch configuration, welding procedure, and electrode type. Eight combinations of these five parameters resulted in forty design points for a statistically designed virtual experiment matrix. Each of the forty design points was an individual virtual experiment simulation that was compiled according to the welding conditions specified in the test matrix. Each simulation output included cooling time predictions $\Delta t_{800-500}$ and $\Delta t_{800-400}$ for the HAZ thermal cycle at fill pass one as well as the hardness profile along the weld centerline and across the weld at the middle plane of the pipe.

Another application of the thermal analysis software was the torch distance analysis for dual torch welding procedure design. During the plate welding design stage, the researchers needed to estimate appropriate range of torch distance for setting up the experiment. Therefore, a set of thermal simulations for dual torch welding was performed to investigate the dependency of cooling times ($\Delta t_{800-500}$ and $\Delta t_{800-400}$) on torch distance for a fixed heat-input welding procedure. The baseline dual torch GMAW-P process under consideration was a six pass dual torch procedure. Three torch spacings were selected for simulations: 2, 7, and 12 in. Each simulation

result included the cooling time $\Delta t_{800-500}$ for the HAZ thermal cycle associated with the lead torch of fill pass 1 and the “residual” temperature behind the lead torch right before the heating cycle by the trailing torch. The team found that the dependency of the cooling time $\Delta t_{800-500}$ and the residual temperature on torch distance is quite significant, especially for torch spacing below 7 in. From 7 to 12 in., the impact of the torch distance becomes much less significant.

4.1.9 Thermal Analysis Tool

The thermal analysis procedure developed for this project fulfilled the primary objective in the effort to identify essential welding variables. In addition, it proved valuable in two other areas. It was instrumental in establishing test conditions for the thermal simulations experiments and in determining how torch distance affects the cooling times.

For GMAW-P processes, it is clear that the True Heat Input instead of the Average Heat Input should be used to achieve an accurate assessment of welding process variables. Thermal simulations for GMAW-P using Average Heat Input always under-predict the peak temperature of the thermal cycle while using True Heat Input consistently predicted thermal cycles with satisfactory peak temperatures.

Through a new heat flux formulation that combined the modified Goldak model with the moving-source solution in the characterization of the transient properties of the electrode, the accuracy, consistency, and robustness of the thermal analysis procedure was demonstrated for GMAW-P over a range of heat inputs. Because the thermal analysis procedure was implemented as a stand-alone software tool, it offers several advantages compared to using a commercial finite element package.

- 1) Automation of a complicated modeling procedure, including its integration with a microstructure model, streamlines some of the very time consuming modeling steps, such as weld partitioning and meshing for a multi-pass girth weld.
- 2) Procedure automation makes the analysis tool highly efficient and far less error prone compared to a manual process of model development.
- 3) Because it is written in generic finite element method, new features can be readily incorporated and implemented in the procedure.

4.2 **Microstructure Models and Hardness Predictions**

4.2.1 Methodology

In selecting the method for microstructure modeling of GMAW processes, the weld metal and its HAZ were treated differently due to their marked differences in chemical compositions, grain structures, and, to certain extent, phase transformations. For HAZ microstructure simulation, a number of approaches, including those by Kirkaldy and Venugopalan [41] and Watt [42], were examined and used in the implementation of the model. For the weld metal microstructure simulation, a combination of the approaches by Bhadeshia and Svenson [43] was adopted.

The major outputs of the microstructure model include the volume fractions of constituents, locally averaged grain sizes, and the local hardness. In the verification of the microstructure

model, comparisons were made between the predicted hardness value and hardness measurements from real welds. Hardness was chosen due to two primary reasons:

- 1) Hardness is a measurable mechanical property for steels and provides a good indication of material strength, and
- 2) For steels, hardness has constantly demonstrated excellent correlation with tensile strength.

The microstructure model was integrated with the thermal model. In principle, the transient thermal cycles and microstructure evolution or phase transformation were simulated in parallel. With each increment of the simulation, the thermal cycles were calculated first. The incremental changes of temperatures were then fed into the microstructure model to calculate the phase transformation, averaged grain growth, and local hardness.

For both weld metal and HAZ, the microstructure model consists of three major modules. First, a thermodynamics module calculates the critical phase transformation temperatures and reaction rates. These include the A_{e3} temperature, the eutectoid temperature (A_{e1}), the bainite start temperature (BS), the martensite start temperature (MS), and the precipitate dissolution temperature.

The results from the first module are used in the second grain growth module that determines the prior-austenite grain size. In this module, the locally averaged austenite grain sizes are calculated according to formula by Ashby and Easterling [44]. Empirical parameters in the formula were correlated and modified according to the HAZ Gleeble® grain size data. For the weld metal, the grain size was estimated according to Bhadeshia [43].

The third module simulates the austenite decomposition process. The empirical equations developed by Kirkaldy and Venugopalan [41] described the reaction rates at which the austenite decomposes into its child products such as ferrite, pearlite, and bainite. Detailed description of the reaction kinetics is reported by Chen et al [39]. At the end of the welding cycles, the final hardness values are calculated in a weight-averaged manner according to the volume fractions of microstructure constituents. The formula for the evaluation of local hardness is reported in detail by Chen et al [39].

In its initial ABAQUS® implementation, two of the three components in the microstructure model, grain growth and austenite decomposition, were coded in an ABAQUS user subroutine. The volume fractions of constituents and hardness distribution were defined as nodal state variables in the subroutine in the finite element mesh. In the final stand-alone software analysis tool, the microstructure model was implemented in two components. The first component was for the thermodynamics calculation of phase transformation temperatures and kinetics reaction rates for austenite decomposition, which was coded as a separate dynamically-linked library. The second component included grain growth and the austenite decomposition which were coded within the framework of the thermal model.

4.2.2 Verification - Comparison between Measurements and Model Predictions

In the process of development and implementation of the microstructure model, several sets of experimental data were used to calibrate and verify the procedure. The major data sets include:

- 1) Hardness measurement data by Hudson [21],
- 2) HAZ thermal simulation results,
- 3) Weld metal thermal simulation results, and
- 4) Flat plate welds and Round 1 and 2 X100 pipe girth welds.

The microstructure model was calibrated and verified in order to establish it as a prediction tool for the microstructure and hardness evaluation of a girth weld. In addition to the verification, the microstructure model was used to perform the virtual experiment in the effort to identify and quantify the essential welding variables.

4.2.2.1 WERC Research Hardness Data by Hudson

The microstructure model was implemented first with ABAQUS® finite element software and its microstructure predictions were compared against the hardness measurements by Hudson. The experimental measurements had two series of data: preheat variation trials and process variation trials. The first series included girth welds made under different pre-heat temperatures. The second series included girth welds made with different GMAW-P variants, namely, single wire, tandem wire, and dual torch processes. With the exception of the dual torch case, the predicted hardness profiles along the weld centerlines showed good agreement with the general trend of the measurement data. The predicted hardness distributions in both weld metal and HAZ by the microstructure model correctly demonstrated the influences of preheat temperature and different welding types (single-wire vs. dual-torch, for instance).

4.2.2.2 HAZ Thermal Simulation Hardness Data

In order to calibrate the microstructure model for its effectiveness in simulating the phase transformation in the HAZ, a set of thermal simulation tests were performed on one of the vintage X100 pipe steels at CANMET. Thermal cycles with a peak temperature of 1350°C and different cooling times, $\Delta t_{800-500}$, were applied to X100 steel. After the calibration, the microstructure model demonstrated its consistency in predicting the trends in volume fractions of constituents, grain growth, and final hardness, Figure 23.

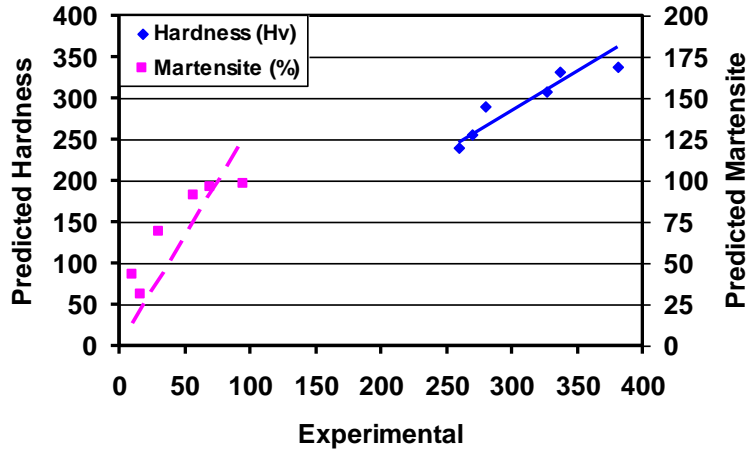


Figure 23. Microstructure and hardness predictions for thermal simulation

4.2.2.3 Plate and Pipe Girth Welds Hardness Data

In further verifying the microstructure model, one plate weld made with a prototype welding consumable and one X100 pipe girth weld made under practical welding conditions were selected. The plate experimental weld was made with consumable PT1 with no pre-heat application or interpass heating. It featured a unique combination of welding passes with typical low heat input for pipeline welding and a cap pass with relatively high heat input. The microstructure model correctly predicted the trend of hardness variation throughout the thickness of the weld and across the weld metal and HAZ. For the X100 girth weld, the model was able to capture the bands of hardness produced by the reheating of subsequent weld passes, though the absolute values of the predicted hardness are higher in general than the measured values. The comparison between the prediction and the measured micro-hardness mapping is shown in Figure 24.

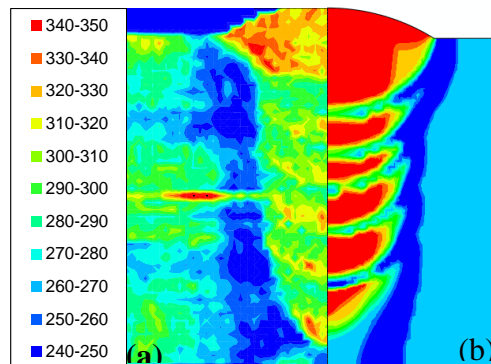


Figure 24. Comparison of micro-hardness distribution, (a) measured vs. (b) predicted

4.2.3 Microstructure and Hardness Prediction Tool

A microstructure model, as a companion to the thermal model, was developed for the purpose of making self-consistent estimates of weld microstructure and hardness with changes in welding variables. The microstructure model was calibrated and verified against a large amount of measured microstructure data. This model was also implemented through finite element method

as a stand-alone analysis software tool. After the calibration and verification, the model was used to perform virtual experiments.

Overall, the microstructure model demonstrated its capability of predicting the trend of microstructure and hardness variations as a function of chemical compositions of pipe and weld metal, welding processes, and welding parameters. Further research effort is needed to improve the model's accuracy of hardness prediction, particularly in terms of its ability to predict the hardness of the RH regions. For weld metal, more systematic and consistent metallurgical measurements are needed and alternative approaches such as direct correlation between chemical composition, cooling rates, and hardness need to be considered.

5 MATERIALS AND PIPE WELD PERFORMANCE

5.1 Heat Affected Zones

Base pipe compositions are summarized in Table 11. All are based on variations of a C-Mn-Si-Ni-Mo-Cr-Cu-Nb-Ti alloy system. The three base pipe samples investigated (X100-2, X100-4, and X100-5) are all similar in terms of C-Mn-Si levels, but differ in the overall alloy content. At $CE_{IIW} = 0.55$, X100-4 has the highest alloy level and at $CE_{IIW} = 0.43$, X100-2 has the lowest alloy level. For these three base pipes, there is enough difference in chemical composition that some variation in microstructure and properties can be expected.

X100-2 and X100-5 microstructures were predominantly bainitic with some banding at mid-thickness, which contained a mixed bainitic-martensitic microstructure [28, 33]. The banding is much more pronounced in X100-5 with higher amounts of martensite evident in the mid-thickness region. In contrast, a more uniform, predominantly bainitic microstructure was observed in X100-4 [33]. Welding thermal cycles cause all three steels to soften, but to varying degrees as a result of general grain coarsening and other microstructural changes that occur during the thermal cycle. The cross weld hardness traverses indicated most of the softening in the ICR-GHAZ with the single cycle GHAZ actually harder than the base pipe. Figure 25 illustrates the influence of cooling time, $\Delta t_{800-500}$, on the simulated GHAZ hardness [33]. X100-2 and X100-5 are similar with X100-2 exhibiting a slightly steeper slope, indicating a higher degree of cooling rate sensitivity. The relatively flat curve for X100-4 indicates this steel does not soften as readily under the influence of weld thermal cycles and plateaus over 30 Hv higher than the others. For X100-5 used in Round 1 and 2 pipe welds, through thickness HAZ hardness was generally below 250 Hv, down from the 270-300 Hv, in the unaffected base pipe. This reduction in hardness corresponded with generally coarsened grain structure, roughly 20-40 microns equiaxed. Both dual torch and single torch weld GHAZ softened to the same degree, but the dual torch weld created a wider HAZ with grain size roughly 30-60 microns equiaxed. In effect, the dual torch GHAZ experiences a longer cooling time (i.e. slower cooling rate) than the single torch GHAZ. The fact that both the dual torch and single torch weld HAZ experience roughly the same degree of softening is consistent with the general flattening of the Figure 25 curves at longer cooling times.

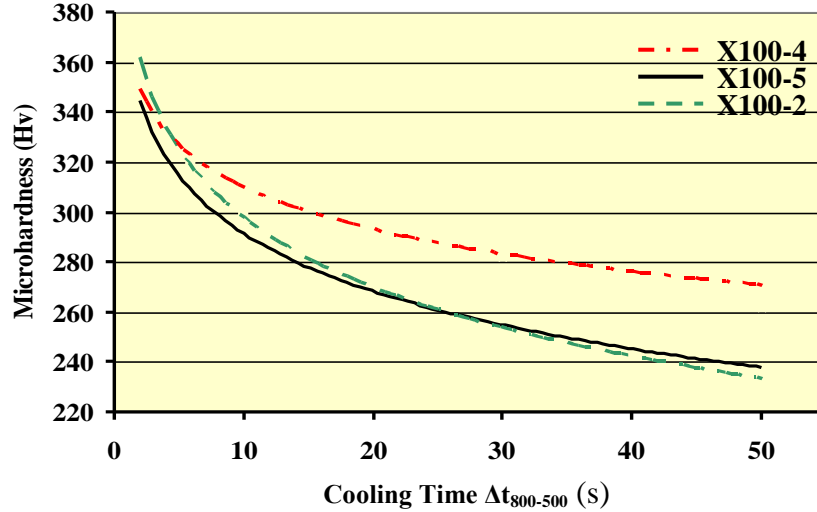


Figure 25. Comparison of simulated HAZ softening for three pipe steels [33]

Impact toughness also is influenced by the microstructure changes that occur in the HAZ, Table 17. In the simulated GCHAZ at 6 and 10 s $\Delta t_{800-500}$, the Charpy V-notch energy transition temperature (ETT) for all three pipe steels increased by 37-50°C for $\Delta t_{800-500} = 6$ s. For X100-2 and X100-5, there was an additional 10-18°C increase for $\Delta t_{800-500} = 10$ s. The ICRGCHAZ in X100-4 and X100-5 exhibit an additional 4-10°C increase in transition temperature as well as a reduction in upper shelf energy on the order of 50-80 J. The upper shelf energy for all three pipe steels is in excess of 250 J [33]. Even though X100-4 and X100-5 exhibited a substantial reduction in upper shelf energy in the simulated HAZ, the energy levels are still high, on the order of 200-250 J.

Table 17. Summary simulated HAZ Charpy V-notch properties

Pipe	X100-2			X100-5			X100-4		
	ETT T (°C)	CVN Energy (J)		ETT (°C)	CVN Energy (J)		ETT (°C)	CVN Energy (J)	
		-60°C	-20°C		-60°C	-20°C		-60°C	-20°C
As-received	-87	259	272	-70	237	287	-98	289	315
GCHAZ, 6s	-50	92	247	-25	17	145	-50	100	254
GCHAZ, 10s	-40	38	152	-7	26	76	-50	69	254
ICRGCHAZ	-	-	-	-11	16	48	-40	38	234

The highest alloy steel, X100-4 at $CE_{IIW} = 0.55$, exhibits superior HAZ CVN performance overall. This is correlated with the higher proportions of low carbon lath martensite and fine bainite that forms at cooling times $\Delta t_{800-500} \leq 10$ s. On the other hand, X100-5 HAZ exhibits the lowest toughness overall with the highest transition temperatures and lowest CVN energies through the transition region. The increasing proportions of coarse bainite observed in the X100-5 GCHAZ and second phase precipitation in the ICR-GCHAZ distinguish it from the other two steels [28, 33].

The purpose of conducting CVN tests for simulated GCHAZ and ICR-GCHAZ was to gain some understanding of the inherent toughness of the various microstructures formed in the HAZ and to

reveal relative differences among pipe steels having the same chemical compositions. The correlations with microstructure observations are approximate, at best. Resolution of the second phases and detailed characterization of the microstructures requires more advanced methods than the optical metallography used in this project. Therefore, the microstructure observations should be taken as general approximations. Further, the CVN results from simulated HAZ should be considered as a lower bound of what is possible and as a tool for screening pipe steel capability.

These points are illustrated in Figure 26 with a comparison among the X100-5 CVN transition curves from the pipe welds [29] and the HAZ simulations. The increase in energy transition temperature previously discussed for the GCHAZ and ICR-GCHAZ relative to the base pipe is apparent. In contrast, there is almost no shift in transition temperature for the single torch HAZ-fusion line (ST 807F) compared to the base pipe. Recall that the CVN notch at the HAZ-fusion line location samples a wide range of microstructures and is not exclusive to the GCHAZ, particularly for the single torch weld with a relatively narrow HAZ. For the dual torch weld with a wider HAZ and greater coarsening of the microstructure, the HAZ-fusion line transition temperature increase is on the order of 35°C and is approaching the performance of the simulated HAZ. The reduction in upper shelf energy for all X100-5 HAZ relative to the base pipe, suggests that there may be some second phase precipitation occurring that was observable by optical microscopy only in the ICR-GCHAZ.

The relative CTOD SE(B) results at room temperature for the single and dual torch welds at the HAZ-fusion line location are consistent with the relative CVN behavior, with average CTOD of 0.38 mm and 0.27 mm respectively [29]. At lower test temperatures there was little distinction with all CTOD at 0.15 to 0.20 mm, except for one low value of 0.04 mm for a single-torch weld specimen at -20°C. Most of the HAZ specimens showed brittle cleavage (although generally after some ductile crack growth), especially for the dual-torch welds. Nevertheless, CTOD values were generally quite good (0.14 mm or higher).

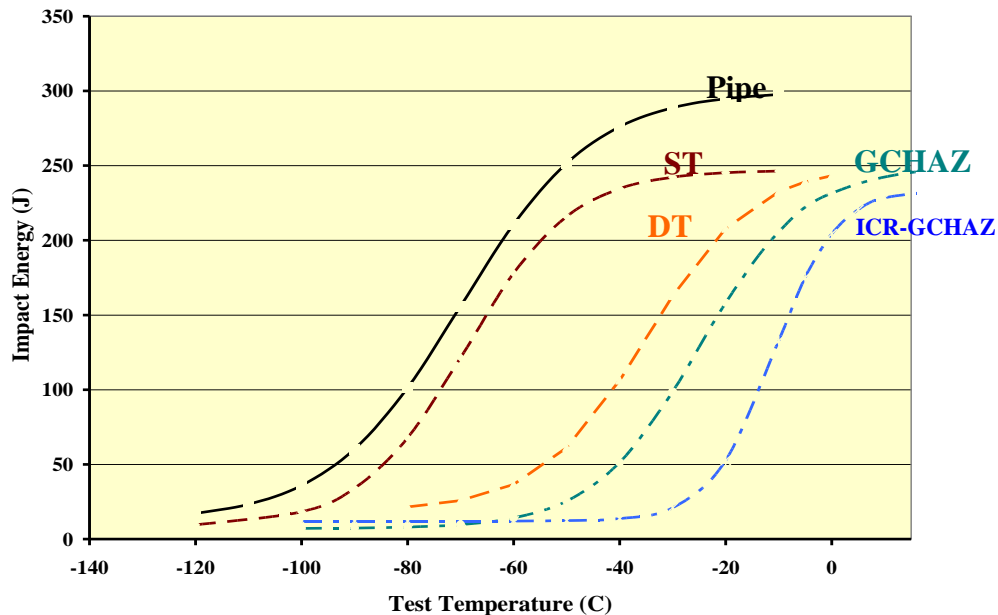


Figure 26. Comparison of CVN transition behavior for pipe steel X100-5

The practical implications of this investigation on X100 heat affected zone behavior is that HAZ simulations can be used effectively to assess the impact of welding thermal cycles on pipe steel HAZ performance. In order to mitigate the negative impact of welding on X100 HAZ properties, there are a limited number of options. The welding process, procedures and practice have the greatest influence on the cooling time, while the base pipe selection has the greatest influence on the magnitude of change that is likely to occur in mechanical performance. For the three pipe steels considered here, the steel with the highest alloy, X100-4, achieved the highest level of HAZ performance in terms of resistance to softening and in terms of CVN performance. The performance of X100-2 and X100-5 is not as easily predicted from chemical composition. The CE_{IIW} is significantly different at 0.43 and 0.47, respectively, yet they perform similarly in terms of resistance to HAZ softening and very differently in terms of CVN performance, as indicated in the simulation tests. Distinguishing the performance of these two steel requires a more fundamental knowledge of how their respective microstructures change under the welding thermal cycle.

5.2 Weld Metal

Various welds were produced during this program and characterized for mechanical and chemical properties. The alloy systems included C-Mn-Si-Ni-Mo, C-Mn-Si-Ni-Mo-Ti and C-Mn-Si-Ni-Mo-Ti-Cr, Table 12. Some of these, particularly those with the lowest CE_{IIW} or P_{cm} , were used to introduce specific chemical composition variants for the flat plate experiments or the thermal simulations and were not expected to achieve strength levels any higher than would nominally match the X100 SMYS. These are discussed in context elsewhere [32,34,35]. This section addresses the weld metal alloy systems that were expected to achieve some level of overmatching of the pipe strength. Consequently, the focus is on the weld performance in the pipe welds for which the detailed results have been reported by Gianetto et al [29-31]. Weld properties are discussed in terms of weld metal microstructures, chemical composition and welding conditions.

5.2.1 NiMo80 Weld Metal

NiMo80 weld metal produces a C-Mn-Si-Ni-Mo-Ti weld metal. This alloy system was selected to establish baseline X100 weld performance because of its history in the WERC development and the X100 field demonstrations.

Weld metal strength for the Round 1 and 2 pipe welds is summarized in Figure 27 and compared with longitudinal pipe strength for both single torch and dual torch GMAW-P in both the 1G rolled and 5G welding positions. All data for each condition were compiled in this statistical summary of strength properties. YS was determined by both the 0.2% offset method and by the 0.5% total strain method. The error bars represent ± 1 standard deviation scatter about the average strength value.

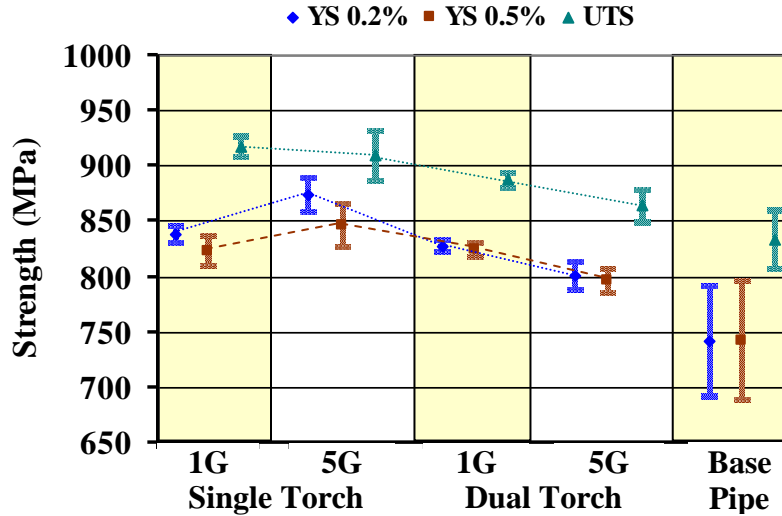


Figure 27. Tensile test summary NiMo80 and X100-5

The mixed microstructure of relatively fine martensite, bainite, and acicular ferrite with a CE_{ITW} on the order of 0.50 is responsible for YS consistently over 800 MPa. These welds consist of alternating bands of as-deposited and reheated material, which is best illustrated in the microhardness maps in Figure 11 and Figure 12. The dual torch welds differ somewhat in that the grain interiors contain some fine lath structure with occasional polygonal ferrite and the trail beads exhibit coarser overall structures. The result is that the dual torch welds contain few, if any, of the very high hardness bands that are characteristic of the as-deposited weld metal in the single torch welds. The through thickness hardness generally is less variable for the dual torch, which translates into less scatter in strength than the single torch welds for a given welding position. The drop in strength on the order of 50 MPa from single torch to dual torch is consistent with slower weld cooling rates for the dual torch and the effective reheating of the lead torch deposit by the second torch [28,38].

In these pipe welds, where the welding procedures were highly controlled with minimal variation around the pipe circumference, there is much less scatter in the weld metal YS than in the pipe YS. In all cases the YS overmatches the X100 pipe SMYS, but not the actual pipe YS. In the case of the dual torch 5G weld, both the YS and ultimate tensile strength are nominally matched with the top of the respective pipe strength scatter bands. If overmatching the actual pipe strength is required, these results suggest that welding conditions can have a significant influence on the ability to achieve that objective with this weld composition.

CVN toughness transition curves are presented in Figure 28. As is typical for most weld metal, transition curves have lower upper shelf energies and longer, flatter transition regions than the corresponding base material. In all cases, weld metal upper shelf exceeds 100 J and transition temperatures are similar to the pipe at approximately -70°C , which is consistent with the observation that a relatively consistent microstructure exists under both single and dual torch welding conditions. In the single torch case, there is a greater difference in the upper shelf energies with the root 80 J higher than the cap. In the dual torch case, there is little difference in impact toughness between root (ID) and cap (OD) locations, with upper shelf energies within 30 J. Changes in upper shelf are most often associated with an increased frequency of second

phase precipitates and/or non-metallic inclusions. Gianetto [28] noted the precipitation of a second phase along grain boundaries in the intercritically reheated region just below the cap pass in the single torch welds, which coincides with the Charpy V-notch location. It is plausible that the drop in upper shelf energy is associated with this microstructure feature, which is not observed in the dual torch welds. More advanced metallographic methods than used in this investigation will be needed to characterize these features and determine their relevance to weld toughness properties.

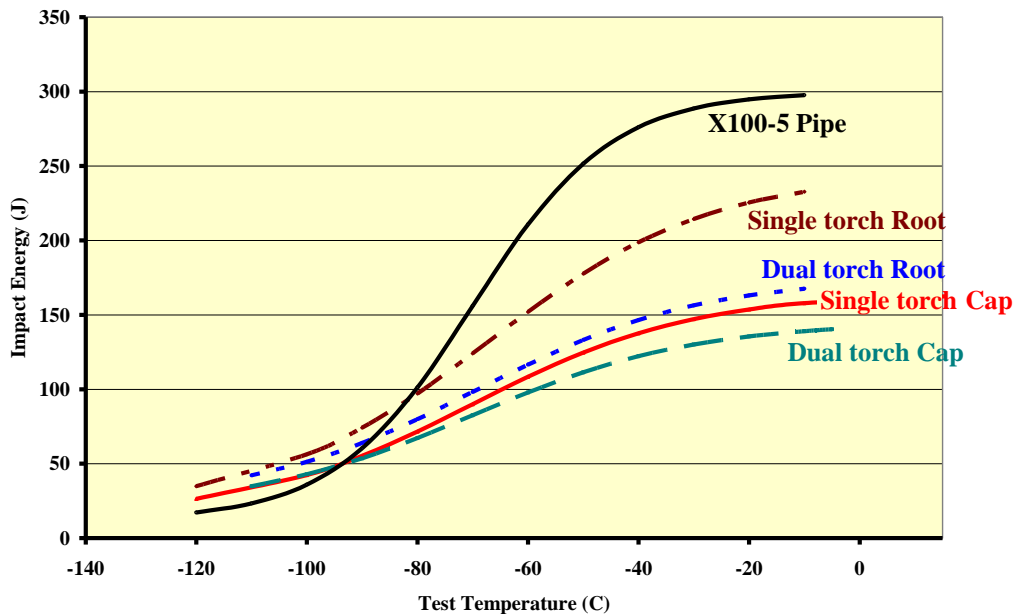
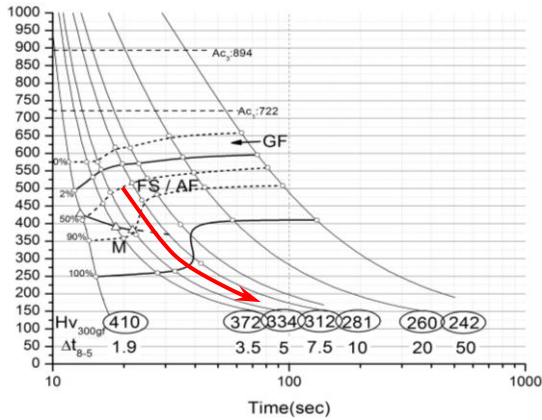
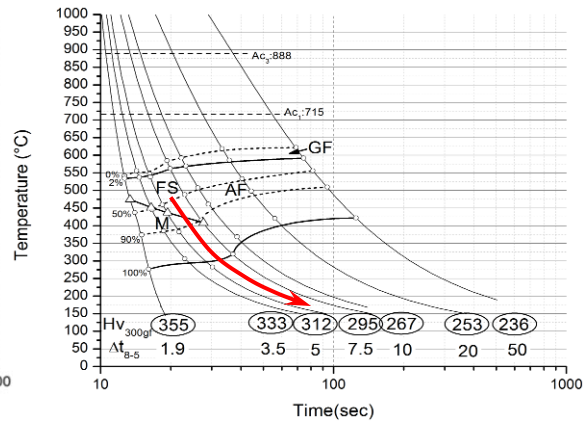


Figure 28. Charpy V-notch impact toughness, NiMo80

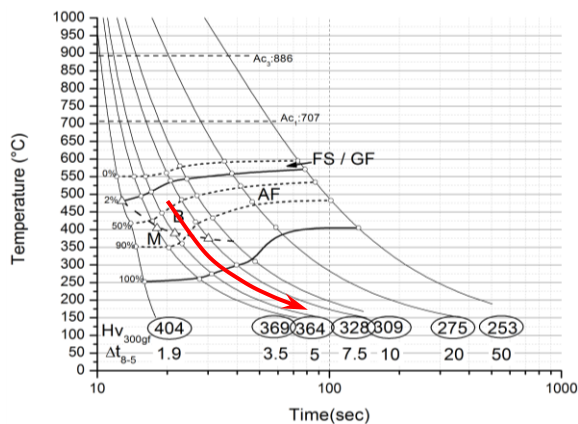
Consideration of the CCT behavior provides additional insight as to the performance possible with this weld metal alloy, Figure 29(a). A review of the welding data for the Round 1 and 2 single torch welds indicates weld metal cooling times $\Delta t_{800-500}$ for the fill passes were on the order of 2 to 3 s. Cooling times $\Delta t_{800-500}$ for dual torch welds are expected to vary from approximately 5 to 15 s for these narrow gap joints depending on welding process and torch spacing. The estimates for the Round 2 welds are closer to 5 s. The mixed martensite, bainite, acicular ferrite microstructures observed are consistent with what would be predicted from the CCT diagram for cooling times at and to the left of the red arrow placed at approximately 4 s. It is apparent that any change in welding practice that slows the cooling rate by a small amount will begin to alter the microstructure significantly. At cooling times over 7.5 s the fine martensite, bainite, ferrite mix will be replaced completely by coarser structures containing higher fractions of acicular ferrite with aligned second phase, which are not likely to achieve the same strength or toughness levels. In fact, the S-hook in the CCT diagram is fairly well centered in the normal range of operation for narrow gap GMAW ($\Delta t_{800-500}$ of 2 to 15 s). Achieving weld strength that consistently overmatches the pipe, clearly will require welding procedures and a level of control that ensure cooling times below ~5 s. Without the mixed microstructure that includes some martensite, X100 strength levels will not be possible with this alloy system.



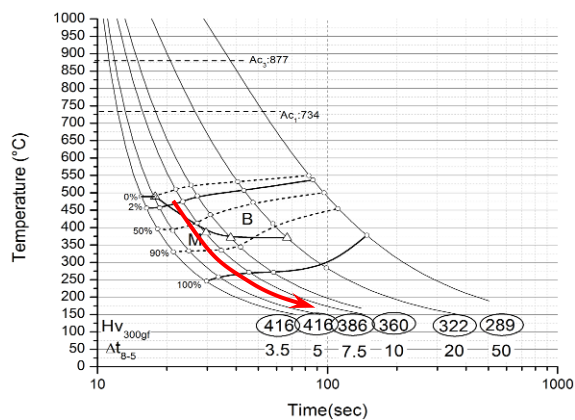
(a) NiMo80, $CE_{IIW}=0.48$, $P_{cm}=0.24$



(b) LA100, $CE_{IIW}=0.52$, $P_{cm}=0.21$



(c) PT1, $CE_{IIW}=0.56$, $P_{cm}=0.25$



(d) PT2, $CE_{IIW}=0.65$, $P_{cm}=0.28$

Figure 29. Continuous cooling transformation behavior

5.2.2 Other Weld Metal Alloy Systems

To investigate the potential for alternative alloys to achieve targeted strength levels over a wider range of welding conditions, indicated by $\Delta t_{800-500}$, one additional C-Mn-Si-Ni-Mo-Ti weld metal and two C-Mn-Si-Ni-Mo-Ti-Cr weld metals were considered. The C-Mn-Si-Ni-Mo-Ti alternative differs from the NiMo80 in that C-Si-Ti are lower and Ni-Mo are higher. The net result is a higher CE_{IIW} , ~ 0.53 compared with ~ 0.50 , but with lower P_{cm} , ~ 0.22 compared with ~ 0.25 . The two C-Mn-Si-Ni-Mo-Ti-Cr weld metals have the same nominal alloy balance with one having a generally higher overall alloy level with PT1 at $CE_{IIW} \cong 0.59$ and PT2 at $CE_{IIW} \cong 0.65$. The detailed chemical compositions are presented in Table 12.

Comparing the transformation behavior for NiMo80 and LA100 weld metal in Figure 29(a) and (b) it is apparent that both weld metals will form similar microstructures at the shorter cooling times (to the left of the red arrow). However, higher strength is expected from the NiMo80 owing to the influence of the higher carbon content on the martensite. This is consistent with the tensile properties from LA100 plate welds that indicate YS on the order of 700-724 MPa and ultimate tensile strength on the order of 820-850 MPa compared with NiMo80 at over 800 and 900 MPa, respectively, under similar conditions. Even though the LA100 chemical composition maintains consistent strength over a wider range of cooling rates than NiMo80, it

does not achieve sufficient strength even at the slowest cooling rates for the application. In this case, CE_{IIW} did not provide even a relative indication of strength performance between these chemical compositions. Clearly P_{cm} is a better indicator of potential weld metal strength than CE_{IIW} in this case.

Like LA100, PT1 and PT2 have greater potential for consistency over a wider range of cooling rates, given the more gradual shift in microstructure as cooling time increases, Figure 29. Overall alloy levels are sufficiently high to promote the formation of the mixed martensite, bainite, acicular ferrite microstructures needed for strength and toughness at longer cooling times.

This discussion illustrates how an understanding of the weld metal transformation behavior can provide a basis for selection of candidate weld metal compositions for the range of cooling conditions. The red arrows on each graph in Figure 29 represents a cooling rate roughly intermediate between the single torch and dual torch techniques used in this project. Based on the nature of the NiMo80 phase boundaries in this region, a recommendation can be made for using this material in single torch welding (<4 s) provided that the strength overmatch requirement is based on specification minima and not the actual pipe strength. For overmatching actual strength at any level, alternative chemical compositions are needed. The PT1 tested here is viable for X100 single torch (<5-7 s). However, it is not likely to achieve sufficient strength at the longer cooling times (~15 s) consistent with a direct current GMAW dual torch process. Under these circumstances the higher alloy levels of PT2 would be needed.

6 WELDING CONSIDERATIONS

6.1 Essential Welding Variables

The preceding discussion illustrates how an understanding of the transformation behavior can provide a basis for selection of candidate weld metal composition for a range of weld cooling conditions. Since the welding process variables essentially control the cooling conditions, the determination of essential welding variables was the next area of focus.

6.1.1 GMAW-P Welding Variable

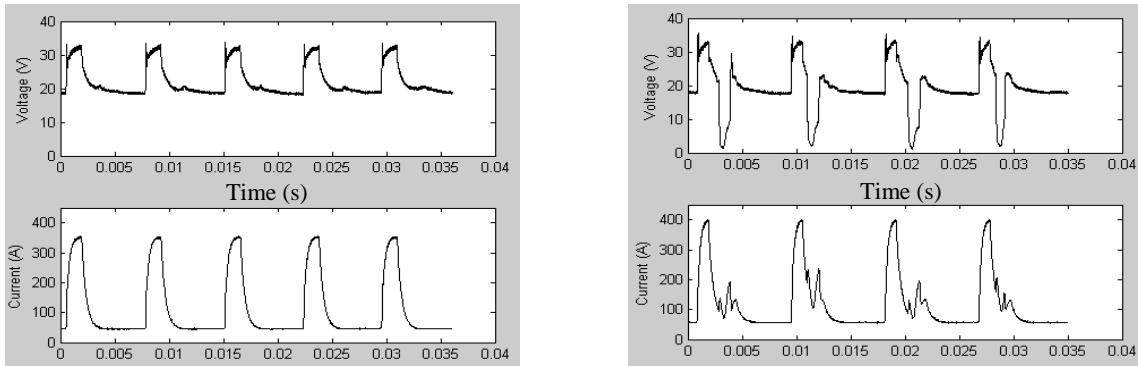
Table 9 lists twenty-nine welding variables considered by one code or standard to be essential in terms of welding procedure specification for GMAW-P. Conclusions arising from the State of the Art Review suggested that at least another half dozen are critically important to the welding of X100 pipe lines, including the consumable design, the welding torch design, power source type and model number, etc. While it is clear that X100 welding requires a higher level of precision than lower strength pipe grade, specification over thirty welding variables is beginning to look like a shotgun solution to a problem that could benefit from a more fundamental approach.

Accordingly, this project considered some aspect of thirteen of the twenty-nine listed variables in the context of their potential to influence either the welding thermal cycle or microstructure through chemical composition. The details have been reported by Rajan and Daniel [34, 35]. One of the essential variables that are known to have a major influence on cooling rate is the heat

input. The traditional approach to controlling heat input by calculation from average current, voltage and travel speed measurements. While wire feed speed, current and voltage can be measured independently in some manner, they are all interactive and cannot be controlled separately. Their interaction is characteristic of the welding power source being used and all are correlated with contact tip to work distance. With GMAW using modern power sources and pulsed waveforms, it is often difficult to obtain a measure of current and voltage that is meaningful [27].

While heat input is measured value with conventional meters, True Heat Input determined by measurement of True Energy™ is the most accurate measurement of this variable and makes possible very accurate determinations of weld thermal cycles [38]. Heat input measurement in this fashion also renders this variable independent of the type of waveform or the power source that is used in welding, eliminating them as individual essential variables. Taking the focus away from the waveform itself as an essential variable and focusing on direct measurement of the True Energy™ parameter has several additional advantages:

- In practice, True Energy™ can be measured directly with existing technology and audited by an inspector, whereas the complexity in specifying and verifying all of the subtle nuances of a waveform that might impact the thermal cycle is simply not practical. Consider the differences in complexity between two waveforms in Figure 30, for example.
- The True Energy™ data files can be used for post weld evaluations should it become necessary to determine what was happening at a specific point in the weld progression. This feature was used often by the project team in evaluating observed or perceived variations in performance.
- The intellectual property of welding contractors that customize waveforms to enhance productivity and weld quality remains a private matter between the contractor and his customer.



(a) Traditional GMAW-P waveform

(b) RapidArc® GMAW-P waveform

For WFS/TS Ratio = 19.1, True Heat Input - 0.47 kJ/mm
 For WFS/TS Ratio = 26.2, True Heat Input - 0.83 kJ/mm

For WFS/TS Ratio = 19.1, True Heat Input - 0.55 kJ/mm
 For WFS/TS Ratio = 26.2, True Heat Input - 0.91 kJ/mm

Figure 30. Schematic comparison of GMAW-P waveforms

The first assessment of essential welding variables was made using the analytical methods previously described. The objective was to assess the relative importance of several variables. The experimental design matrix included True Heat Input, number of welding torches, preheat and interpass temperature, welding consumable composition, and bevel groove offset, with other variables held constant. Bevel groove offset was included because of anecdotal claims in the industry the small changes on the order of 0.01 in. have a significant impact on mechanical properties. The thermal-microstructure model produced the results for this virtual experiment. The statistical analysis of this experiment resulted in a much focused experimental trial.

Plate welding experiments were conducted as a design of experiments (DOE) to corroborate and validate the essential variable predictions of the model. These experiments reiterated the importance of consumable or weld chemical composition as the most important variable, followed by preheat and interpass temperature, true heat input and torch configuration in their effect on mechanical properties. HAZ softening was also influenced by preheat and interpass temperature, true heat input and torch configuration. Figure 31(a) illustrates the effect of preheat and interpass temperature in conjunction with True Heat Input. Note the slight curvature in the surface plot indicating the compounding effect of these two variables together.

Groove offset as an independent variable was not identified as a major factor in either case. Figure 31(b) indicates a small influence in conjunction with preheat and interpass temperature on HAZ cooling time. If there is substance to the perception that groove offset is a major factor, the results here suggest that some other aspect of the welding process with a more direct impact on thermal cycle is changing at the same time.

Statistical analysis of the results produced linear models with very good fit between the essential variables and weld tensile strength, YS and CVN toughness. This enabled the development of transfer functions between the essential variables and the mechanical properties, allowing graphical optimization of the underlying response surface. The transfer functions became the basis for implementation of control limits on the essential variables to ensure the desired tensile and YS for a given consumable composition, weld composition and welding torch configuration.

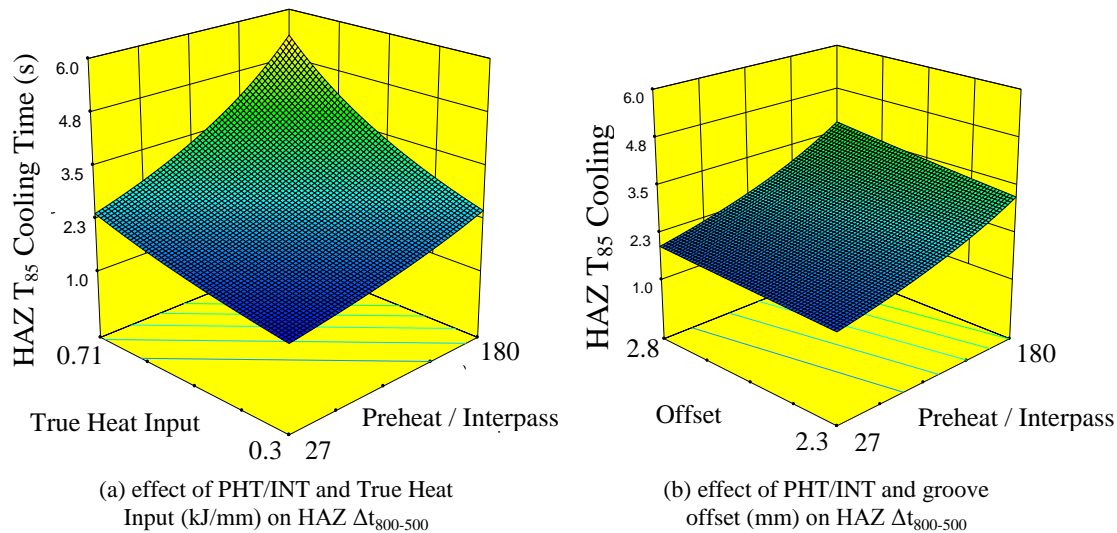


Figure 31. Effect of welding variables on HAZ cooling time

Using this approach, recommendations for control of essential welding variables were drafted to supplement the API requirements listed in Table 9. Additional guidance is provided as to the measurement of preheat and interpass temperature to ensure consistency around the pipe circumference. The recommendations are as follows:

- Preheat and interpass temperatures to be maintained at $100^{\circ}\text{C} +15^{\circ}\text{C}/-0^{\circ}\text{C}$. Temperature to be measured at 12:00, 3:00 , 6:00 and 9:00 clock positions around the pipe
- Wire feed speed (WFS)/Travel Speed (TS) ratio to be maintained as consistent as possible for all fill passes. For the final fill passes, TS could vary as much as 15% or WFS could vary as much as 10% from nominal settings.
- Heat input (HI) is to be based on True Energy™ continuously and maintained at $\pm 2\text{kJ/in}$ (0.08 kJ/mm) for all fill passes.
- HI/(WFS/TS ratio) tolerance of ± 0.04 for all passes
- Contact tip to work distance to be maintained at $\pm 1/8$ in. (3.2 mm) for all passes.
- Groove offset tolerance of ± 0.01 in. (0.3 mm).
- Preferred location for any high/low root fit up condition is at the 12:00 or 6:00 clock position

6.1.1.1 Contractor Validation

These control limits were transmitted to pipeline contractors to see the efficacy of this control methodology in actual field welding. Several 5G pipe welds were produced in this Round 3 of welding by each contractor using their own welding procedures and the additional constraints indicated above. The normal welding practices at each facility differed with one contractor using GMAW in a globular transfer mode and the other using GMAW-P similar to the Round 1 and 2 pipe welds. The trial included pipe from two new sources and both single and dual torch welding.

Both feedback from the contractors and analysis of their respective welding practices demonstrated that they were able to control the essential variables for the most part with some intermittent deviations. One contractor sometimes deviated from the $\pm 2\text{kJ/in}$ (0.08 kJ/mm) True Heat Input limit as welding progressed around the pipe, while the other sometimes deviated from the prescribed preheat and interpass temperature targets. For many weld passes, the variation achieved was significantly better than the targets. In spite of the minor variations experienced, the stress-strain curves from the different clock positions, for the most part, nearly matched, and overmatched the pipe stress-strain curves, as well as, tensile strengths obtained in the longitudinal and hoop directions. CVN toughness values of the welds were also high and barring some minor differences, showed consistent behavior around the pipe. These results indicate that with control methodology implemented in this study, consistent mechanical properties can be obtained in the pipe welds.

This was the first assessment of the practical implementation of the proposed changes in welding process control. Both contractors considered that the proposed methodology can be implemented and is within their capabilities. There is some concern about the more demanding preheat and interpass temperature requirements and the impact this may have on cost and

schedule for an active project on a right of way. There were many questions as to how industry might integrate the proposed methodology into existing codes and standards. Both contractors expressed a desire to remain involved with future efforts to refine and improve the approach.

6.2 Considerations for Other Welding Processes

6.2.1 Double Jointing

Double jointing of line pipe is generally done with SAW. However, double jointing of X100 in this manner has not been applied in practice [4]. Because double joint girth welds are subject to the same performance requirements as main line girth welds, other processes such as dual torch GMAW are being considered. Whichever process is ultimately used for this purpose, double jointing of X100 is considered a technology gap that must be satisfied for any large project to be feasible.

In double joint welding with SAW, the grooves are much wider than that employed in main line girth welding, and the heat inputs used are much higher. Consequently, the weld metal composition and properties are influenced to a large extent by the amount of dilution of the weld metal from the base pipe. The extent of this influence varies depending on the pipe compositions and consumable compositions employed. Furthermore, the extent of this dilution is determined by the welding practice (e.g. number of passes, bead placement, current type and polarity, etc.) The resulting heat input becomes one of the primary variables that determine weld and HAZ properties. Often, SAW is done with AC/DC machines with varying polarity. While this makes determination of True Heat Input a bigger challenge, it is very important to the SAW in determining the following:

- Extent of base metal dilution in the weld which in turn determines the weld metal properties, and
- HAZ properties, particularly with SAW where the heat inputs are potentially much higher than for GMAW.

Models for SAW can be developed using the same methodology reported for GMAW [34, 35]. However, the models can be expected to be more complex because at the higher heat inputs commonly employed, the weld composition will vary with both consumable selection and amount of dilution, and likely will have a significant impact on the weld mechanical properties. As a result, significant interaction between the essential welding variables such as True Heat Input, preheat and interpass temperature, consumable composition, pipe composition and groove geometry can be expected to effect the weld and HAZ mechanical properties. The relatively simple linear correlations developed for the narrow groove GMAW welds will not apply for SAW. Rather, significant non-linearity leading to more complex models is expected.

6.2.2 Flux Cored Arc Welding

FCAW is commonly used in line pipe construction, particularly with lower strength pipe grades. FCAW-G has been used for tie-in or repair welding of pipe in some X100 demonstration projects [4]. Self shielded flux cored arc welding (FCAW-S) consumables with the ability to satisfy the mechanical properties requirements for X100 pipeline applications are yet to be

developed. Both of these FCAW processes employ tubular wires with fill ingredients that produce slag during welding. FCAW-G resembles GMAW except for the fact that the slag-metal reactions can be significant in determining effective heat inputs and cooling rates. FCAW-S does not utilize shielding gas, and its fill ingredients are even more influential in the heat input and mechanical properties of the weld. The fill ingredients contain active ingredients that undergo oxidation or react with each other resulting in a very complex heat balance during the welding process. Furthermore, the heat balance associated with these fill ingredients will also be affected by the heat input employed during welding. Consequently, measurements of True Heat Input will not provide the full picture of the total heat input into the process. As a result, modeling the correlation between essential welding variables and mechanical properties is expected to be very complex.

6.2.3 Shielded Metal Arc Welding (SMAW)

In high strength pipelines, SMAW is used almost exclusively for tie-in and repair. SMAW is a manual process and welding is done in the constant current mode. Because of the manual nature of this process, the heat input is not monitored as stringently as for the automatic welding processes. Control of heat input is often dependent on the dexterity and skill level of the welder. Current is usually monitored and recorded by visual observations of the current meter on the welding machine, and the travel speed is determined by the welder. While this process does not lend itself easily to control in the conventional sense as obtained with the GMAW process, some measures can be taken to reduce the variation in heat input. If True Power can be recorded in the machine continuously, then efforts can be made to reduce variation in the power input into the weld. If the travel speed can be kept within reasonable control, efforts to minimize heat input variation around the pipe can be implemented. As with the fill material in FCAW wire electrodes, the coating of the SMAW electrodes can have active ingredients that influence the heat input into the weld, and to that extent, True Power monitoring will not capture these effects. But within a constant set of conditions of consumable composition, pipe composition and groove geometry, True Power monitoring could still provide a means to reduce variation in the welding process.

7 CONCLUDING REMARKS

The experience gained in this study with X100 highlights a need to consider the welding procedure as a tool in achieving the required weld properties. The researchers found that there is sufficient interaction between welding practice and material chemical composition (base pipe or weld) that the control of both of these inputs is necessary to achieve the level of consistency and predictability desired for strain based design. This is a paradigm shift from traditional practice which has considered the welding procedure almost exclusively as a tool in achieving productivity and weld soundness. The greatest value for the industry lies in a methodology that strikes the optimum balance on all fronts: productivity, soundness, and mechanical performance.

The primary objective of the research was a rational approach to essential welding variables that would ensure reliable and consistent mechanical performance in X100 girth welds.

The research team developed an approach to GMAW-P process control based on the concept and measurement of True Energy™ which allows for informed choices about welding process changes that can minimize variation in weld performance. They also established and monitored procedure limits in real time with the appropriate instrumentation. The data was used also for post weld assessment of test results.

The research demonstrated that using the True Heat Input derived from True Energy™ measurements ensures accurate prediction of welding thermal cycles using the thermal analysis tool. The research team found they could use cooling times $\Delta t_{800-500}$ estimates from the thermal cycles in conjunction with the CCT diagrams generated from the thermal simulation experiments to assess the robustness of various welding materials under different scenarios.

The research also showed that connecting the welding process knowledge with the fundamental understanding of how the materials will respond to the process is key to making the best welding consumable selection. Conversely, it showed that same kind of analysis will identify the boundaries of a welding process required to ensure a given weld metal performs.

The same methodology applies to the assessment of the HAZ. The evaluation of simulated HAZ regions provided an excellent method for comparing and ranking the pipe steels. This approach is expected to minimize the complexity and cost associated with the evaluation of real welds where complex distributions and narrow width of HAZ regions are often encountered.

A higher level of predictability and consistency for X100 was achieved with this approach than has been previously possible. Even though this project was focused on X100, the research team expects to apply the technical approaches and general problem solving methods to any GMAW application to improve reliability and consistency.

The research showed that to answer any question about weld performance, one must consider the interaction of the starting materials with the welding process. This introduces a level of complexity that often requires the development of new tools and methods. In this case, researchers made significant improvements to existing analytical tools and employed conventional assessment procedures in new ways in order to understand X100 weld performance on a root cause level. Many tools were developed during the course of this work that also have applicability beyond X100. This process of developing the technical tools and methods resulted in several findings that are worth noting:

The team demonstrated the viability of combining experimental and analytical approaches for effective problem solving. Analytical methods need not be perfect in order to deliver consistent predictions of trends that aid in complex decision making, but they do need to have basis in fundamental principles.

Furthermore, it was found that continuous cooling transformation diagrams provide insight into the weld metal behavior that is not possible to determine from a lot certificate or manufacturer's specification sheet. Although such diagrams are not often used as a tool in material selection, the strong interaction between welding materials and welding process in determining a satisfactory result makes them uniquely applicable.

Their microhardness measurements, presented in the form of contour and topographical maps, provided the best visual indication of weld macrostructure and were invaluable in assessing the magnitude of variation in physical properties across the weld regions.

The use of staggered welds was essential in developing a better understanding of the evolution of microstructure with successive weld passes. It also clearly showed the range of weld bead thicknesses, the relative distributions of as-deposited and reheated weld metal, as well as, the change weld metal and HAZ microhardness, that occur with deposition of successive weld passes (i.e., the influence of reheating and tempering).

In closing, this project accomplished much in terms of advancing our understanding of welding process and materials as it applies to X100. The challenge of implementing this understanding in practical ways that benefit industry is the essential next step.

8 FUTURE RESEARCH OPPORTUNITIES

The research team believes that the work presented herein should be considered a foundation for ongoing improvement in weld performance and the methodology could be refined further.

The project identified the major welding process variables influencing performance, but did not determine the influence of the secondary variables and their interactions. There is still much work to be done in mitigating the impact of the welding process on HAZ softening. Reducing variability in the welding process will make it possible to investigate other factors in more detail whose data is often masked by noise in the welding process. For example, the industry is aware that clock position affects weld performance, but the relationship is not yet well understood.

The detailed evaluation of high strength pipe and various welds in this investigation illustrated some of the limitations of conventional metallographic examination for characterizing the very fine weld metal and HAZ microstructures formed in advanced pipeline girth welds. In the X100 welds, the structures are so fine and there is so much short range variation, that it was difficult to resolve all of the important features using optical methods. The team recommends that future investigation using advance metallographic methods would be beneficial for resolution of effective grain size, identification of second phase precipitates, etc.

The project established a solid foundation for understanding the influence of phase transformations on weld metal and HAZ properties. The team did not yet characterize discontinuities in the dilation curves which indicate the occurrence of potentially important phase transformations. Resolution of these phase transformations will require more advanced metallographic methods than employed in this project. The research team considers that additional research in this area will help determine the relevance of microstructure variation to weld toughness properties.

This project addressed only a few of the X100 technology gaps and priority needs identified in Hammond's State Of The Art Review [4]. The work on essential welding variables provides a framework for better definition of the field welding parameter envelope and establishes an

approach for welding consumables improvements for GMAW. Other opportunities for further X100 technology development and research for onshore applications include:

- Welding process and material optimization for SAWL and SAWH pipe seams to mitigate excessive hardening that occurs at girth weld intersections
- Welding process and material optimization for double jointing
- Mitigation strategies for HAZ softening adjacent seam welds
- Process development for continuous improvement of productivity in the field
- FCAW-G procedures and consumables optimized for tie in and repair
- X100 fittings including induction bends, reducers, tees and flanges.

Additional opportunities for offshore pipeline applications are assumed to relate to seamless X90Q/X100Q line pipe intended for risers and flow lines. Use of large diameter X100 is not expected to find application offshore. These include:

- Field qualification of 2G position welding procedures for J-Lay
- Determine fatigue performance of X90/X100 girth welds in air and in seawater
- Determine corrosion-fatigue behavior for X90/X100 flow lines or risers for aggressive well streams
- Collapse testing of X90Q/X100Q seamless pipe
- Electrochemical studies of weld/HAZ/parent pipe zones for corrosive well streams

9 ACKNOWLEDGEMENTS

The support of the Pipeline Research Council International, Inc. (PRCI) and the Pipeline and Hazardous Materials Safety Administration (PHMSA) of the U.S. Department of Transportation (DOT) as well as the support of organizations that have provided in-kind support are gratefully acknowledged. These include the Canadian Federal Government Program of Energy Research and Development (PERD), TransCanada Pipelines Ltd., CANMET-MTL, CRES, Electricore, and The Lincoln Electric Company (LEC). CRC-Evans and Serimax North America also are recognized for their contributions to the pipe welding and perspectives relative to field application.

10 REFERENCES

1. Hammond, J. and Millwood, N.A., “Construction Of Ultra-High Strength Steel Pipelines”, Third International Conference on Pipeline Technology, Brugge, Belgium, 21-24 May 2000.
2. Sanderson, N., Ohm, R.K. and Jacobs, M., “Study Of X100 Line Pipe Costs Points To Potential Savings”, Oil & Gas Journal, 97, pp 54-57, March 15, 1999.
3. Energy Information Administration (EIA) (2010), International Energy Outlook 2010 - World Energy Demand and Economic Outlook, <http://www.eia.doe.gov/oiaf/ieo/world.html>
4. Hammond, J., “State of the Art Review”, Final Report 278-T-01 to PHMSA per Agreement # DTPH56-07-T-000005, September 2011.
5. Quintana, M. and Hammond, J., “X100 Welding Technology – Past, Present and Future”, International Pipeline Conference, ASME, IPC2010-31421, pp. 1-10, 2010, Calgary, Alberta, Canada, September 27– October 1.
6. Ryan, R.S., “First X-100 Line Pipe Tested by Columbia Gas”, The Oil and Gas Journal pp. 92-96, June 14, 1965.
7. Glover, A.G., Horsley, D.J. and Dorling, D.V., “High Strength Steel Becomes Standard On The Alberta Gas System”, Oil & Gas Journal pp 44-50, 4 January 1999.
8. Glover, A., Horsley, D., Dorling, D. and Takehara, J., “Construction And Installation Of X100 Pipelines”, Paper IPC04-0328 IPC Conference, Calgary, Oct 4-8, 2004.
9. Glover, A., Zhou, J., Suzuki, N. and Ishikawa, N., “The Application Of X100 To Gas Pipeline Projects”, International Symposium on Microalloyed Steels for the Oil & Gas Industry, Araxa, MG, Brazil, 23-26 January 2006.
10. Barsanti, L., Bruschi, R. and Donati, E., “From X80 To X100 Know-How Reached By ENI Group On High Strength Steel”, SNAM Rete Gas Spa, Milan Italy and Snamprogetti Spa, Fano Italy. Proceedings of Pipe Dreamer’s Conference, Application and Evaluation of High Grade Line Pipes in Hostile Environments, Yokohama, Japan, 7-8 November 2002.
11. Demofonti, G., Mannucci, G., Harris, D., Hillenbrand, H-G. and Barsanti, L., “Fracture Behavior Of X100 Gas Pipeline By Full Scale Tests”, CSM Spa, Rome, Italy, Corus, London UK, Europipe GmbH, Ratingen, Germany and SNAM Rete Gas, Milan Italy, Proceedings of Pipe Dreamer’s Conference, Application and Evaluation of High Grade Line Pipes in Hostile Environments, Yokohama, Japan, 7-8 November 2002.
12. Horsley, D., Taylor, D., Hudson, M. and Johnson, J., ”X100 Field Welding Experience”, APIA-EPRG-PRCI 18th Biennial Joint Technical Meeting, Canberra, Australia, April 2007.
13. Johnson, J., Hudson, M.G., Takahashi, N., Nagase, M. and Yamamoto, S., “Specification And Manufacturing Of Pipes For The X100 Operational Trial”, IPC 2008-64653, Proceedings of International Pipeline Conference IPC 2008. Calgary, Alberta, Canada, September 2008.
14. Johnson, J., Sanderson, N., Hudson, M.G. and Murdoch, C., “The X100 Operational Trial - Operational Validation of X100 Grade Steel Line pipe”, PITSO Conference. October 2007
15. Takeuchi, I., Fujimo, J., Yamamoto, A. and Okaguchi, S., “Prospect Of High Grade Steel Pies For Gas Pipelines”. Sumitomo Metal Industries, Proceedings of Pipe Dreamer’s Conference, Application and Evaluation of High Grade Line Pipes in Hostile Environments, Yokohama, Japan, 7-8 November 2002.
16. Hillenbrand, H-G. and Kalwa, C., “Production And Service Behavior Of High Strength, Large Diameter Pipes”, Europipe GmbH, Ratingen, Germany, Proceedings of Pipe

- Dreamer's Conference, Application and Evaluation of High Grade Line Pipes in Hostile Environments, Yokohama, Japan, 7-8 November 2002.
17. Hudson, M., Blackman, S., Hammond, J. and Dorling, D., Girth Welding of X100 Pipeline Steels", Paper IPC2002-27296, International Pipeline Conference, Calgary, Alberta, September 29-October 3, 2002.
 18. Hillenbrand, H-G., Niederhoff, K.A., Amoris, E., Perdrix, C., Streisselberger, A. and Zeislmaier, U., "Development Of Linepipe In Grades Up To X100", Proceedings of Biennial Joint Technical Meeting EPRG/PRC, Paper 6, Washington DC USA, April 1997.
 19. Hillenbrand, H-G., Liessem, A., Knauf, G., Niederhoff, K.A. and Bauer, J., "State Of The Art Report From The Manufacturer's Point Of View", International Pipeline Technology Conference, Brugge, Belgium, May 2000.
 20. Gräf, M.K., Hillenbrand, H-G., Heckmann, C.J. and Niederhoff, K.A., "High-Strength Large-Diameter Pipe For Long-Distance High Pressure Gas Pipelines", Proceedings of The Thirteenth International Offshore and Polar Engineering Conference, Honolulu, Hawaii, USA, pp. 97-104, 25-30 May 2003.
 21. Hudson, M., "Welding of X100 Line Pipe", PhD Thesis, School of Industrial and Manufacturing Science, Cranfield University, March 2004
 22. ASME Boiler and Pressure Vessel Code, Section IX, "Qualification Standard for Welding and Brazing Procedures, Welders, Brazers, and Welding and Brazing Operators", American Society of Mechanical Engineers, 2010.
 23. API 1104, "Welding of Pipelines and Related Facilities, 5.4 Essential Variables", American Petroleum Institute 1999.
 24. CSA Z662-03, "Oil and Gas Pipeline Systems", Canadian Standards Association, 2003.
 25. BS 4515-1:2004 "Specification For Welding Of Steel Pipelines On Land And Offshore - Part 1: Carbon And Carbon Manganese Steel Pipelines", British Standards Institute, 2004.
 26. EN 288-9:1999, "Specification And Approval Of Welding Procedures For Metallic Materials, Welding Procedure Test For Pipeline Welding On Land And Offshore Site Butt Welding Of Transmission Pipeines", European Committee for Standardization, 1999.
 27. Panday, R. and Daniel, J., "Materials Selection, Welding And Weld Monitoring", Final Report 278-T-02 to PHMSA per Agreement # DTPH56-07-T-000005, September 2011.
 28. Gianetto, J.A., Goodall, G.R., Tyson, W.R., Quintana, M.A., Rajan, V.B and Chen, Y., "Microstructure And Hardness Characterization Of Girth Welds", Final Report 278-T-03 to PHMSA per Agreement # DTPH56-07-T-000005, September 2011.
 29. Gianetto, J.A., Tyson, W.R., Park, D.Y., Shen, G., Lucon, E., Weeks, T.S., Quintana, M.A., Rajan, V.B. and Wang, Y.-Y., "Small Scale Tensile, Charpy V-Notch, and Fracture Toughness Tests", Final Report 277-T-05 to PHMSA per Agreement # DTPH56-07-T-000005, September 2011.
 30. Park, D.Y., Tyson, W.R., Gianetto, J.A., Shen, G., Eagleson, R.S., Lucon, E. and Weeks, T.S., "Small Scale Low Constraint Fracture Toughness Test Results", Final Report 277-T-06 to PHMSA per Agreement # DTPH56-07-T-000005, September 2011.
 31. Park, D.Y., Tyson, W.R., Gianetto, J.A., Shen, G., Eagleson, R.S., Lucon, E. and Weeks, T.S., "Small Scale Low Constraint Fracture Toughness Test Discussion and Analysis", Final Report 277-T-07 to PHMSA per Agreement # DTPH56-07-T-000005, September 2011.

32. Gianetto, J.A., Goodall, G.R., Tyson, W.R., Quintana, M.A., Rajan, V.B. and Chen, Y., "Microstructure and Properties of Simulated Weld Metals", Final Report 278-T-04 to PHMSA per Agreement # DTPH56-07-T-000005, September 2011.
33. Gianetto, J., Goodall, G.R., Tyson, W.R., Quintana, M.A. and Chen, Y., "Microstructure and Properties of Simulated Heat Affected Zones", Final Report 278-T-05 to PHMSA per Agreement # DTPH56-07-T-000005, September 2011.
34. Rajan, V.B., "Essential Welding Variables", Final Report 278-T-06 to PHMSA per Agreement # DTPH56-07-T-000005, September 2011.
35. Rajan, V.B. and Daniel, J., "Application to Other Processes", Final Report 278-T-09 to PHMSA per Agreement # DTPH56-07-T-000005, September 2011.
36. Rajan, V.B., Daniel, J., Chen, Y., Quintana, M. and Souza, A., "Welding process selection and control for high strength pipeline applications", Paper IBP1506_09, Rio Pipeline Conference and Exhibition, Rio de Janeiro, Brazil, September 2009.
37. Bosworth, M. R., "Effective Heat Input in Pulsed Current Gas Metal Arc Welding with Solid Wire Electrodes", Supplement to the Welding Journal, May 1991.
38. Chen, Y., Wang, Y.-Y., Quintana, M.A. and Rajan, V.B., "Thermal Model for Welding Simulations", Final Report 278-T-07 to PHMSA per Agreement # DTPH56-07-T-000005, September 2011.
39. Chen, Y., Wang, Y.-Y., Quintana, M.A. and Rajan, V.B., "Microstructure Model for Welding Simulations", Final Report 278-T-08 to PHMSA per Agreement # DTPH56-07-T-000005, September 2011.
40. Rosenthal, D., "Mathematical Theory Of Heat Distribution During Cutting And Welding", Welding Journal, pp. 220s-234s, 1941.
41. Kirkaldy, J.S. and Venugopalan, D., in Phase Transformation In Ferrous Alloys (Edited by Marder, AR and Goldstein, JI), Philadelphia, pp. 125-48, October 1983
42. Watt, D.F., Coon, L., Bibby, M.J., Goldak, J.A. and Henwood, C., "An Algorithm For Modeling Microstructural Development In Weld Heat Affected Zones", Acta Metal, Vol. 36, No 11, pp. 3029-3035, 1988.
43. Bhadeshia, H.K.D.H. and Svensson, L.E., in Mathematical Modeling of Weld Phenomena, H. Cerjak and K. E. Easterling , eds., Institute of Materials, London, pp. 109-180., 1993
44. Ashby, M.F. and Easterling, K.E., "A First Report On Diagrams Of Microstructure And Hardness For Grain Growth In Welds," Acta Metall., Vol 30, No 11, pp. 1969-1978, 1982.